MAY, LESTER THEODORE

ISOCITRATE DEHYDROGENASE AND ITS RELATIONSHIP TO GLUCONEOGENESIS IN TETRAHYMENA

City University of New York PH.D. 1981

PLEASE NOTE:

In all cases this material has been filmed in the best possible way from the available copy. Problems encountered with this document have been identified here with a check mark __√__.

1. Glossy photographs or pages __✓__
2. Colored illustrations, paper or print _____
3. Photographs with dark background __✓__
4. Illustrations are poor copy _____
5. Pages with black marks, not original copy _____
6. Print shows through as there is text on both sides of page _____
7. Indistinct, broken or small print on several pages _____
8. Print exceeds margin requirements _____
9. Tightly bound copy with print lost in spine _____
10. Computer printout pages with indistinct print _____
11. Page(s) _____ lacking when material received, and not available from school or author.
12. Page(s) _____ seem to be missing in numbering only as text follows.
13. Two pages numbered _____. Text follows.
14. Curling and wrinkled pages _____
15. Other _____

ISOCITRATE DEHYDROGENASE AND ITS RELATIONSHIP TO GLUCONEOGENESIS IN TETRAHYMENA

by LESTER T. MAY

A dissertation submitted to the Graduate Faculty in Biochemistry in partial fulfillment of the requirements for the degree of Doctor of Philosophy, The City University of New York.

1981

This manuscript has been read and accepted for the Graduate Faculty in Biochemistry in satisfaction of the dissertation requirement for the degree of Doctor of Philosophy.

9/4/81
date

Chairman of Examining Committee
James F. Hogg

September 16, 1981
date

Executive Officer
Aaron Lukton

John Berech

Walter Essman

William G. Robinson

Donald Sloan

Supervisory Committee

ABSTRACT

ISOCITRATE DEHYDROGENASE AND ITS RELATIONSHIP TO GLUCONEOGENESIS IN TETRAHYMENA

by

Lester T. May

Adviser: Professor James F. Hogg

It is reported in this thesis that Tetrahymena pyriformis does have an NAD-linked isocitrate dehydrogenase. This enzyme was assayed in both crude particle and mitochondrial preparations. However, all of its activity was lost upon solubilizing mitochondria in detergents or disruption with sonication. Since solubilization of this enzyme was unsuccessful all kinetic constants reported here were derived from mitochondria that had been separated by isopycnic density centrifugation in a sucrose gradient. Storage of these mitochondria in 50% aqueous-glycerol (v/v) at -20°C showed no loss of activity of the NAD-linked isocitrate dehydrogenase for up to 3 weeks. The NAD-linked isocitrate dehydrogenase from these mitochondria was stimulated by adenine nucleotides (AMP, ADP and ATP), with ADP having the greatest effect. ADP lowered the apparent K_m for NAD (from 225 to 45 micromolar) and increased the V_{max} with respect to threo-D_s-isocitrate. This ADP stimulation was found to be pH dependent, and was optimal at pH 7.0. This NAD-isocitrate dehydrogenase was inhibited by NADH, but not NADPH.

Homogenates or buffered extracts of freeze-dried cells do show

a significant amount of NAD-isocitrate dehydrogenase activity. However, this activity was observed only at high NAD concentrations (greater than 1mM). Attempts to separate this enzyme from a co-extracted NADP-isocitrate dehydrogenase activity showed that both coenzyme activities eluted together off Sephadex G-200, DEAE-Sephacel and Blue Dextran-agarose (Affi-Gel Blue) columns. Also, both activities had identical electrophoretic mobilities on a polyacrylamide gel and had equivalent molecular weights (90,000) as determined by gel chromatography. Finally the severe inhibition by NADPH, but not NADH on both coenzyme activities supports the conclusion that this NAD-activity from freeze-dried cells is a non-specific activity of the NADP-linked isocitrate dehydrogenase. The reductive carboxylation of α-ketoglutarate could be catalyzed by this enzyme with NADH. The physiological importance of this reaction, in regards to gluconeogenesis through the glyoxylate cycle is discussed.

An attempt to physiologically link a decrease in the specific activity of the NAD-linked isocitrate dehydrogenase in T. pyriformis with increasing gluconeogenesis through the glyoxylate cycle is made. Results of these studies do not definitively confirm nor refute this, but suggest a novel set of controls for the activation of gluconeogenesis from fats in T. pyriformis. Biochemical and electron microscopic evidence shows a distinct reorganization of the cytoplasm while

T. pyriformis develop the capacity to synthesize glycogen from exogenous acetate or endogenous phospholipids. Specifically enzymes required for gluconeogenesis from fats become sequestered in a fraction that is rich in autophagic vacuoles. Evidence is presented that implicates these autophagic vacuoles in the synthesis of glucose and/or glycogen from fats.

ACKNOWLEDGEMENTS

I would like to thank Dr. James F. Hogg for his patience in teaching biochemistry to me. His philosophical approach combined with an insistence on experimental details provided an ideal learning environment. I would also like to thank Zen Majuk and Marc Tissot who put up with me in the last few anxious months of my graduate work. A special thanks to O. Roger Anderson who contributed all of the electron micrographs and his expertise in their interpretation. It was a truly rewarding experience to have collaborated with him. To my good friend Dan Hryb and the many ideas and hours that we have spent together which in no small way contributed to this thesis as well as my enjoyment-Thanks! I would also like to thank Donald Sloan for taking time from his own vacation to read and review this dissertation and for his support during my years at the City University.

Finally, to my wife Debbie, for whom gratitude and thanks are simply not enough-I love you! Her encouragement and love were and are my greatest assets.

TABLE OF CONTENTS

LIST OF TABLES

LIST OF FIGURES

CHAPTER 1

THE NADP-ISOCITRATE DEHYDROGENASE OF *TETRAHYMENA PYRIFORMIS*.

INTRODUCTION

Tetrahymena pyriformis is a ciliated protozoan that has been used as a model system for the study of the metabolism of eucaryotic cells. Aerobically glucose is converted to CO_2, and anaerobically lactic acid accumulates from glucose fermentation. When the cells are grown without vigorous aeration, glycogen synthesis and storage constitutes a major metabolic diversion. Up to 23% of the dry weight of this organism when grown in a noncarbohydrate medium (1) and 50% when grown in the presence of glucose (2) is found as glycogen. The pathway towards glycogen synthesis from glucose resembles that found in mammalian systems with UDP-glucose as the immediate donor of glucosyl units. Also, the glycogen found in T. pyriformis resembles that of rabbit liver, both in frequency and types of branch points (3) and in particle size range (4). All of the glycolytic enzymes have been identified, and it does seem that the path from endogenous glycogen or exogenous glucose to pyruvate or acetyl-CoA is similar to that found in most animals (5). Unlike mammalian glycogen phosphorylase and glycogen synthetase, these enzymes in T. pyriformis have not been found to be reciprocally repressed and induced (6) , but remain in active forms.

T. pyriformis diverges markedly from animals however, in its ability to convert fats to carbohydrates. Exogenous acetate and

endogenous phospholipids may be rapidly converted to glycogen (2) under appropriate conditions. Thus, like plants, molds and many other microorganisms T. pyriformis contains a glyoxylate cycle. The key enzymes (isocitrate lyase and malate synthase) have been studied and found to be elevated during conditions favorable to gluconeogenesis from fats (7, 8). In their absence, no gluconeogenesis from lipids could be elicited.

Recent findings implicate the presence of the glyoxylate pathway in animals. Goodman et al. (9, 11) have identified isocitrate lyase and malate synthase in toad bladder mucosa. These enzymes were also shown cytochemically in the peroxisome of toad bladder mucosa. However, increased glycogen synthesis through the glyoxylate cycle occurred only after toads had been placed on a regimen of aldosterone. It may be that the development of the glyoxylate cycle in mammals requires the presence of specific hormones and/or be the result of a specific nutritional state of the animal studied. Since fetal guinea pig liver (10) also appears capable of converting fats to to carbohydrates, it may be that the study of the controls and regulation of the glyoxylate cycle are of far greater importance than previously thought.

It was originally demonstrated by C. Wagner (2) that lipid conversion to glycogen occurs in T. pyriformis. He also determined that only phospholipids of the cellular lipids decreased as the glycogen

content of the cell increased. This occurred in stationary phase cells, but not in cells that were in the logarithmic (exponential) phase of growth. A year after Wagner's work was published (1957) the glyoxylate cycle was proposed by Kornberg and Krebs (12) as the enzymatic route for the conversion of fats in carbohydrates. The demonstration of the glyoxalate cycle rested on two novel enzymes; isocitrate lyase and malate synthase. The discovery of isocitrate lyase (13) showed that isocitrate could be split into succinate and glyoxylate, as well as being dehydrogenated and decarboxylated. Malate synthase condensed the glyoxylate with acetyl-CoA to form malate. Both malate and succinate could then be oxidized to oxaloacetate by well-known enzymes of the tricarboxylic acid cycle. The oxaloacetate could then be converted to phosphoenolpyruvate (PEP) by adenosine triphosphate (ATP) and phosphoenolpyruvate carboxykinase. PEP, in turn fuels gluconeogenesis. Thus, finding both of the key enzymes in the glyoxylate bypass present in extracts from cells that are oxidizing fats (i.e. producing acetyl-CoA) offered an enzymatic path to glucose synthesis.

When Hogg and Kornberg in 1963 (7) showed that intracellular activity of these key enzymes was induced by acetate and/or ketogenic amino acids to produce cells capable of gluconeogenesis from fats, the glyoxylate cycle was invoked as the means to generate glycogen from fats. Levy and Scherbaum (14) suggested that decreasing oxygenation also induced gluconeogenesis, since they could induce log

phase cells (normally incompetent for gluconeogenesis from lipids) to synthesize glycogen from acetate by maintaining them for several hours at low oxygen. Hogg confirmed their observations under more rigorously controlled experimental conditions (8).

Intracellular localization experiments revealed that the various enzymes required for the glyoxalate cycle were found in at least two different organelles (mitochondrion and peroxisome) and the cytosol (15). This led Hogg to propose a complex scheme for glucose synthesis from fats involving a four membrane-transport step pathway to correspond with the various locales of the requisite enzymes (8). The apparent complexity of this pathway baffled even the author. Intercompartmental transport of substrates and intermediate products might be expected to divert a large portion of them away from glucose synthesis. Furthermore, the presence of at least a partial pentose phosphate cycle (16) should result in "carbon scrambling" of the substrates for glycogen synthesis. Yet, the labeling pattern from 1-[^{14}C]-labeled acetate, either in resting cells or in growing cultures, is marked by its purity (greater than 95% is found in the third and fourth carbons of the glucose in glycogen), while at least 50% of the 2-[^{14}C]-labeled acetate was found in glycogen (8). Thus, the path to glycogen from exogenous acetate (and presumably endogenous lipids) appears undiverted by any side reactions. Further scrutiny of the glyconeogenic process reveals other paradoxes.

Induction of glyconeogenesis in log phase cells by decreasing oxygen tension (14) obscures the fact that glycogen synthesis absolutely requires good oxygenation. In fact anaerobic conditions are well-known to produce glycolysis in T. pyriformis (17). This need for oxygen in gluconeogenesis from fats was more precisely established by Cooper and Beevers (18) for peroxisomes of castor bean endosperm. Addition of palmitoyl-CoA to peroxisomes resulted in oxygen uptake, NADH accumulation and acetyl-CoA formation. These findings paved the way for the discovery of a peroxisomal β-oxidation system not coupled to mitochondrial respiration in T. pyriformis (19). In fact the first enzyme in this extramitochondrial β-oxidation system has been localized in the peroxisome. This novel enzyme (fatty acyl-CoA oxidase) has an FAD dependence, as does the first enzyme involved in the mitochondria (fatty acyl-CoA dehydrogenase). However, it contributes its electrons directly to oxygen, thereby producing H_2O_2 and explaining the oxygen dependency of gluconeogenesis from fats. Thus, the condition that induces gluconeogenesis from fats in T. pyriformis also necessarily prevents it until oxygen is reintroduced into the cellular environment.

Although the enzymatic pathway of glyconeogenesis from endogenous lipids or exogenous acetate has been worked out, the intracellular determinants activating this path are not understood at all. Induction of this pathway in log phase cells cannot be adequately

explained by synthesis of isocitrate lyase and/or malate synthase. The levels of each were found to be high enough in log phase cells, before any hypoxicinduction, to support high rates of gluconeogenesis from fats. Activation of these key enzymes offers a possible explanation. However, the three to four hours required for full activation of this pathway in log phase cells seems too long for such a process. Very little else is known about the regulation of gluconeogenesis. This thesis is an attempt to gain some understanding of the factor(s) that are involved within the cell in activating gluconeogenesis.

My initial approach to this problem involved isocitrate metabolism. Since isocitrate lies at a strategic junction between the initial site of glyoxylate bypass reactions (i.e. isocitrate lyase) , and the first site of oxidation in the tricarboxylic acid cycle (i.e. isocitrate dehydrogenase) it seemed a good candidate for involvement in some form of metabolic regulation. As the site of the glyoxylate bypass reactions (the peroxisome) and the locale of isocitrate synthesis (the mitochondrion) within T. pyriformis are cytologically separate (15), isocitrate formed in the mitochondrion must be exported to the peroxsome in order for the glyoxylate cycle pathway to continue. Thus, the requirement of isocitrate for carbohydrate synthesis through the glyoxylate bypass reactions makes the availability of isocitrate be of primary importance. There are also significant amounts of NADP-linked isocitrate dehydrogenase (EC1.1.1.42) in the mitochondrion,

peroxisome and cytosol of T. pyriformis (15). The availability of isocitrate to the glyoxylate cycle may therefore be dependent on the extent to which total isocitrate is oxidized and decarboxylated by this enzyme. Thus, isocitrate dehydrogenase activity (NADP) could dictate the availability of isocitrate. The specific activity of the NADP-linked isocitrate dehydrogenase (NADP-Icdh) remains essentially constant, under variable growth conditions (20, 21) in both particles (20, 21) and cell extracts (20) and during various stages of growth (20, 21). The levels of total NADP remain constant during conditions favorable (static) and unfavorable (shaken in air) for gluconeogenesis (22). The level of isocitrate in the cell, under conditions of active gluconeogenesis was found to be 5.1 μM (23). This is twenty-fold smaller than the $K_m^{\text{isocitrate}}$ for isocitrate lyase established by the same researcher. Thus the kinetic and metabolite data would seem to imply that gluconeogenesis through the glyoxylate cycle cannot be occurring. Yet, it most certainly is. I must therefore beg your indulgence on this point, since it is clear that isocitrate does go through the glyoxylate bypass reactions while gluconeogenesis from fats is occurring. It must also be conceded that, if isocitrate is coming from the mitochondria it is not effectively deterred in getting to isocitrate lyase by the NADP-Icdh despite the fact that the specific activity of this enzyme and the level of total NADP are invariant with age. Moreover, it is the NAD-linked isocitrate dehydrogenase (EC 1.1.1.41) that has been

implicated as an important site in the regulation of oxidation within the mitochondrion (24, 25, 26). Since its discovery in yeast (27), almost all eucaryotic organisms have been shown to possess both an NAD- and NADP-linked isocitrate dehydrogenase. T. pyriformis has been a notable exception because only the NADP-Icdh has been found. Since ∝-ketoglutarate dehydrogenase (EC 1.2.4.2) also has not been found in T. pyriformis, the possibility of an abbreviated tricarboxylic acid cycle cannot be overlooked. However, the stimulation of oxygen uptake in purified mitochondria by both isocitrate and ∝-ketoglutarate (15, 28) argue against such an interpretation. The subcellular distribution of NADP-Icdh revealedabout 5% of this enzyme to be in the T. pyriformis mitochondria (15). Muller et al. further claimed that this small percentage of the enzyme's total activity could not account for the "isocitrate oxidase" activity found in mitochondria from T. pyriformis. They concluded that an NAD-Icdh must be responsible for this activity (15). Unfortunately no specific activities for the mitochondrial-associated NADP-Icdh were shown to compare with the specific activities of their "isocitrate oxidase" in support of their conclusion.

Prior to my involvement in this project, D. J. Hryb had observed an NAD-linked isocitrate dehydrogenase activity in aqueous-glycerol extracts of lyophilized cells. T. Dorsey (23) had shown that 50% (v/v) glycerol acted as an extremely effective preservative for isocitrate

lyase activity. Thus it was concluded that the discovery of an NAD-linked isocitrate dehydrogenase from dry cell extracts was contingent on the maintenance of its stability and that 50% glycerol had this ability. My job was to characterize its activity with respect to its potential to regulate the isocitrate flux out of the mitochondrion.

MATERIALS AND METHODS

Growth of cells. Tetrahymena pyriformis, strain E (ATCC 30005) was cultured axenically as described by Hogg and Kornberg (8). The culture medium contained 1% (w/v) proteose-peptone (Difco), 0.1% D-glucose, 0.1% sodium acetate, 0.1% dipotassium phosphate, 0.01% yeast extract and 0.002 micrograms/ml of thiamine HCl. Stock cultures were kept in 19mm screw-cap test tubes containing 10 ml of medium and fitted with plastic caps permeable to O_2 and CO_2. Mass cultures were grown in flat cylindrical flasks, 7 inches in diameter, provided with a side neck (Jobling No. 1420 culture flasks, Laboratory Glassblowers Company, Sands, High Wycomb, Bucks, England), containing 500 ml of medium. All cultures were inoculated with a 1% volume (5ml) of a growing stock culture. Cultures were then grown without shaking at 25 C for 2-7 days before harvesting.

Cells were harvested in a modified plankton centrifuge as described by Conner et al. (102). After the cells were collected they were immediately washed, while in the centrifuge, with an equal volume of dilute Ringer phosphate solution (17). All washed cells were resuspended in dilute Ringer phosphate solution to a concentration of cells between 4 and 6% (v/v) as estimated in Constable protein tubes by centrifugal packing (1000 x g for 10 minutes) in an International centrifuge. The cell suspensions were frozen in dry ice-acetone and

and dried at high vacuum in an all glass Kontes lyophilizer.

Extraction of isocitrate dehydrogenase. All isocitrate dehydrogenase was extracted by suspending the freeze-dried cell powders in 10mM Hepes buffer, pH 7.0 (10mg of dried cells/ml of buffer) in a precooled Brendler homogenizer tube and grinding with a teflon pestle for one minute at 1000 rpm. Homogenates were centrifuged at 30,000 x g for 20 minutes in a Sorvall RC-2 centrifuge with an SS-34 fixed angle rotor. The resultant clear supernatant contained all of the detectable isocitrate dehydrogenase activity and was used for most studies presented here. Variations in the extraction procedure will be noted and detailed in each specific case.

Enzyme assay. Isocitrate dehydrogenase was assayed by the method of Kornberg (29) For NAD and NADP enzyme activities. Both activities (NAD and NADP) were routinely measured in the presence of 50 mM Hepes buffer, pH 7.3, 1mM $MnCl_2$ or $MgCl_2$ and 10mM NAD or 0.4mM NADP. The reaction was initiated by the addition of D,L isocitrate to 5 mM and the increasing absorbance at 340nm was followed with respect to time in a Gilford 240 or 2400 recording spectrophotometer at 30°C.

Separation of NAD- from NADP- isocitrate dehydrogenase. Separation of potential isozymes of the isocitrate dehydrogenase activities found in extracts of dry cells was performed on columns packed and equilibrated at 5°C with Sephadex G-200 (superfine grade), DEAE-Sephacel (pre-swollen) and Affi-Gel Blue (pre-swollen). The

Sephadex G-200 was equilibrated in 50 mM Hepes (pH 7.3) and packed in a Pharmacia K26/40 column. A constant flow rate of 1.5 ml/hour was maintained. The void volume was determined with Dextran Blue. DEAE-Sephacel, also packed in a Pharmacia K26/40 column, was washed with 5 mM potassium phosphate buffer (pH 7.2) before use. A constant flow rate of 17 ml/hour was maintained. Cibacron Blue 3GA-bound agarose (Affi-Gel Blue) was packed in a 1 x 10 cm column with a sintered glass support and washed with 5 mM potassium phosphate buffer (pH 7.2). Dry cell extracts were concentrated by taking the 70% $(NH_4)_2SO_4$ precipitate (after 40% precipitate had been removed), which always contained greater than 90% of the isocitrate dehydrogenase activity (NAD or NADP) and resuspending in the buffer used to equilibrate the column. The resuspended precipitate was then dialyzed against the same buffer overnight. No more than 5% of the total activity was lost during dialysis at 5°C. 5 ml of the dialysate was then applied to each column.

Molecular weight determination. The molecular weight was estimated by gel filtration through Sephadex G-200 in accordance with the method described by Andrews (30). Column packing and equilibration were identical to those used for the attempted separation of isocitrate dehydrogenases described above.

Disc gel electrophoresis. Electrophoresis of isocitrate dehydrogenase activities (NAD and NADP) was also used in the attempts to

separate potential isozymes of these activities. The separating gels were composed of 7.5% acrylamide and 0.2% N,N'-methylenebis-acrylamide. The stacking gels were composed of 1.25% acrylamide and 0.31% N,N'-methylenebisacrylamide. Gels were prepared in .5cm x 7.5cm tubes according to the method of Gabriel (31) for the separation of molecules between 10,000 and 1,000,000 molecular weight in a running buffer of Tris-barbital (System II-pH7.0). Extracts of dried cells were prepared as in the chromatography work described above, except that dialysis was against Tris-barbital in 10% (v/v) glycerol. Glycerol was included in order to maintain an interface (to avoid mixing) between the enzyme extract applied atop the gels and the running buffer initially. About 200μg of protein from the dialysate was layered on the gels and then carefully covered with buffer. The samples were then run at 10°C for 2 hours at 2 mAmperes/gel tube for a total of 36mAmperes. The staining solution for isocitrate dehydrogenase activity was a modification of the solution used for lactate dehydrogenase by Dietz and Lubrano (32). The solutions were identical to that of the routine assay solution described above, except that $MnCl_2$ was used exclusively to fulfill the metal requirement, and phenazine methosulfate and nitroblue tetrazolium were added to concentrations of 0.027 mg/ml and 0.270 mg/ml respectively.

pH dependence of forward and reverse reaction. The dependence of reaction velocities on pH was measured in both the forward

and reverse directions with NAD or NADP (forward) and NADH or NADPH (reverse) from pH 5.5 to 8.2, using 50 mM MES (2-(N-morpholino) ethanesulfonic acid), MOPS (morpholinopropane sulfonic acid), Hepes (N-2-hydroxyethylpiperazine-N'-2-ethane sulfonic acid) and bicine (N,N-bis[2-hydroxyethyl] glycine). The activity in dry cell extracts was concentrated as before in 70% $(NH_4)_2SO_4$, resuspended in 50 mM Hepes (pH 7.3) and dialyzed overnight against the same buffer at 0°C.

Protein concentrations were determined by the method of Weichselbaum (33) after the protein had been precipitated with 0.5M perchloric acid, and then washed with 0.5M perchloric acid followed by absolute ethanol. Crystallized and lyophilized bovine serum albumen (Sigma) was used as the standard protein.

Materials. Acrylamide monomer and N,N'-methylenebisacrylamide were bought from Eastman-Kodak Chemical Co., Rochester, N.Y. DEAE-Sephacel, Sephadex G-200 (superfine grade) and the protein calibration kit (ribonuclease A, ovalbumin, chymotrypsinogen A, aldolase and Blue Dextran) were obtained from Pharmacia Fine Chemicals, Uppsala, Sweden. Affi-Gel Blue was obtained from Bio-Rad Laboratories. All other chemicals were of analytical reagent grade.

RESULTS

The observation that an NAD-linked isocitrate dehydrogenase (NAD-Icdh) was extractable in 50% (v/v) glycerol was readily confirmed. However, the NAD-Icdh activity was also found for dry cell homogenates in water and buffer, as well as in their extracts. In other words, glycerol was not needed to preserve the activity. Tablel shows some of the homogenates and extracts in which NAD-Icdh activity was found, as well as the substantially higher NADP-Icdh activity that coextracted. What seemed to characterize this NAD-Icdh activity was its unusually high concentrational requirement for NAD (less than 1mM NAD showed no observable rate of enzyme activity). We attributed our success and others' failures (15, 21) in finding this activity to the use of high concentrations of NAD (10mM). The NAD- and NADP-Icdh activities do observe Michaelis-Menten kinetics. A compilation of the kinetic constants for these enzyme activities from dry-cell extracts is shown in Table 2. The apparent K_m for NAD, using either $MnCl_2$ or $MgCl_2$, is 4-5mM. NAD-Icdh from other sources have K_m values for NAD that are one to two orders of magnitude lower (24, 34, 35). The apparent K_m found for NADP is more consistent with values published for mammalian cells (36, 37). Under optimal conditions, the concentrational dependencies for the natural isomer, threo-D_s-isocitrate, are identical with each coenzyme. When an equal concen-

TABLE 1. Isocitrate dehydrogenase activities assayed according to methods previously described. All homogenates and extracts were prepared from freeze-dried cells (10mg/ml). Final concentrations of NAD and NADP used in the assay were 10mM and 0.4mM respectively. All specific activities are in terms of moles of NAD(P)H formed/minute/mg of protein.

	Specific Activity	
A. Homogenates	NAD-Icdh	NADP-Icdh
50% glycerol	0.033	0.289
25% glycerol	0.031	0.257
10% glycerol	0.035	0.302
distilled water	0.029	0.257
50mM potassium phosphate(pH7.2)	0.033	0.287
50mM Hepes (pH 7.2)	0.034	0.306
B. Extracts		
50% glycerol	0.065	0.424
25% glycerol	0.067	0.413
10% glycerol	0.070	0.408
distilled water	0.052	0.362
50mM potassium phosphate (pH 7.2)	0.050	0.355
50mM Hepes (pH 7.2)	0.048	0.330

TABLE 2. Comparison of kinetic properties of NAD-and NADP-isocitrate dehydrogenase activities. All kinetic parameters were established for dry cell extracts assayed in Hepes buffer, pH 7.3, 1mM $MnCl_2$ or $MgCl_2$, 5mM D, L isocitrate when NAD or NADP were varied and 10mM NAD or 0.4mM NADP as threo-D_s-isocitrate was varied.

	Specific Activity, micromoles NAD(P)H/min/mg
V_{max} for NAD-activity using $MnCl_2$	0.07
V_{max} for NADP-activity using $MnCl_2$	0.47
V_{max} for NAD-activity using $MgCl_2$	0.04
V_{max} for NADP-activity using $MgCl_2$	0.30
	Concentration, micromoles/liter
K_m^{NAD} using $MnCl_2$	4000
K_m^{NADP} using $MnCl_2$	10
K_m^{NAD} using $MgCl_2$	5000
$K_m^{Ds\text{-isocitrate}}$ for NAD-activity using $MnCl_2$	5
$K_m^{D_s\text{-isocitrate}}$ for NADP-activity using $MnCl_2$	5
$K_m^{D_s\text{-isocitrate}}$ for NAD-activity using $MgCl_2$	15
$K_m^{D_s\text{-isocitrate}}$ for NADP-activity using $MgCl_2$	15

tration of $MgCl_2$ is used in place of $MnCl_2$ to fulfill the metal requirement, the apparent K_m for isocitrate increases from 5 to 15 M. The K_m values for threo-D_s-isocitrate listed in Table 2 for T. pyriformis isocitrate dehydrogenase(s) are consistent with published values for the NADP-Icdh from other cell types (36, 37, 38), but considerably lower than those reported for the NAD-Icdh (24, 35, 37).

The apparently low affinity for NAD of this NAD-Icdh activity was troublesome. Table 3 provides a list of metabolites that might have the potential to increase this low affinity of NAD for this enzyme activity. Both citrate and ATP at lmM inhibit activity, and GTP did to a smaller degree. However, these effects were abolished by decreasing the in vitro concentrations of citrate and ATP or by increasing the concentration of $MnCl_2$. Thus, chelation of the required metal cation is involved in this inhibition. The differential effect of GTP on this proposed inhibition by chelation is not understood at this time.

Attempts to separate the two coenzyme-specific activities were unsuccessful. Figures 1, 2 and 3 show that both activities eluted together, regardless of the nature of the chromatography. Figure 4 illustrates that the NAD- and NADP-Icdh activities are inseparable by disc gel electrophoresis. Both have identical electrophoretic mobilities in a polyacrylamide gel. A molecular weight determination on Sephadex G-200 indicates that both activities are

TABLE 3. Effect of some metabolites on sub-maximal NAD-isocitrate dehydrogenase activity. Assays are in 50mM (pH 7.3) Hepes, 1mM $MnCl_2$, 5mM D, L isocitrate and 2mM NAD, except where noted. All activities are from dry cell extracts and are listed in micromoles of NADH formed/minute/mg of protein.

	Activity
+10mM NAD	0.046
Control (2mM NAD)	0.023
+1mM AMP; 1mM ADP; 1mM 3, 5-cyclic AMP	0.023
+1mM ATP	0.013
+0.25mM ATP	0.024
+1mM ATP + 2mM $MnCl_2$	0.022
+1mM citrate	0.012
+0.25mM citrate	0.023
+1mM citrate + 2mM $MnCl_2$	0.021
+1mM phosphoenolpyruvate; 1mM pyruvate	0.022
+1mM acetyl-CoA	0.021
+1mM malate; 1mM fumarate	0.022
+1mM succinate; 1mM ketoglutarate	0.024
+1mM GDP	0.021
+1mM GTP	0.018

FIGURE 1. Elution pattern from gel filtration on Sephadex G-200 of isocitrate dehydrogenase activities. Experimental details are described in text. The void volume was determined as 26ml with Blue Dextran. Elution volumes shown represent all of the recovered isocitrate dehydrogenase activities (both NAD and NADP).

FIGURE 1

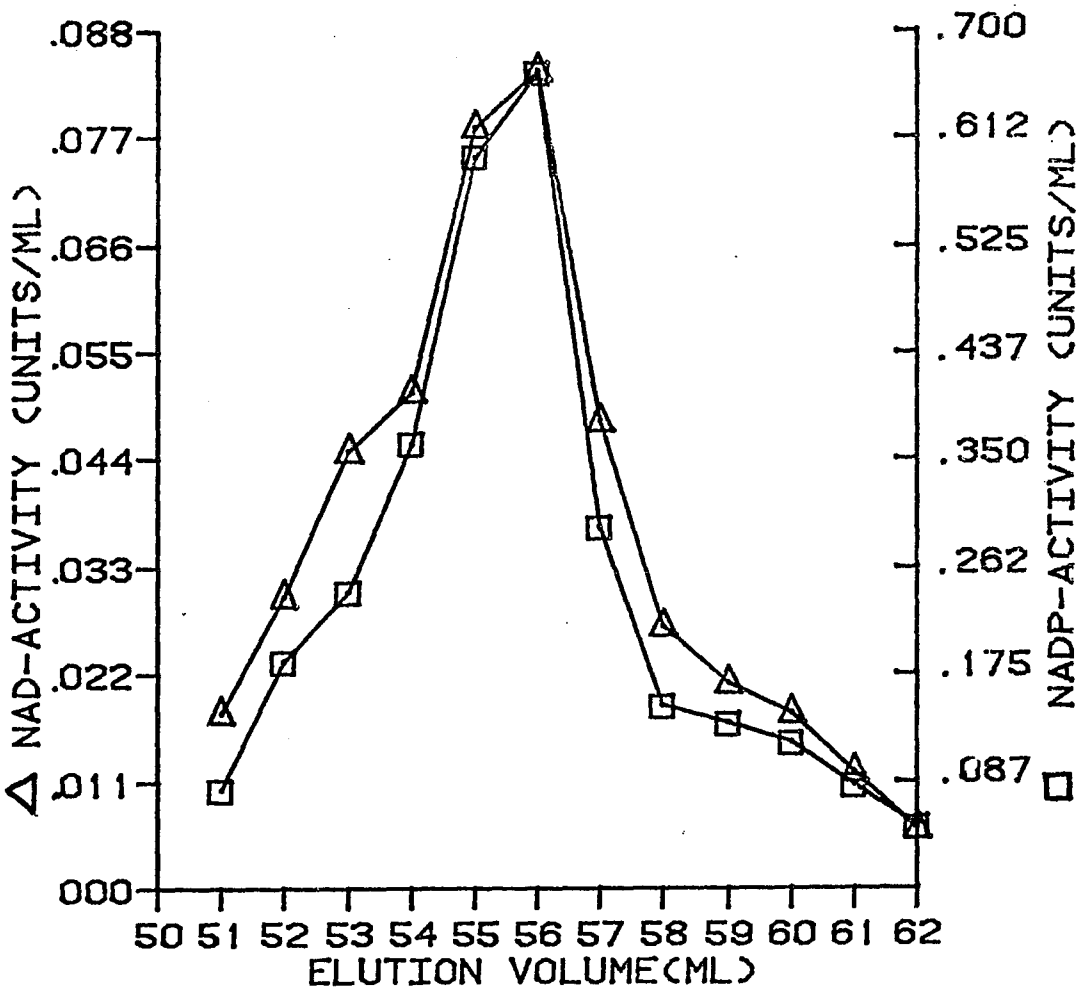
.088
.077
.066
.055
.044
.033
.022
.011
.000
Δ NAD-ACTIVITY (UNITS/ML)
.700
.612
.525
.437
.350
.262
.175
.087
□ NADP-ACTIVITY (UNITS/ML)
50 51 52 53 54 55 56 57 58 59 60 61 62
ELUTION VOLUME(ML)

FIGURE 2. Elution pattern from DEAE-Sephacel of isocitrate dehydrogenase activities. The increasing potassium phosphate buffer concentrations (5mM-30mM) were used to elute isocitrate dehydrogenase activities (both NAD and NADP) are indicated by broken line. Elution volumes shown represent all of the recovered isocitrate dehydrogenase activities.

FIGURE 2

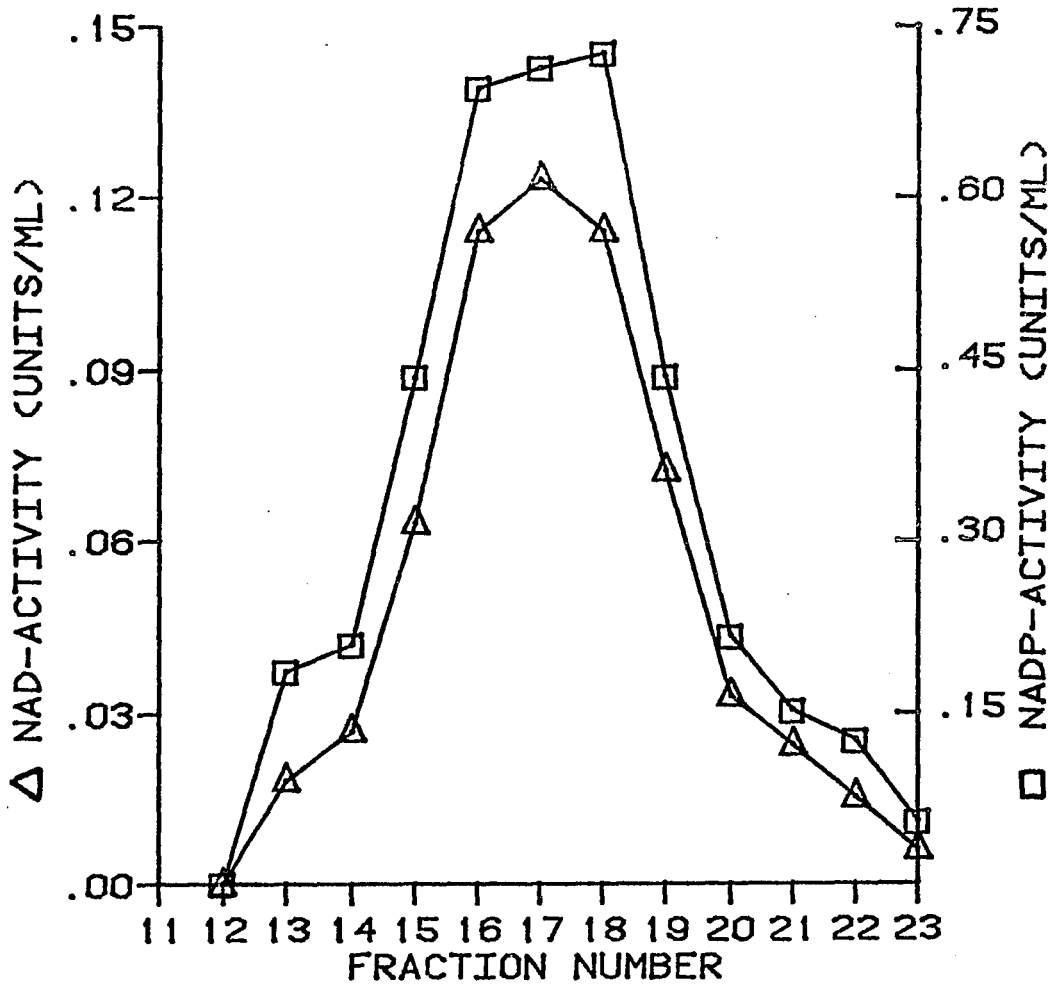
.15
.12
.09
.06
.03
.00
Δ NAD-ACTIVITY (UNITS/ML)
.75
.60
.45
.30
.15
□ NADP-ACTIVITY (UNITS/ML)
11 12 13 14 15 16 17 18 19 20 21 22 23
FRACTION NUMBER

FIGURE 3. Elution pattern from Blue-Dextran bound agarose (Affi-Gel Blue) of isocitrate dehydrogenase activities. All isocitrate dehydrogenase activity remained on column when washed with 5mM potassium phosphate buffer (pH 7.2) with or without 10mM NAD. All isocitrate dehydrogenase activity (both NAD and NADP) were eluted with 5mM NADP. Elution volumes shown represent all of the recovered isocitrate dehydrogenase activities.

FIGURE 3

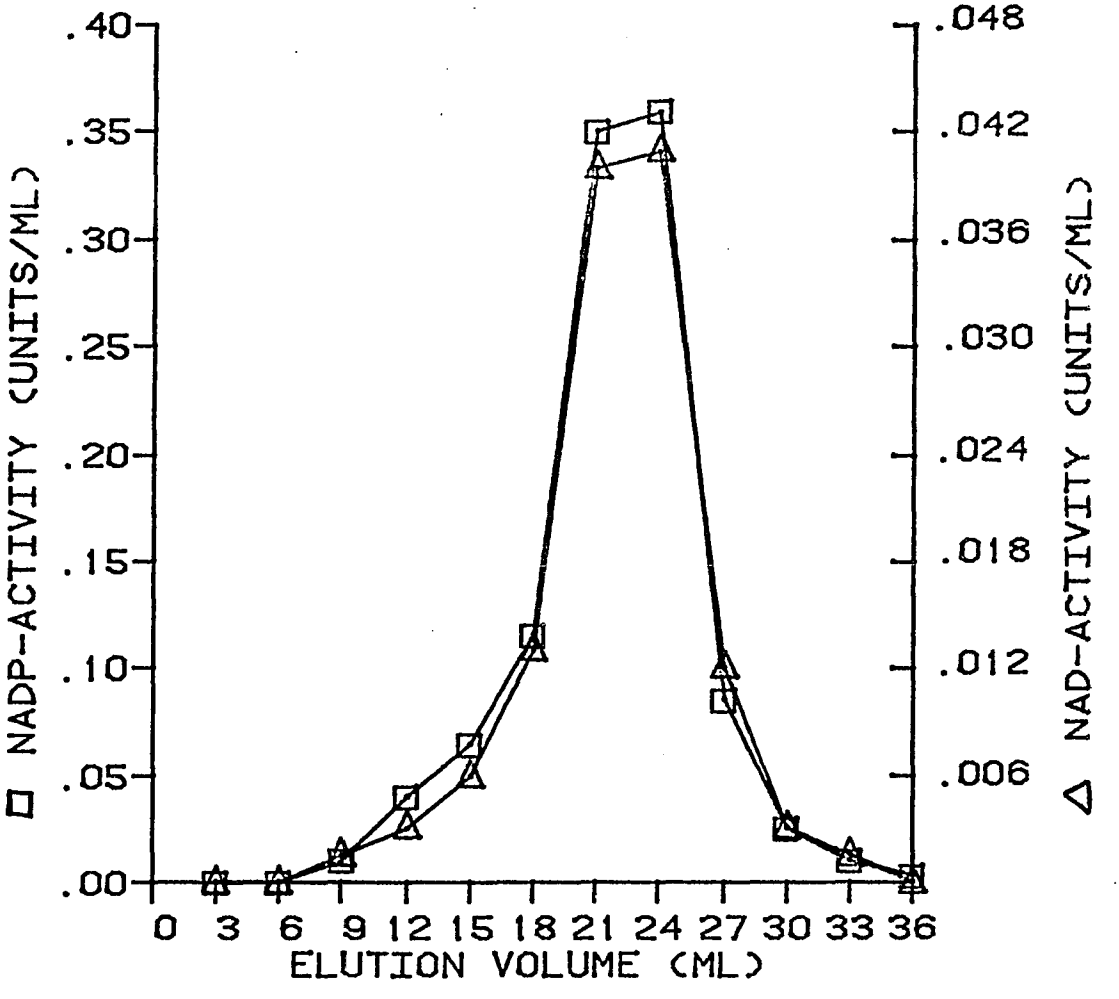
.40
.35
.30
.25
.20
.15
.10
.05
.00
□ NADP-ACTIVITY (UNITS/ML)
.048
.042
.036
.030
.024
.018
.012
.006
Δ NAD-ACTIVITY (UNITS/ML)
0 3 6 9 12 15 18 21 24 27 30 33 36
ELUTION VOLUME (ML)

FIGURE 4. Polyacrylamide-gel electrophoresis of isocitrate dehydrogenase activities. Experimental details are described in Materials and Methods section.

A-Incubation with NAD as the only coenzyme

B-Incubation with NADP as the only coenzyme

C-Incubation with both NAD and NADP

FIGURE 4

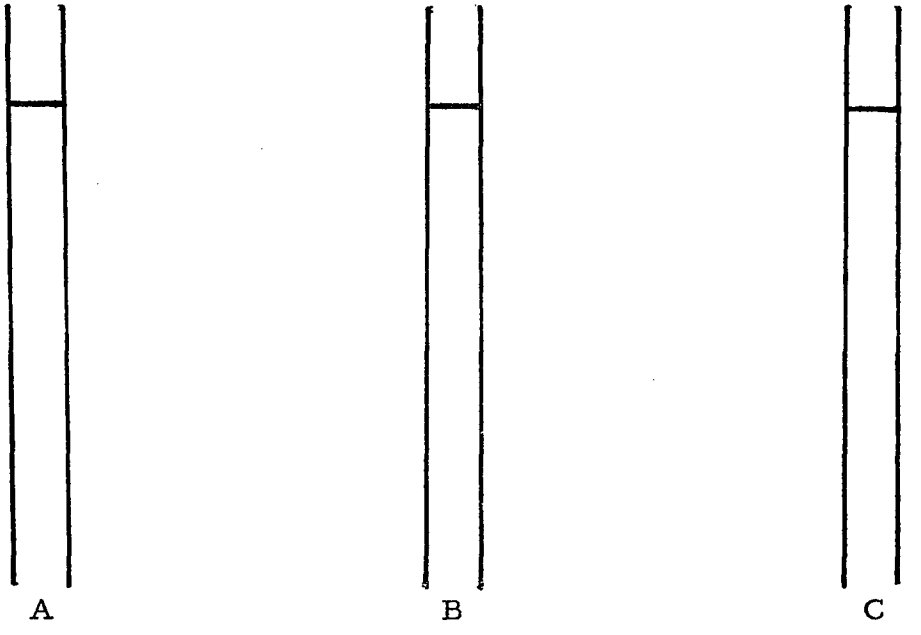

FIGURE 5. Estimation of the molecular weight of isocitrate dehydrogenase by gel filtration through Sephadex G-200. The molecular weights of marker proteins are plotted on a logarithmic scale against $K_{average}$ ($K_{average}$ as defined by Pharmacia is "the fraction of the stationary gel volume which is available for diffusion of a given solute species", which is calculated by the following equation: (Elution volume-void volume)/(total volume of packed bed-void volume)). The marker proteins used were: 1. ribonuclease A (13,700), 2. chymotrypsinogen A (25,000), 3. ovalbumin (43,000) and 4. aldolase (158,000). The $K_{average}$ for isocitrate dehydrogenase activities (both NAD and NADP) is indicated by a bar and corresponds to a molecular weight of 90,000.

FIGURE 5

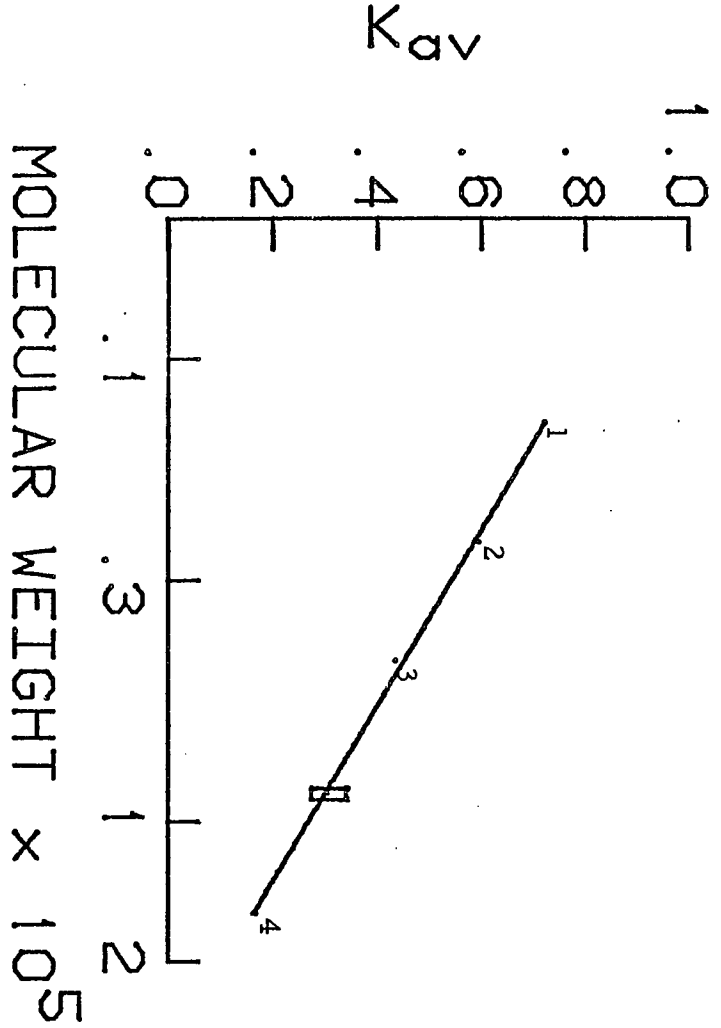

associated with a protein of approximate molecular weight of 90,000 (Figure 5).

Denaturation studies using different concentrations of urea (Table 4) and varying exposures to heat (Table 5) show the NAD-Icdh activity to be much more labile than the NADP-Icdh activity. Varying the amount of glycerol had a differential effect on the two coenzyme-specific activities. Both activities are effectively protected by 50% glycerol and moderately protected in 25% glycerol. In 10% glycerol only the NADP-Icdh activity was even partially preserved.

Inhibition studies with reduced pyridine nucleotides show that NADPH is far superior to NADH with respect to inhibiting the NAD- and NADP-Icdh activities (Table 6). This provides further evidence that the NAD-Icdh activity is a nonspecific activity of the NADP-Icdh.

Since both activities work in the forward and reversedirections, pH effects were studied in both directions. In the forward direction, decreasing pH has a greater effect on the rate of NADPH formation. This is shown in Table 7 by the ratio of the rates of NADPH to NADH formation. At the lowest pH (5.6) at which I was able to assay effectively, the ratio of activities (NADPH/NADH formation) was 3.4, while at the highest pH (8.2) the ratio was found to be 13.6. For the reverse reaction, i.e. the oxidation of both reduced coenzymes in the presence of HCO_3^-, $MnCl_2$ and α-ketoglutarate, increasing pH had a greater effect on NADPH oxidation. At the lowest pH studied (pH 5.8)

the ratio of activities (NADPH/NADH oxidation) was 81, while at the highest pH (7.8) the ratio was 7.6. It should be noted that when the reaction is run in reverse, optimal rates could not be established for NADH oxidation. The spectrophotometer used could not offset much more than 1.2 absorbance units (about 200 micromolar NAD(P)H). Thus, increased NADH may close the gap in the ratio of activities since the rate for NADPH was already maximal at 200 micromolar.

TABLE 4. Urea denaturation of NAD- and NADP-isocitrate dehydrogenase activities. Dry cell extracts were exposed to varying concentrations of urea for 30 minutes at 4 C. All assays were in 50mM Hepes (pH 7.3), 1mM $MnCl_2$, 10mM NAD or 0.4mM NADP and 5mM D,L isocitrate. After 30 minutes, treated extracts were pipetted into the assay mixture, thus resulting in a 15-fold dilution of the urea concentrations shown. All activities are in terms of micromoles of NAD(P)H formed/minute/ml of extract.

Urea(moles/liter)	NAD-activity	NADP-activity
0	0.138	1.190
2.0	0.019	1.003
2.5	0.011	0.939
3.0	0.005	0.682
3.5	0.000	0.271
5.5	0.000	0.143

TABLE 5. Heat denaturation of NAD- and NADP-isocitrate dehydrogenase activities. Dry cell extracts in varying concentrations of glycerol were exposed to a temperature of 50 C in a water bath for varying amounts of time. Assay solutions are identical to those in Table 4. Samples of the extracts were assayed at the time exposure indicated. Activities are in terms of micromoles of NAD(P)H formed/minute/ml of extract.

Extract	Exposure time(hrs)	NAD-activity	NADP-activity
50% glycerol(v/v)	0	0.144	0.990
	1	0.095	0.940
	2	0.093	0.940
	3	0.096	0.940
	4	0.093	0.900
25% glycerol(v/v)	0	0.094	1.030
	1	0.051	0.680
	2	0.057	0.680
	3	0.048	0.530
	4	0.042	0.530
10% glycerol(v/v)	0	0.089	0.930
	1	0.000	0.290
	2	0.000	0.190
	3	0.000	0.069
	4	0.000	0.000
0.01M Hepes(pH 7.3)	0	0.104	0.890
	1	0.000	0.062
	2	0.000	0.000

TABLE 6. Effects of reduced pyridine nucleotides on NAD- and NADP-isocitrate dehydrogenase activities. All enzyme assays are in 50mM Hepes (pH 7.3), 1mM $MnCl_2$, 10mM NAD or 0.4mM NADP and 5mM D,L isocitrate.

NAD-activity	Relative activity (%)
Control	100
+0.474mM NADH	33
+0.047mM NADH	104
+0.410mM NADPH	0
+0.041mM NADPH	14
NADP-activity	
Control	100
+0.474mM NADH	88
+0.410mM NADPH	47

TABLE 7. The effects of pH on the initial velocities of NAD- and NADP-isocitrate dehydrogenase activities. Activities were assayed in the forward and reverse reaction. In the forward reaction the assay included 50mM buffer, 1mM $MnCl_2$, 10mM NAD or 0.4mM NADP and 5mM D,L isocitrate. In the reverse reaction the assay included 67mM buffer, 1mM $MnCl_2$, 0.2mM NADH or NADPH, 67mM $KHCO_3$ and 7mM α-ketoglutarate. The zwitterionic buffers used were MES (pH 5.6-6.2), MOPS (pH 6.2-7.0), Hepes (pH 7.0-7.6) and Bicine (pH 7.6-8.2). All enzyme activities were measured on dry cell extracts purified 15-fold on a Sephadex G-200 gel, as described in Materials and Methods, and are recorded in terms of micromoles formed/minute/mg of protein.

pH	NADH formation	NADPH formation	Ratio of activities (NADPH/NADH)	NAD formation	NADP formation	Ratio of activities (NADP/NAD)
5.5	0.145	0.493	3.4	-	-	-
5.8	0.150	0.825	5.5	0.006	0.486	81.0
6.2	0.185	1.195	6.5	0.021	0.468	22.3
6.6	0.193	1.475	7.6	-	-	-
7.0	0.280	2.200	7.9	0.018	0.314	17.1
7.4	0.203	2.237	11.0	0.018	0.250	13.9
7.8	-	-	-	0.010	0.076	7.6
8.2	0.155	2.106	13.6	-	-	-

DISCUSSION

The NAD-dependent isocitrate dehydrogenase activity in extracts of lyophilized cells of Tetrahymena pyriformis with which we began our study has been found to be a nonspecific activity of the NADP-Icdh, albeit an unusual one. Although a scheme for complete purification of either coenzyme-specific activity has not been developed, it is clear from the separation techniques employed (Sephadex G-200, DEAE-Sephacel and Affi-Gel Blue chromatography; disc gel electrophoresis) that both activities reside in the same protein. The kinetic data supporting this conclusion show that both activities have an equal affinity for threo-D_s-isocitrate, prefer Mn^{+2} over Mg^{+2} at an equimolar concentration but differ in their affinity and inactivation for their respective coenzymes. The NAD-Icdh activity that was extracted and separated along with the NADP-Icdh activity shows none of the regulatory control with AMP, ADP or citrate that is associated with other NAD-Icdh (24, 39). Even the intriguing possibility of these enzymatic activities being part of a double-headed enzyme seems remote. The severe inhibition exerted on the NAD-Icdh activity by NADPH should preclude any reaction in the direction of NAD reduction since the proportional amounts of NAD/NADPH under the most favorable conditions were found to be 6:1 (22, 40). My results show no activity at an NAD/NADPH ratio of 25:1 and only 14% at a ratio of 250:1 (Table 6). This data casts doubt on any physiological role for

the nonspecific NAD-Icdh activity in cellular oxidations. Thus, the apparent greater susceptibility of this activity to urea and heat denaturation may reflect the fact that the NADP binding domain is separate from the NAD binding domain.

The kinetic data presented in Table 2 for the NADP-Icdh activity suggest that it is quite similar to other NADP-Icdhs from mammals (36, 37, 38). Furthermore, the molecular weight as determined by gel chromatography was 90,000 which is in agreement with values determined for the NADP-Icdhs of ox heart, beef and pig liver (41, 36, 42). This molecular weight for an NAD-Icdh would be considered unusually small in comparison (24, 38).

It is apparent from the results presented here that within T. pyriformis there is a single NADP-Icdh that is extractable from freeze-dried cells. Identical results have been found for whole cell homogenates, but they have not been presented in order to avoid duplication and unnecessary bulk. To some extent this work confirms the work of Vidal and Machado (43) on T. pyriformis. They found an NAD-Icdh activity that copurifies with the NADP-Icdh. Moreover, they were also not able to show the presence of any isozymes by disc gel electrophoresis. Although they did not characterize this NAD-activity, believing it to be completely unphysiological, they did find it to have a very high K_m for NAD (about five-fold higher than we have found).

Since the NADP-Icdh of T. pyriformis is known to be located in the mitochondrion, peroxisome and cytosol (15) it is interesting to note that no isozymes of this enzyme was found in the work presented here or that of Vidal and Machado (43). However, Nanney et al. (44) have compiled a large amount of data characterizing different strains of Tetrahymena by their isozymes of NADP-Icdh, as well as other enzymes, using starch gel electrophoresis. Their method of electrophoresing and staining for enzyme activity rests on very dubious procedures. Running time in a Tris-citrate buffer was 17 hours at 75 milliamperes and 200 volts. Citrate is a peculiar choice for a buffer since their homogenate should contain aconitase activity. Electrophoresing NADP-Icdh in the probable presence of its substrate (isocitrate) may have variable effects on the mobility of this enzyme, if some enzyme binds isocitrate and some does not. Both the pH and the amount of time involved in staining the gel for enzyme activity suggest a considerable loss of enzyme activity over the 17 hours of electrophoresis. It should not be necessary to pull the NADP-Icdh reaction to the right by running at pH 9; nor should it take "several hours" to achieve adequate staining. Also, the possibility of a monomer-dimer equilibration has not been considered at all. Since the mammalian enzyme has been noted to occur in both forms without any apparent effects on its enzyme activity (41) it should not be ignored for Tetrahymena.

If the NAD-Icdh activity we have measured is, in fact, an unphysiological, nonspecific activity originating from the NADP-Icdh, as Vidal and Machado propose (43), then what enzyme is responsible for the oxidation of isocitrate that has been observed in the mitochondrion of T. pyriformis (15,28)? It should be recalled that it is this oxidation, or rather a failure to achieve complete isocitrate oxidation, that I proposed as a cause for isocitrate accumulation and eventual exportation from the mitochondria for use in the glyoxylate cycle. Since a small shoulder of NADP-Icdh activity occurs in the mitochondrial fractions (15) of density gradients, it may be sufficient to meet the needs of isocitrate oxidase activity of mitochondria if there is a transhydrogenase activity within the mitochondria: $NADPH + NAD(\overset{+}{-}ATP) \rightleftharpoons NADP + NADH(\overset{+}{-}(ADP+P_i))$ In pig heart the high levels of mitochondrial NADP-Icdh and transhydrogenase have been used to account for the high levels of isocitrate oxidase activities there (37). However, I found no direct transhydrogenase activity. Similarly, it seemed plausible that a phosphatase could act on NADPH to form NADH, and account for the oxygen uptake upon isocitrate administration to mitochondria. This enzyme also was not found. Thus, I still have no way to reconcile the isocitrate oxidase activity known to be present in T. pyriformis mitochondrion (15,28), nor have I presented here any direct experimental support for the proposition that isocitrate exit from the mitochondria

is necessary for gluconeogenesis through the glyoxylate bypass reactions.

On the other hand, the results from Table 7 indicate that the reverse reaction of NADP-Icdh could act to synthesize isocitrate from α-ketoglutarate. In this reductive carboxylation of α-ketoglutarate, either coenzyme (NADH or NADPH) is able to supply the requisite reducing power. Since it is now known that the T. pyriformis peroxisome has a β-oxidation system that generates NADH (19), it appears possible that the nonspecific isocitrate dehydrogenase reductive carboxylation using NADH and CO_2 may be important in the synthesis of isocitrate for the glyoxylate cycle and gluconeogenesis. The relatively large amount of NADP-Icdh within the peroxisome of T. pyriformis (40% or more of the cell's total), as shown by Muller et al. (15), may represent a selective advantage of the peroxisome in that it may be used to synthesize isocitrate rather than to act in competition with isocitrate lyase for the consumption of isocitrate. I will return to this possibility in chapter III, which is antagonistic to the proposition that isocitrate is exclusively synthesized in the mitochondria and any isocitrate use outside of it must necessarily be dependent on mitochondrial metabolism.

At this point I still believed there was an NAD-Icdh in T. pyriformis that was responsible for the previously observed isocitrate oxidase activity in mitochondria, and that this enzyme con-

trolled the flux out of the mitochondria for gluconeogenesis. The next chapter deals with the discovery of the NAD-Icdh of T. pyriformis and its putative role in regulating isocitrate metabolism outside of the mitochondria.

CHAPTER II

THE NAD-ISOCITRATE DEHYDROGENASE OF

TETRAHYMENA PYRIFORMIS

INTRODUCTION

A new method of approach was in order, if I was ever to associate the 'isocitrate oxidase' activity with a mitochondrial NAD-isocitrate dehydrogenase. Muller et al. (15) had already made this claim but there was no clear basis for the assertion. In fact, Vidal and Machado were (and are) convinced that Tetrahymena pyriformis did not have an NAD-Icdh, as appears to be the case for many procaryotes (43, 45, 46, 47). My own results agreed with those of Vidal and Machado for both fresh whole cell homogenates (total disruption, with no subcellular organelles spared) and extracts of freeze-dried cells. If there was an NAD-Icdh, it was extremely labile. I reasoned that at least partial maintenance of the subcellular integrity was the only way to conserve this enzymatic activity without spending even more effort and time on the in vitro conditions necessary for its preservation. Both Kobiyashi and Muller, Hogg and deDuve (28, 15) had assayed 'isocitrate oxidase' in what they felt were well-preserved mitochondria. Thus, I approached the problem of demonstrating an NAD-Icdh by its particulate (mitochondrial) nature.

Breaking cells by means of one or two passages through a coarse sintered glass filter had been shown to yield relatively undamaged subcellular particles (7, 15, 48). It was this technique that became the cornerstone of all subsequent subcellular fractionations

that would yield a legitimate and specific NAD-Icdh from T. pyriformis. I was aware that previous use of these particles had not succeeded in helping to identify an NAD-Icdh (15, 21). However, I was fortunate to be privy to precise methodological details regarding those experiments since I worked with one of the coauthors (15). He emphasized that there was a significant amount of time that elapsed (6 to 12 hours) between breaking of the cells and actual performance of the assays (J.F. Hogg, personal communication). Thus, I gained from prior failures, and would assay only fresh particulate preparations (obtained within three hours of cell disruption).

There still remained a very significant interpretational problem. Once I accepted the nonspecific nature of the NAD-Icdh activity I had been studying, how could I distinguish whatever NAD-Icdh activity I might find from a simple nonspecific NADP-Icdh activity? Moreover, about 50% of the total cellular NADP-Icdh had been found to be specifically associated with subcellular particles (15, 21, 20), thus making any claims to finding the NAD-Icdh fraught with ambiguity. However, characterization of the nonspecific activity had shown little or no activity at NAD concentrations of 1mM or less. Since, to the best of my knowledge, there is no NAD-Icdh that has a K_m of even one-half that concentration (1mM), enzyme activity found at 1mM or less should be a minimal criterion.

Further clarification of this T. pyriformis NAD-Icdh did

finally require a fairly sophisticated separation procedure. Once it was established as an NAD-linked isocitrate dehydrogenase, and marked as purely mitochondrial, I was able to delve into its potential control over isocitrate metabolism with respect to gluconeogenesis.

MATERIALS AND METHODS

Growth and harvesting of cultures was the same as described in the Materials and Methods section in chapter 1. Instances where there were minor variations in the growth conditions will be individually noted and details of those differences will be described.

Cell disruption. After cells are resuspended in dilute Ringer phosphate solution, they are washed twice in cool (10-15°C) 0.25M D-mannitol by centrifugation for 3 minutes at 1000 rpm (250 x g) in an International centrifuge. After the last washing 0.25M D-mannitol was added to bring the cell concentration to 3-5% (v/v) as determined by centrifugal packing at 1000 x g in a Constable protein tube cell suspension was then placed in ice for 5-10 minutes. Cellular disruption was achieved by passage of the chilled cell suspension through a sintered glass filter (SF 113, pore size 20 to 30 microns, obtained from Laboratory Glassblowers Co.) under light suction (7). Two passages always resulted in complete breakage, as determined by examination under a phase contrast microscope. Most importantly the structural integrity of subcellular particles seems to be preserved better by this method than all others tried (7, 48).

Subcellular fractionation methods. Fractionation of the cell homogenate into particulate and soluble fractions was accomplished by centrifuging the homogenate at 25,000 x g for 10 minutes in a pre-

cooled (5°C) Sorvall RC-2 centrifuge with an SS-34 rotor. The supernatant was transferred to a clean centrifuge tube, and constituted the soluble fraction. The pellet was suspended into ice cold 0.25 M D-mannitol equal to half the volume of the supernatant, and constituted the particulate fraction.

Fractionation of the homogenates in a discontinuous sucrose density-gradient was performed to obtain organellar separations. A discontinuous sucrose density-gradient was prepared by pipetting into a 38ml polyallomer centrifuge tube (1" x 3 1/2") 4ml each of a 50%, 48%, 46%, 44%, 42%, and 40% (w/w) sucrose solution, in that order, on top of a 7ml cushion of 60% (w/w) sucrose solution. Each gradient was allowed to stand for 4-5 hours at 0-5°C before 6ml of freshly prepared homogenate was layered on top of the gradient. The gradient tube was then centrifuged in a precooled SW27 rotor in a Beckman Model L-2 (50) ultracentrifuge operated at 26,000 rpm (120,000 x g) for 2 hours at 5°C. After centrifugation a 4ml volume was removed from the top of the gradient and marked fraction 9. The bottom of each gradient tube was then punctured with a 21 gauge needle and eight fractions were collected dropwise; the first fraction was 5ml in volume, and the next seven were 4ml each. Thus, fractions 2-8 represent 2ml above and 2ml below each successive density interface, with higher numbers representing lower densities. All densities were determined with a Bausch and Lomb Refractometer (Abbe 3L) on

an equivalent gradient run with just 6ml of 0.25M D-mannitol.

For much of the work presented in this chapter, the peak mitochondrial fraction (#5), which contains the interface between 46 and 44% (w/w) sucrose was processed further. After mixing fraction 5 with two volumes of ice-cold 0.25M D-mannitol, I was able to pellet virtually all of the NAD-Icdh by centrifugation for ten minutes at 25,000 x g in a Sorvall RC-2 centrifuge with an SS-34 rotor. The pellet could then be resuspended in 50% (v/v) glycerol and stored for at least three weeks at -20°C without any loss in activity. Storage for one year in 50% glycerol at -20° C left about 40% of the original NAD-Icdh activity.

Enzyme assays. NAD-linked isocitrate dehydrogenase was assayed by a modification of the method of Kornberg (29). Activity was routinely measured in 67mM potassium phosphate buffer (pH 7.0), 1mM $MnCl_2$ and 0.067% (v/v) Triton X-100. Variations in the concentrations of NAD, threo-D_s-isocitrate and in the identity and concentration of adenine nucleotides accompany the Tables and Figures. NADP-Icdh was measured in 67mM potassium phosphate buffer (pH 7.0), 0.40 mM NADP (or as indicated), 1mM $MnCl_2$ and 0.067% (v/v) Triton X-100; the increase in absorbance at 340nm was followed after addition of threo-D_s-isocitrate or D,L isocitrate up to 5mM (29). Catalase was assayed by a modification of the method of Luck (49). Activity was measured in 67mM potassium phosphate, pH 7.0, 12.5mM H_2O_2 and

0.067% (v/v) Triton X-100; the decrease in absorbance at 240nm was measured upon addition of enzyme. Succinate dehydrogenase was measured in 67mM potassium phosphate, pH 7.4, 0.033mM 2,6 dichlorophenolindophenol, 1mM phenazine methosulfate, 2mM KCN and 0.067% (v/v) Triton X-100; the decrease in absorbance at 600nm was measured upon addition of sodium succinate to 20mM (15). Citrate synthase was assayed by the method of Dixon and Kornberg (50). Its activity was measured in 70mM Tris-HCl buffer, pH8.0, 3mM $MgCl_2$ and 50 uM acetyl-CoA; the reaction was started by the addition of sodium oxaloacetate to 0.2mM and a decrease in absorbance at 232nm was followed. Fumarase (51) was measured in 100 mM potassium phosphate, pH 7.4, and 0.067%(v/v) Triton X-100; the increase in absorbance at 250nm was followed upon addition of sodium L-malate to 5mM. Glutamate dehydrogenase (52) was assayed in 67mM potassium phosphate, pH 7.4, 50mM NH_4Cl, 0.5mM KCN, 0.15mM NADH, 0.20mM ADP and 0.067% (v/v) Triton X-100; the decrease in absorbance at 340nm was measured after addition of buffered α-ketoglutaric acid to 6.67mM. Acid phosphatase was assayed by the method of Torriani (53), which employs p-nitrophenylphosphate as the substrate. Protein was determined as described in the Materials and Methods section of chapter 1.

Materials. Ultra-pure sucrose (density gradient grade) was purchased from Schwarz/Mann. $MnCl_2$ and $MgCl_2$ were from Fisher

Scientific Co. KCN, NaOH, H_2O_2 and KCl were purchased from J.T. Baker Chemical Co. The yeast extract was from Baltimore Biological Laboratory. The Triton X-100 was from Bio-Rad Laboratories. Proteose-peptone was purchased from Difco Laboratory. Acetyl-CoA was prepared by the method of Stadtman (54). All other reagents were obtained from Sigma Chemical.

RESULTS

At NAD concentrations above 2 or 3mM there is a significant amount of isocitrate dehydrogenase activity that originates from the enzyme in Tetrahymena pyriformis which has the much higher affinity for NADP (See chapter 1). Determining whether or not an NAD-specific isocitrate dehydrogenase exists in these cells could be obscured by this nonspecific activity. In order to measure only the NAD-specific enzyme, two devices were used:

1. Based on the assumption that a T. pyriformis NAD-Icdh is particle-bound (as are all other eucaryotic NAD-Icdhs), approximately one-half of the NADP-Icdh, along with its accompanying nonspecific NAD-activity that is located in the soluble portion of the cell (15,20,21) can be eliminated by sedimenting the homogenate at 25,000 x g for ten minutes. Thus, decanting off the supernatant effectively removes 50% or more of the interfering NADP-Icdh.
2. Assaying the resuspended particle pellet at 1mM NAD should eliminate more than 80% of the nonspecific activity (when the K_m=4mM, as reported in chapter 1) found in the sedimented particle.

Table 8 shows that centrifugation at 250,000 g-minutes sediments enzyme activities associated with mitochondria and perox-

isomes. Citrate synthase and succinate dehydrogenase are attributed to the mitochondria, while catalase and lactate oxidase are found in the peroxisome of T. pyriformis (15). Since all of these known particulate enzymes are found exclusively or predominantly (catalase- 92% particulate:8% soluble) in the pellet of this relatively simple fractionation technique, it is clear that the particulate nature of mitochondrial and peroxisomal enzymes is not disrupted. Thus, the NAD-Icdh activity, at variable NAD concentrations, can be evaluated with respect to its particulate nature. At a high NAD concentration (10mM) a recovery pattern identical to that of the NADP-Icdh is found. At 1 or 0.1mM NAD the recovery pattern becomes characteristically particulate. Using the same separation procedure, I found a substantial variation in particulate NAD-Icdh activity with respect to the age of the culture. The specific activity exhibits a peak at two days of growth and then falls precipitously (Figure 6). Soluble specific activity, presumably the NADP-specific enzyme, remains essentially constant.

Table 9 compares the effects of reduced pyridine dinucleotides (NADH and NADPH) on particulate and soluble isocitrate dehydrogenase activities from cells harvested after two days (log phase). Since NADPH had little or no inhibitory effect on the particle-bound NAD-Icdh activity, this was interpreted as confirmation of the presence of an NAD-Icdh. Furthermore, NADPH inhibition of the soluble NAD-

TABLE 8. Particulate vs. soluble distribution of mitochondrial and peroxisomal marker enzymes in two day cells (log phase). Methods of cell disruption and particulate-soluble fractionation are described in Materials and Methods section.

Enzyme	Distribution		Recovered Activity
	Soluble %	Particulate %	%
Catalase	8	92	102
Lactate oxidase	0.5	99.5	96
succinic dehydrogenase	0	100	94
citrate synthase	2	98	95
NADP-Icdh	54	46	100.9
NAD-Icdh			
(a) NAD=10mM	52	48	101.8
(b) NAD=1mM	8.8	91.2	106.8
(c) NAD=0.1mM	0	100	133

FIGURE 6. Age versus specific activity of NAD-specific isocitrate dehydrogenase from particulate (△) and soluble (□) fractions. NAD-Icdh was assayed in the presence of 50mM potassium phosphate, pH 7.0, 1mM $MnCl_2$, 1mM NAD, 0.067% (v/v) Triton X-100 and 1mM threo-D_s-isocitrate.

FIGURE 6

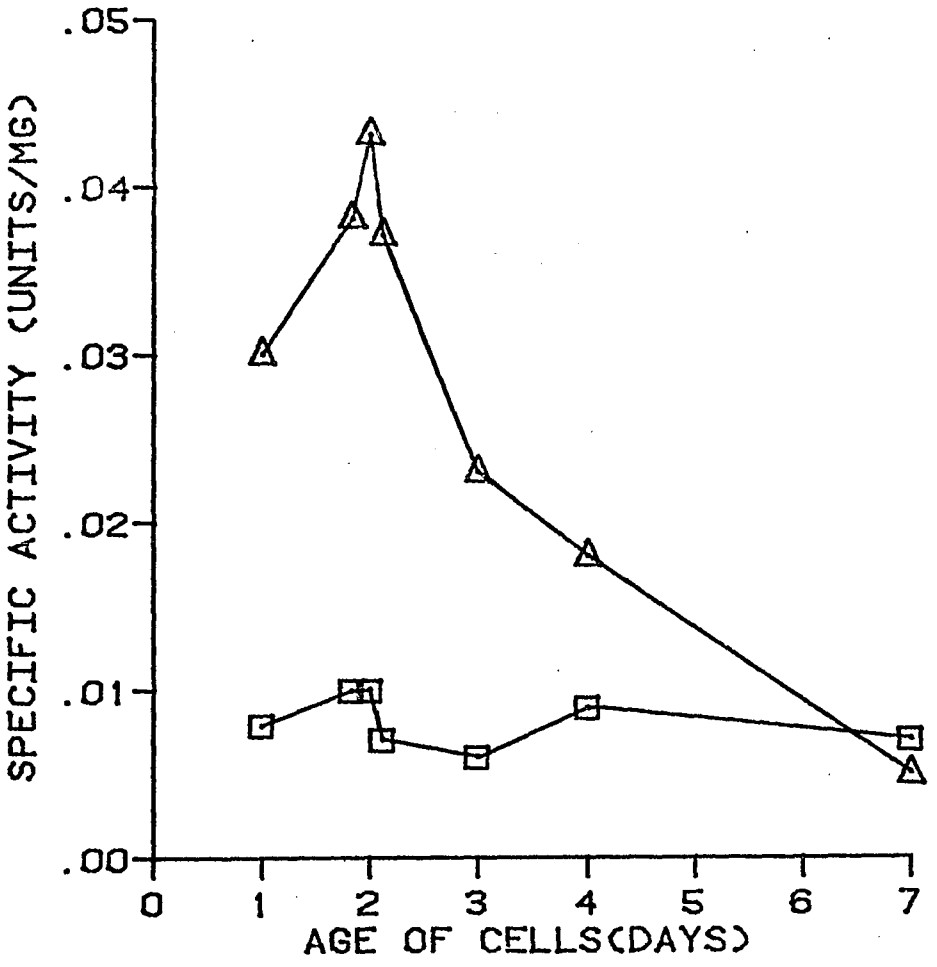
.05
.04
.03
.02
.01
.00
SPECIFIC ACTIVITY (UNITS/MG)
0
1
2
3
4
5
6
7
AGE OF CELLS(DAYS)

TABLE 9. Effect of reduced pyridine dinucleotides on NAD- and NADP-isocitrate dehydrogenase activities from particulate-soluble fractionation as described in Materials and Methods section. All concentrations are in millimolar units, and activities (total activity in the fraction) are listed in terms of micromoles of NAD(P)H formed/minute.

A. Particulate

[NAD]	[NADP]	[NADH]	[NADPH]	Total Activity
10	0	0	0	1.356
10	0	0	0.3	0.958
1	0	0	0	0.904
1	0	0	0.3	0.886
1	0	0.3	0	0.304
0.2	0	0	0	0.467
0.2	0	0.3	0	0.000
0.2	0	0	0.3	0.481
0	0.2	0	0	4.703
0	0.2	0	0.3	2.801
0	0.2	0.3	0	4.248

B. Soluble

10	0	0	0	1.230
10	0	0	0.1	0.289
10	0	0.1	0	1.158
1	0	0	0	0.253
1	0	0	0.1	0.000
1	0	0.3	0	0.198
0	0.2	0	0	7.380
0	0.2	0	0.3	3.760
0	0.2	0.3	0	6.567

Icdh activity confirms that this activity originates from NADP-Icdh.

The possibility that this particulate NAD-Icdh was not mitochondrial still hampered interpretation of the data. By employing a discontinuous sucrose density gradient, based on the median densities of mitochondria and peroxisomes of T. pyriformis as worked out by Muller et al. (15), I was able to show quite conclusively that this NAD-Icdh was localized in the mitochondria.

In order to localize the mitochondrial position in the gradient, marker enzymes were assayed in the nine fractions that composed the gradient (See Materials and Methods). Glutamate dehydrogenase, fumarase, succinate dehydrogenase and malate dehydrogenase mark mitochondria. Catalase marks peroxisomes and acid phosphatase places the lysosomes. NADP-Icdh is known to be mitochondrial, peroxisomal and soluble in T. pyriformis (15). For both log and stationary phase cells, fraction 5 is the cleanest mitochondrial fraction, as indicated by distribution patterns (Figures 7 and 8) and the relative specific activities of its markers (Table 10). The purest peroxisomes (See catalase) are found in fractions 2 (stationary phase) and 3(log phase). The purest lysosomes (See acid phosphatase) are found in fraction 7 in both log and stationary phase cells, but the bulk of the acid phosphatase activity in stationary phase cells is found in fraction 8. The substantial accumulation of all enzymes, as well as protein in fraction 8 of stationary phase cells

FIGURE 7. Enzyme and protein distributions in a discontinuous sucrose density gradient for log phase cells (harvested after 35 to 43 hours). Vertical bars represent the standard deviation. (a) glutamate dehydrogenase-101.3$\pm$ 9.3% recovered (3 trials), (b) fumarase-104.9$\pm$ 7.4% recovered (3 trials), (c) malate dehydrogenase-90.5% recovered (1 trial), (d) succinate dehydrogenase-89.1% recovered (1 trial), (e) NADP-linked isocitrate dehydrogenase-105.3% recovered (1 trial), (f) catalase-98.0$\pm$ 7.4% recovered (3 trials), (g) acid phosphatase-103.6$\pm$12.7% recovered (3 trials) and (h) protein-92.3$\pm$4.6% recovered (5 trials)

FIGURE 7

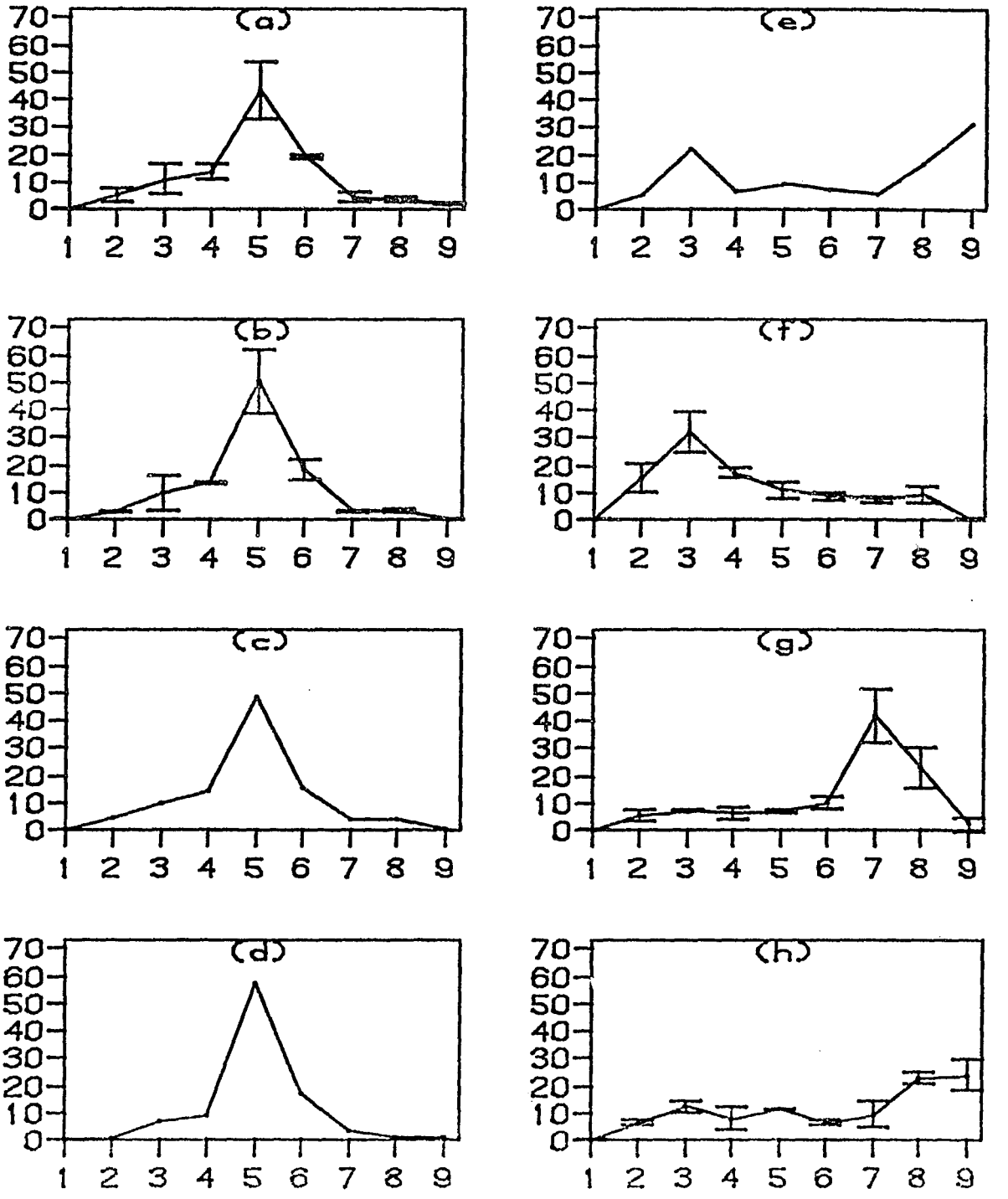

FIGURE 8. Enzyme and protein distribution in discontinuous sucrose density gradient for stationary phase cells (harvested after 135 to 141 hours). Vertical bars represent the standard deviation. (a) glutamate dehydrogenase-110.6±1.4% recovered (3 trials), (b) fumarase-93.8±6.2% recovered (3 trials), (c) malate dehydrogenase-85.6±10.4% recovered (3 trials), (d) succinate dehydrogenase-87.8±9.6% recovered (3 trials), (e) NADP-isocitrate dehydrogenase-108.7±8.3% recovered (3 trials), (f) catalase-101.5±5.9% recovered (4 trials), (g) acid phosphatase-92.3±7.6% recovered (3 trials) and (h) protein-87.7±6.3% recovered (5 trials).

FIGURE 8

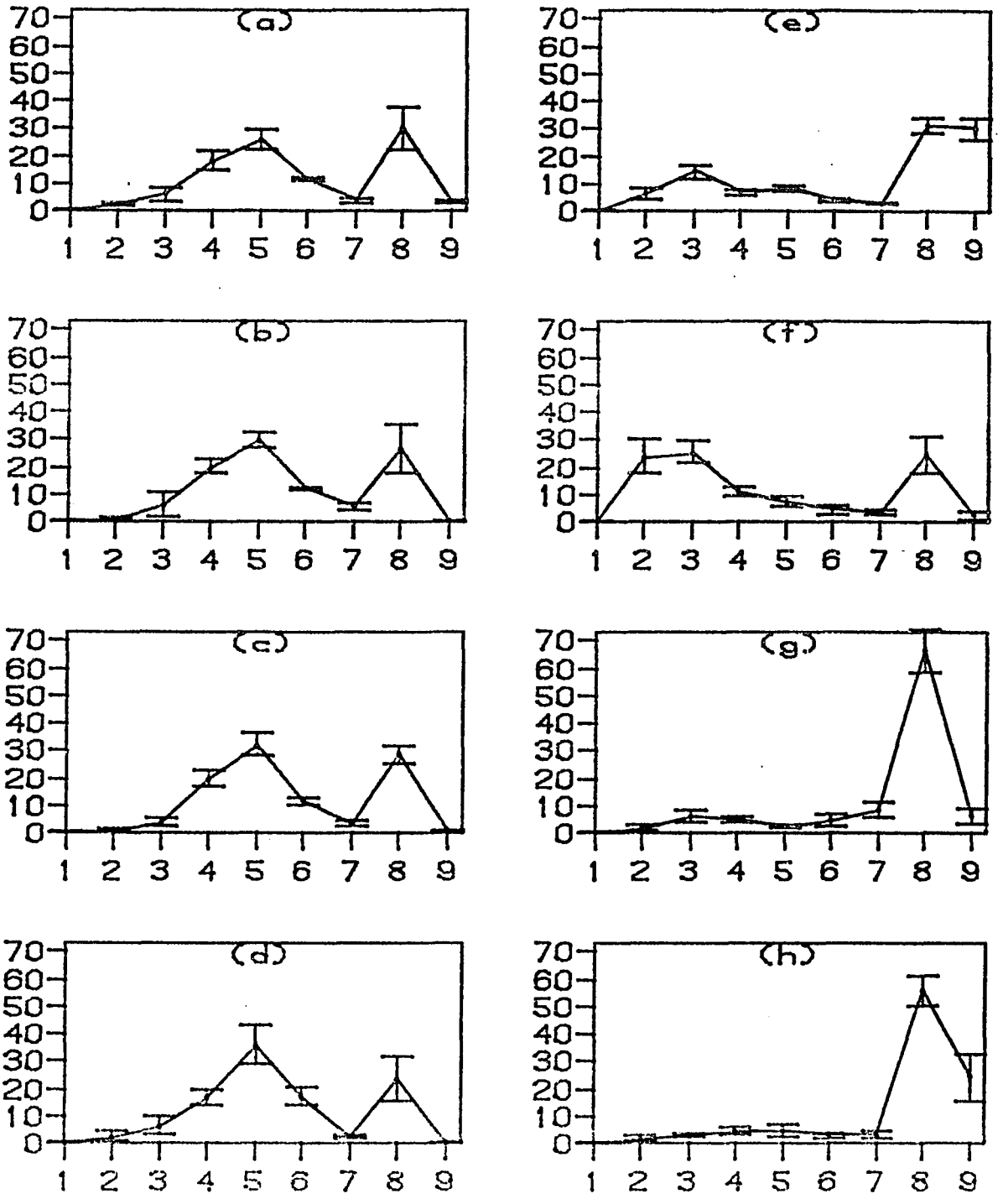

TABLE10. Specific Activity of marker enzymes from gradient fractions (All activities listed in umoles/min/(mg of protein) except Acid Phosphatase which is in terms of O.D.420/min/(mg of protein) with ± S.D. where possible)

	FRACTION NUMBER									
Enzyme	1	2	3	4	5	6	7	8	9	Homo-genate
* 1 GdH-L-3	0	0.027 ±0.012	0.052 ±0.016	0.168 ±0.008	0.394 ±0.031	0.291 ±0.067	0.048 ±0.013	0.018 ±0.003	0.014 ±0.008	0.095 ±0.022
* 2 GdH-S-4	0	0.037 ±0.011	0.045 ±0.013	0.092 ±0.010	0.133 ±0.019	0.100 ±0.012	0.038 ±0.014	0.013 ±0.015	0.001 ±0.001	0.015 ±0.003
* 3 F-L-3	0	0.048 ±0.003	0.061 ±0.025	0.220 ±0.031	0.507 ±0.067	0.311 ±0.083	0.048 ±0.009	0.017 ±0.004	0	0.098 ±0.011
* 4 F-S-4	0	0.014 ±0.018	0.085 ±0.025	0.240 ±0.043	0.523 ±0.158	0.313 ±0.031	0.166 ±0.069	0.020 ±0.005	0	0.036 ±0.002
* 5 MdH-L-1	0	2.47	4.66	8.48	27.63	13.02	3.87	1.03	0.09	6.35
* 6 MdH-S-2	0	1.03 ±0.07	2.78 ±0.12	5.30 ±0.73	27.83 ±0.59	15.94 ±1.32	3.95 ±0.34	0.89 ±0.13	0.05 ±0.04	2.26 ±0.93
* 7 IcdH-L-2	0	0.189 ±0.011	0.393 ±0.080	0.128 ±0.008	0.130 ±0.003	0.105 ±0.003	0.096 ±0.006	0.067 ±0.012	0.381 ±0.066	0.210 ±0.009
* 8 IcdH-S-3	0	0.348 ±0.034	0.346 ±0.051	0.270 ±0.035	0.203 ±0.017	0.180 ±0.014	0.087 ±0.018	0.051 ±0.028	0.379 ±0.016	0.158 ±0.009
* 9 Cat-L-3	0	371.4 ±110.8	837.3 ±131.8	214.7 ±36.9	140.7 ±42.9	158.3 ±44.3	176.3 ±19.3	63.2 ±19.9	2.1 ±2.2	146.7 ±28.9
*10 Cat-S-3	0	288.8 ±63.8	183.3 ±38.3	102.0 ±31.6	91.9 ±35.6	140.3 ±41.6	209.0 ±62.5	110.0 ±12.5	3.1 ±2.3	51.1 ±11.8
*11 A.P.-L-2	0	1.018 ±0.204	0.762 ±0.032	1.410 ±0.040	0.696 ±0.060	2.285 ±0.646	4.809 ±0.981	0.728 ±0.104	0.045 ±0.030	1.087 ±0.303
*12 A.P.-S-2	0	1.763 ±0.112	1.959 ±0.087	1.119 ±0.101	0.556 ±0.074	1.565 ±0.210	4.063 ±0.489	0.878 ±0.132	0.136 ±0.017	0.822 ±0.263

* 1 - glutamate dehydrogenase - Log phase cells - 3 trials
* 2 - glutamate dehydrogenase - stationary phase cells - 4 trials
* 3 - fumarase - Log phase cells - 3 trials
* 4 - fumarase - stationary phase cells - 4 trials
* 5 - malate dehydrogenase - Log phase cells - 1 trial
* 6 - malate dehydrogenase - stationary phase cells - 2 trials
* 7 - NADP-Linked isocitrate dehydrogenase - Log phase cells - 2 trials
* 8 - NADP-Linked isocitrate dehydrogenase - stationary phase cells - 3 trials
* 9 - Catalase - Log phase cells - 3 trials
*10 - Catalase - stationary phase cells - 3 trials
*11 - Acid phosphatase - Log phase cells - 2 trials
*12 - Acid phosphatase - stationary phase cells - 2 trials

only will not be discussed here, but will be covered comprehensively in chapter 3 where electron microscopic data will be compared with the enzyme distributions.

Figures 9 and 10 are especially illustrative of the nonspecific NADP-Icdh in log phase cells. At 10mM NAD, the recovery profile of NAD-Icdh (Figure 9) is identical to that of NADP-Icdh (Figure 10). When the NAD concentration is decreased, the distribution pattern begins to mimic the pattern of the mitochondrial markers in Figure 7, and show that the true NAD-Icdh is mitochondrial.

This mitochondrial NAD-Icdh was also activated by ADP. Figure 11 illustrates this activation by ADP on the specific activity. As would be expected should fraction 5 be the purest mitochondrial fraction and NAD-Icdh located there, the greatest activation by ADP was found to be in that fraction.

Since fraction 5 is the major mitochondrial fraction and the fraction richest in NAD-Icdh, it was used to characterize the NAD-Icdh. However, if the NAD-Icdh remains in the sucrose solution from the gradient, its activity diminishes rapidly after 6-7 hours. Thus, all subsequent studies for characterization of this enzyme were done with a resuspension of fraction 5 in 50% aqueous glycerol, as described in Materials and Methods of this chapter. Storage of this fraction in 50% glycerol at -20°C showed no loss of NAD-Icdh

FIGURE 9. Distribution of NAD-isocitrate dehydrogenase, measured at various NAD concentrations, in a sucrose density gradient. Fractionation procedures are described in Materials and Methods. Enzyme assay is the same as in Figure 6 except NAD= 0.2mM (Δ); 1 mM (□) and 10mM (no symbol).

FIGURE 9

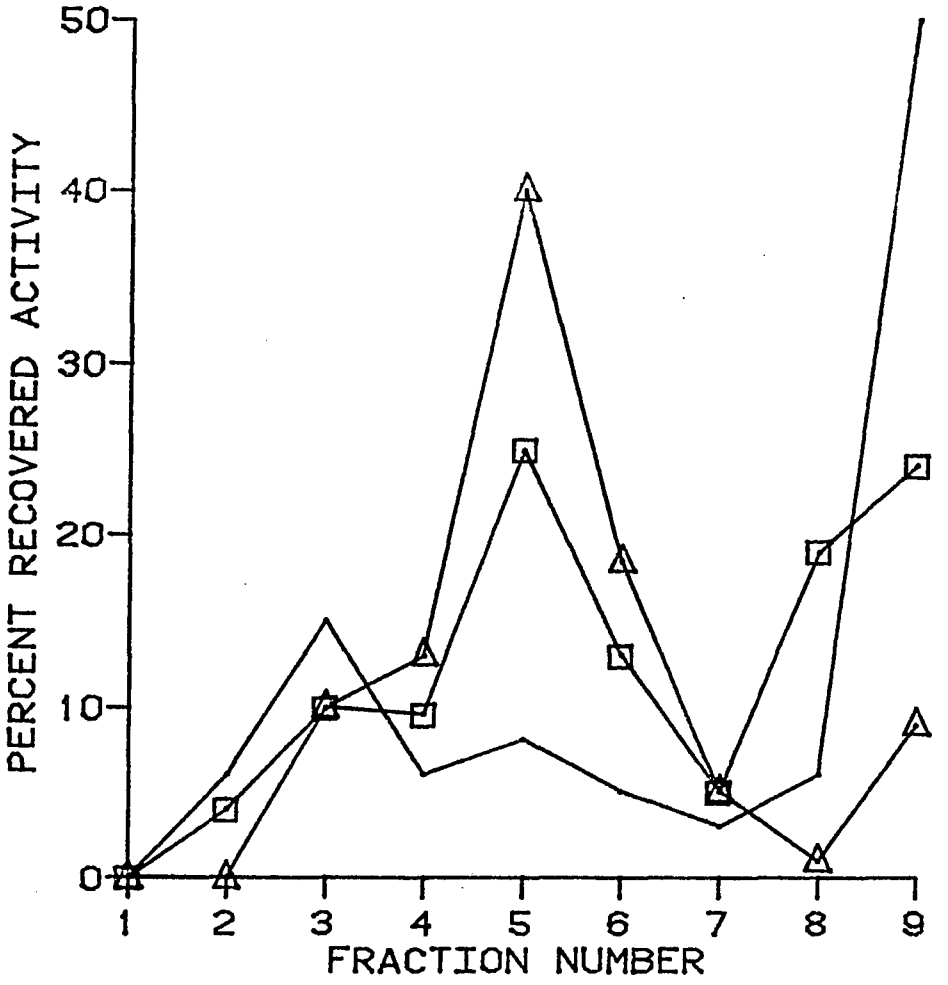
50
40
30
20
10
0
PERCENT RECOVERED ACTIVITY
1
2
3
4
5
6
7
8
9
FRACTION NUMBER

FIGURE10. Distribution of NADP-isocitrate dehydrogenase in a sucrose density gradient. Fractionation procedures are described in Materials and Methods. Enzyme assay methods were identical to those in Figure 6, except NADP at 0.4mM replaces NAD.

FIGURE 10

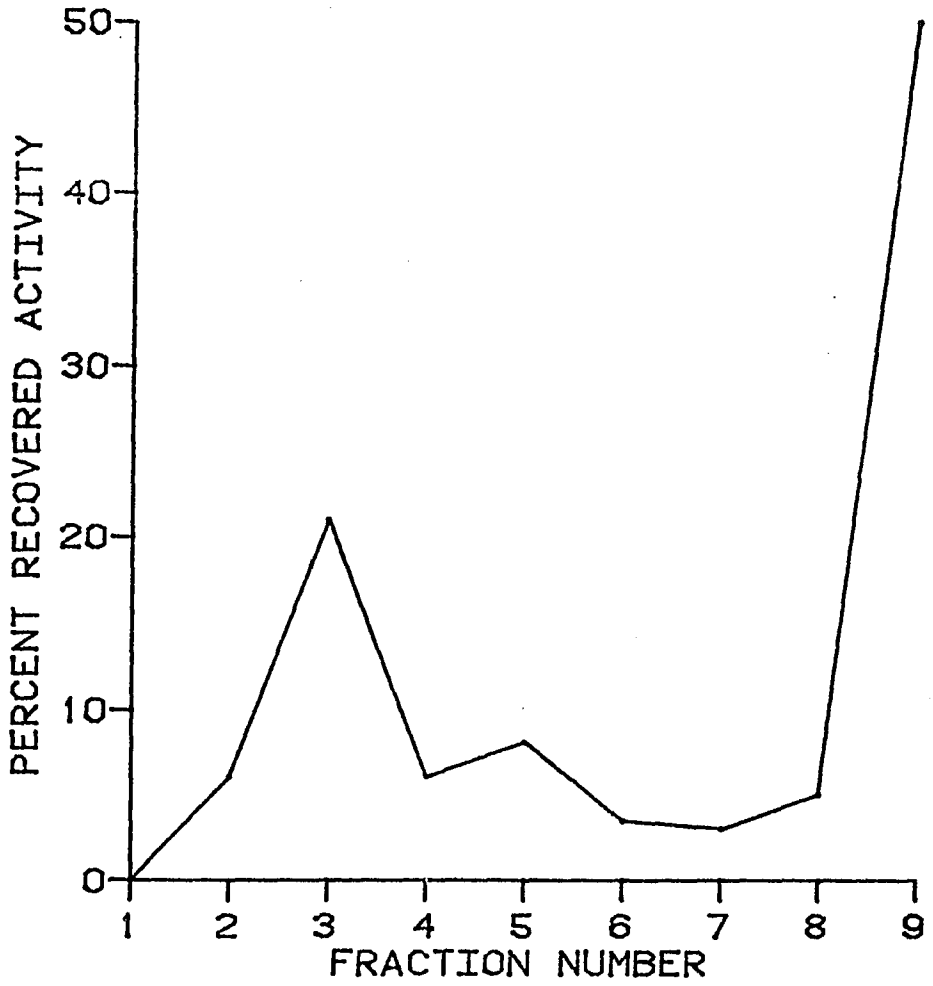
50
40
30
20
10
0
PERCENT RECOVERED ACTIVITY
1
2
3
4
5
6
7
8
9
FRACTION NUMBER

FIGURE 11. Distribution of NAD-isocitrate dehydrogenase specific activities in a sucrose density gradient with (Δ) and without (□) ADP. Enzyme assay is the same as in Figure 6 except ADP (0.2mM) is added to one set (Δ). Specific activity in terms of micromoles of NADH formed/minute/mg of protein.

FIGURE 11

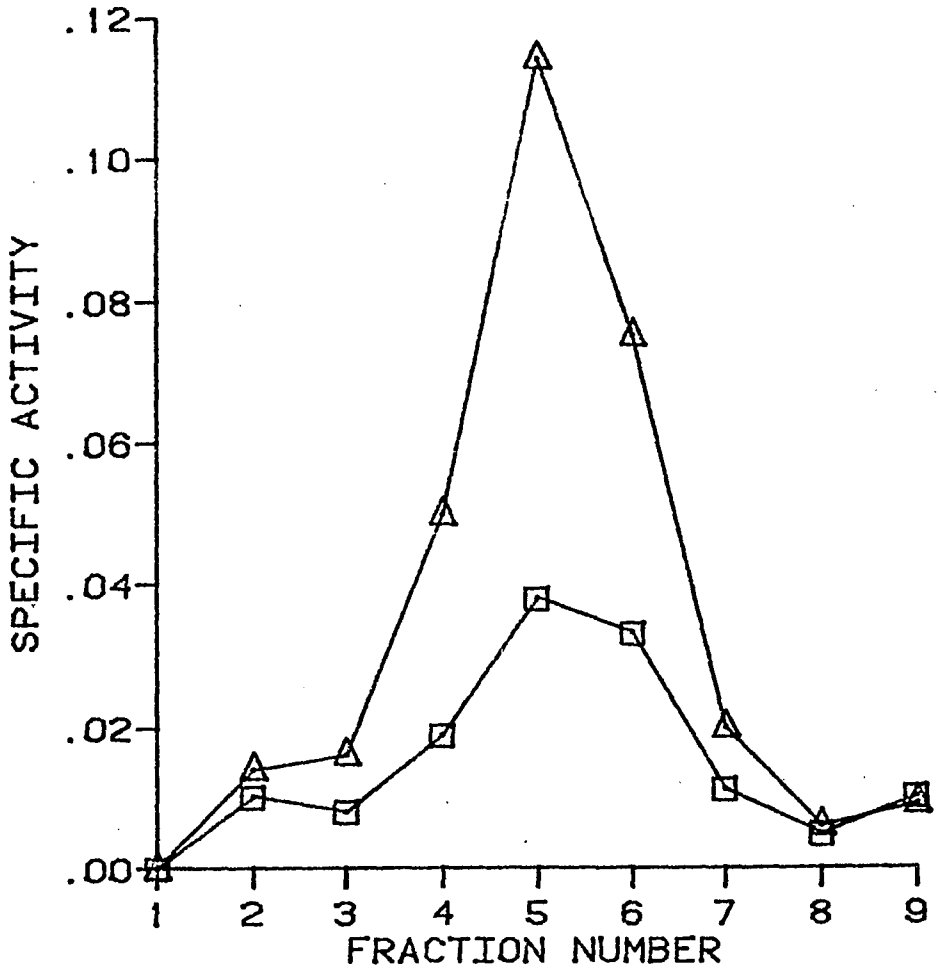
.12
.10
.08
.06
.04
.02
.00
SPECIFIC ACTIVITY
1
2
3
4
5
6
7
8
9
FRACTION NUMBER

activity for up to three weeks. After two months about one-half of its activity was lost, and after one year38% of the original activity was retained.

This stabilized fraction 5 preparation of NAD-Icdh shows stimulation with either AMP, ADP or ATP. Table 11 compares the stimulations by AMP, ADP and ATP. Their order of stimulation of this enzyme is ADP AMP ATP. It does appear that ATP will inhibit the ADP response. However, addition of increased levels of $MnCl_2$ abolishes the ATP inhibition. Citrate has also been found inhibitory to the ADP response, but its inhibitory effect was also abolished by increasing $MnCl_2$ concentration. These effects have been observed with $MgCl_2$, but have not been tabulated here since they are based on one experiment. Generally Mg^{+2} seems to have the same qualitative effect as Mn^{+2} on particulate NAD-Icdh activity, except at equimolar concentration (1mM) Mn^{+2} has a 3-4 fold higher V_{max}. Also Zn^{+2} works slightly better than Mg^{+2}, but worse than Mn^{+2} in fulfilling the metal requirement of NAD-Icdh. No NAD-Icdh activity could be elicited when Ca^{+2} was used. In ox brain Ca^{+2} does result in the highest catalytic activity for NAD-Icdh (55). All of the data on variable metal ion effects is based on a single experiment and is presented here only to verify that other cations may be important in the physiological NAD-Icdh activity of T. pyriformis.

TABLE 11. Effect of adenine nucleotides on the NAD-specific isocitrate dehydrogenase activity from mitochondria of log phase cells. Only those conditions that varied from the routine assay described in Materials and Methods are shown below.

Assay	Relative Activity
0.2mM NAD	1.0
0.2mM NAD + 0.2mM ADP	6.6
0.2mM NAD + 0.2mM AMP	5.4
0.2mM NAD + 0.2 mM ATP	3.1
0.2mM NAD + 1.0mM ATP	1.4
0.2mM NAD + 1.0mM ATP + 2mM $MnCl_2$	3.1
0.2mM NAD + 0.2mM AMP + 0.2mM ADP	5.8
0.2mM NAD + 0.2mM AMP + 0.6mM ATP	3.3
0.2mM NAD + 0.2mM ADP + 0.6mM ATP	4.1
0.2mM NAD + 0.2mM AMP + 0.2mM ADP + 0.6mM ATP	4.1
0.2mM NADP	10.1
0.2mM NADP + 0.2mM ADP	10.1
0.2mM NADP + 0.2mM AMP	10.1
0.2mM NAD + 1.0mM citrate	0.0
0.2mM NAD + 1.0mM citrate + 2mM $MnCl_2$	0.8

Table 12 shows that ADP activation of NAD-Icdh is pH dependent. At pH 7.0 the stimulatory effect of ADP is the most pronounced. Conversely, without exogenous adenine nucleotide addition, the highest activity is found at around pH 6.6. This pH effect is analogous to what has been reported for NAD-Icdh in porcine liver, rat heart and locust flight muscle (24, 56, 57). Figure 12 shows the concentrational dependence of ADP stimulation. Half-maximal stimulation by ADP occurs at about 33 micromolar ADP at pH 7.0.

Kinetic characterization of the substrates for the NAD-Icdh of T. pyriformis was limited to saturation plots since the nonspecific activity of NADP-Icdh with NAD was always present in fraction 5 preparations. Attempts to solubilize and separate the two enzyme activities have failed. The NAD-Icdh remains particle-bound after mild sonication, detergent treatment or both. When any of these techniques were made more drastic to force solubilization, all NAD-Icdh activity was lost. Thus, all kinetic constants may be affected by membrane-associated phenomenon.

Saturation plots for threo-D_s-isocitrate and NAD in the presence or absence of ADP are shown in figures 13 and 14. ADP has little or no effect on the apparent K_m for isocitrate. The approximate value for this apparent K_m is 15 micromolar with or without ADP. This is much lower than values reported for purified prep-

TABLE 12. Effects of pH on NAD- and NADP-isocitrate dehydrogenase activities from mitochondria of two day cells (log phase). All concentrations listed are in millimolarity.

[NAD]	[NADP]	[ADP]	pH	Relative Activity
1.0	0	0	7.4	0.8
1.0	0	0	7.0	1.0
1.0	0	0	6.6	1.5
1.0	0	0	6.2	1.0
0.2	0	0	7.4	0.5
0.2	0	0	7.0	0.7
0.2	0	0	6.6	1.1
0.2	0	0	6.2	0.9
0.2	0	0.2	7.4	4.0
0.2	0	0.2	7.0	6.5
0.2	0	0.2	6.6	3.7
0.2	0	0.2	6.2	2.3
0	0.2	0	7.4	10.3
0	0.2	0	7.0	9.2
0	0.2	0	6.2	4.8
0	0.2	0.2	7.4	9.6
0	0.2	0.2	7.0	9.0
0	0.2	0.2	6.2	5.0

FIGURE 12. Concentrational dependency of ADP on NAD-isocitrate dehydrogenase from mitochondrial fraction stored in 50% (v/v) glycerol. Enzyme assay is identical to that in Figure 6 except variable amounts of ADP were used. Activity is in terms of micromoles of NADH formed/minute/ml. of mitochondrial fraction.

FIGURE 12

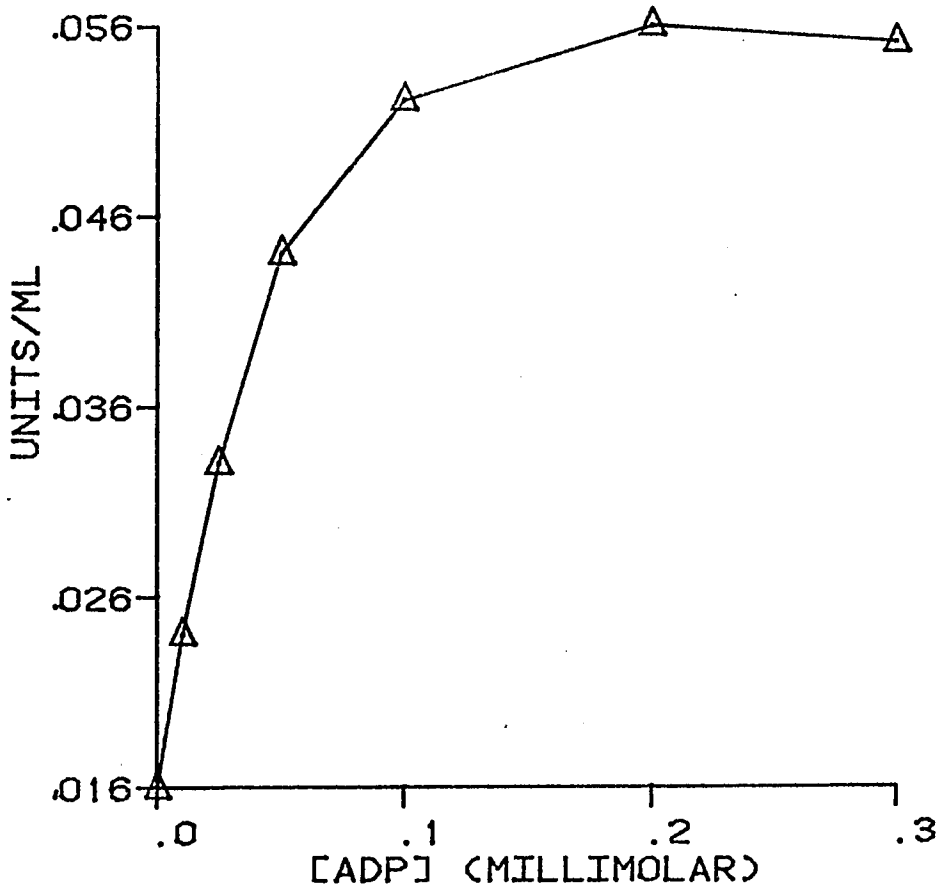

FIGURE 13. Concentrational dependency for threo-D_s-isocitrate of NAD- and NADP-isocitrate dehydrogenases from mitochondrial fraction. NAD-activity measured with (Δ) and without (no symbol) ADP (0.2mM) at NAD=1mM. NADP-activity (□) was measured with and without ADP with identical activities resulting. Activities are in terms of micromoles of NAD(P)H formed/minute/ml of mitochondrial fraction.

FIGURE 13

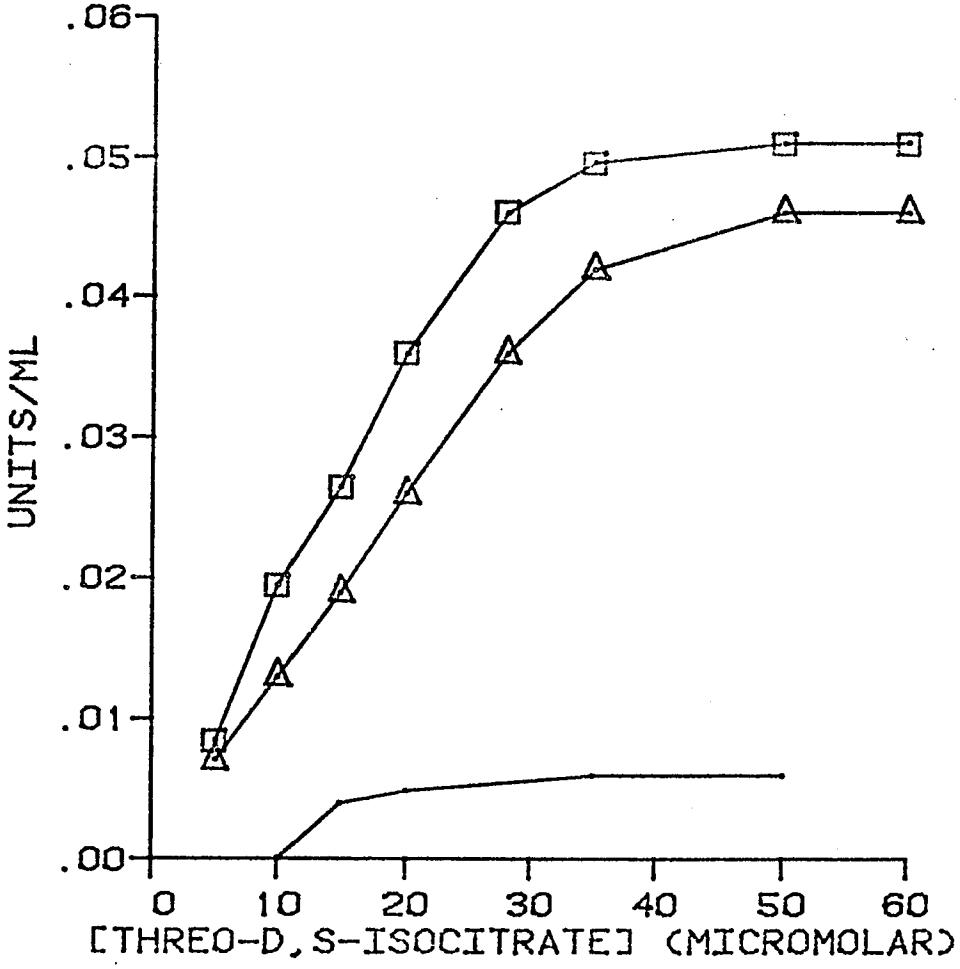
.06
.05
.04
.03
.02
.01
.00
UNITS/ML
0
10
20
30
40
50
60
[THREO-D,S-ISOCITRATE] (MICROMOLAR)

FIGURE 14. Concentrational dependency for NAD of the NAD-isocitrate dehydrogenase from mitochondrial fraction. NAD-activity measured with (△) and without (□) ADP (0.2mM). Activity is in terms of micromoles of NADH formed/minute/ml of mitochondrial fraction.

FIGURE 14

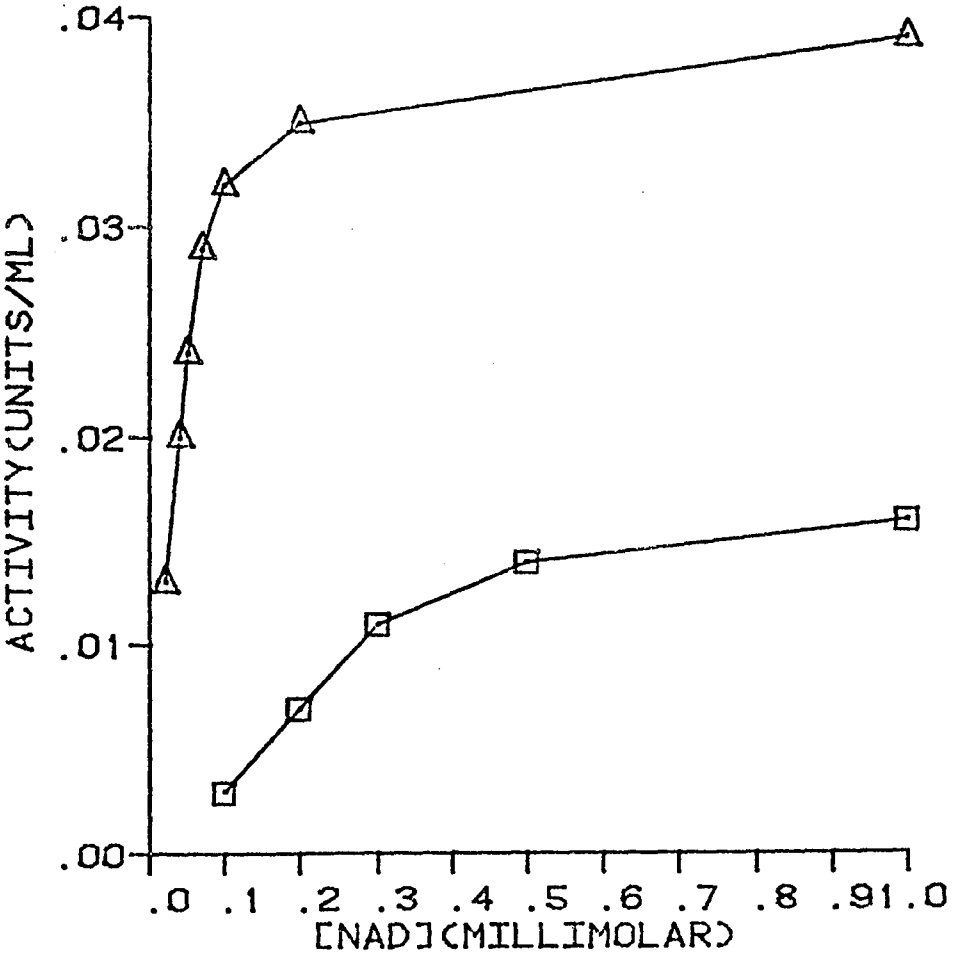
.04
.03
.02
.01
.00
ACTIVITY(UNITS/ML)
.0 .1 .2 .3 .4 .5 .6 .7 .8 .91.0
[NAD](MILLIMOLAR)

arations from mammalian tissues (38, 58). The apparent K_m for NADP-Icdh present in the same fraction preparation for threo-D_s-isocitrate can also be estimated from Figure 13. It was found to be about the same as the K_m of the NAD-Icdh, with or without ADP. A slightly lower value was found in dry cell extracts for NADP-Icdh (See Table 2), but the present value is nearly the same as Levy had found in T. pyriformis (20).

Figure 14 shows that there was a significant change in the concentrational dependence of the NAD-Icdh for NAD in the presence of ADP. The apparent K_m for NAD without ADP stimulation was between 220 and 230 micromolar. In the presence of ADP the K_m decreased to between 40 and 45 micromolar, which is approximately what has been found in mammalian tissues (24).

Since fraction 5 preparations have always contained significant amounts of NADP-Icdh (Figure 13- ◻) it remained possible that these two enzyme activities were from the same molecule. Table 13 confirmed the specificity of the two types of reduced pyridine nucleotides to inhibit isocitrate dehydrogenase. The NADPH inhibition was specific for NADP-Icdh and the NADH inhibition for NAD-Icdh. Furthermore, the NAD-Icdh (+ADP) and NADP-Icdh activities were found to be approximately additive.

At this point the NAD-Icdh had been at least partially characterized. Initially log phase cells had been chosen for these studies

TABLE 13. Effects of reduced pyridine nucleotides on NAD- and NADP-linked isocitrate dehydrogenase activities from mitochondria of two day cells (log phase) with and without ADP added. All concentrations listed are in millimolarity.

[ADP]	[NAD]	[NADP]	[NADH]	[NADPH]	Relative Activity
0	0.2	0	0	0	1.0
0.2	0.2	0	0	0	6.4
0.2	0.2	0	0.2	0	2.4
0	0.2	0	0.2	0	0
0.2	0.2	0	0	0.2	6.9
0	0	0.2	0	0	10.0
0.2	0	0.2	0	0	10.0
0	0	0.2	0.2	0	9.4
0	0	0.2	0	0.2	5.3
0.2	0.2	0.2	0	0	14.0

because stationary phase cells had a considerably lower NAD-Icdh specific activity (see Figure 6) as measured on the 25,000 x g pellet. However, these values were obtained without ADP stimulation. Full fractionation, in the same density gradient used to separate organelles, showed that when ADP was added, the specific activity of NAD-Icdh from the purest mitochondrial fraction was actually higher in stationary phase cells (0.205 ± 0.008 for stationary phase cells versus 0.128 ± 0.021 micromoles of NADH formed/minute/mg of protein for log phase cells). In order to determine whether or not these two sets of seemingly contradictory data had any basis in the metabolic state of T. pyriformis, particulate fractions (250,000 x g-minute resuspended pellet) from cells grown or maintained under different conditions were studied to see what effects these conditions had on the specific activity of NAD-Icdh. Table 14 further establishes that conditions of growth have marked effects on the specific activity of NAD-Icdh. The reduction in specific activity with culture age, as well as the effect of aeration were most pronounced at NAD=0.1mM without ADP addition (When NAD=1mM these effects may be obscured by the contribution of nonspecific NAD-Icdh activity from the NADP-Icdh). Cells subjected to constant shaking (high aeration), and in the log phase of growth (24 hours old) had the highest specific activity of all growth or metabolic conditions studied in Table 14. Cells grown under static conditions, and nearing the end of log phase of growth

TABLE 14. Variations of particulate NAD-linked isocitrate dehydrogenase activity with culture condition. All activities are in terms of micromoles of NADH formed/minute/mg of protein ± standard error for three trials.

	Growth with shaking for 24 hours	Static growth for 48 hours	Static growth for 48 hours+ 3 hours hypoxia	Static growth for 6 days
NAD=1mM	0.061±0.008	0.040±0.008	0.032±0.006	0.007±0.003
NAD=1mM ADP=0.2mM	0.109±0.018	0.075±0.011	0.061±0.009	0.058±0.006
NAD=0.1mM	0.025±0.003	0.011±0.003	0.003±0.002	0.000
NAD=0.1mM ADP=0.2mM	0.058±0.009	0.033±0.003	0.029±0.005	0.033±0.007

(48 hours old) were found to have a specific activity for NAD-Icdh of about half that of the log phase-aerated cells. Cells that were grown under the same static conditions for 48 hours, but subjected to three hours of reduced oxygen tension (see Materials and Methods of chapter 3), a condition shown to activate gluconeogenesis (8, 14) had a barely measureable specific activity when ADP was absent from the assay mixture. Cells grown for 6 days under static conditions had no measureable NAD-Icdh activity when NAD=0. 1mM. However, addition of ADP to the assay for all growth or metabolic conditions studied brought each of the specific activities to about the same levels.

DISCUSSION

Evidence has been presented in this chapter that directly proves the existence of a mitochondrial NAD -Icdh in T. pyriformis. Although this enzyme activity had been previously postulated (15), all attempts to measure its activity had been unsuccessful (15,21,43). My own work has been limited by instability of the enzyme in anything but particulate preparations (purified mitochondria) stored at -20°C in 50% glycerol. However, the enzyme's stability in these glycerol-stored particles was sufficient to allow a determination of some potentially important characteristics of the T. pyriformis NAD-Icdh:

1. Adenine nucleotides (AMP, ADP and ATP) stimulate this enzymatic activity, with ADP having the greatest effect.
2. The stimulation by ADP appears to be a result of increasing affinity (decreasing K_m) for NAD, and increasing the rate of reaction (V_{max}) with respect to threo-D_s-isocitrate.
3. The stimulation by ADP is pH dependent, and is optimal at around pH 7.0.
4. The enzyme is specifically inhibited by NADH, but not by NADPH.

It is possible that any or all of these kinetic properties are involved in regulating the T. pyriformis NAD-Icdh.

Since this enzyme has been localized in the mitochondrion,

the physiological importance of the kinetic results are contingent on the intramitochondrial conditions within which this enzyme functions. Unfortunately there is little known about intramitochondrial conditions in T. pyriformis. It is known that ATP levels within the whole cell do not vary in going from the logarithmic to the stationary phase of growth (59). Even "atypical" increases in ATP during heat-induced synchronous cell division were rapidly normalized by a decrease in ATP to the levels found in both logarithmic and stationary growth phase cells. Thus, significant variations in ATP of each cell may only occur just prior to cell division. The fact that the ATP produced by glycolysis and that produced by respiration can be used equally well for this ciliate's motility implies that separate pools of glycolytic ATP and respiratory ATP do not exist in T. pyriformis (60).

In higher animals, substrate pooling in specific organelles occurs because of permeability barriers in which specific transport proteins permit unidirectional movement of certain metabolites. Studies with liver and heart have delineated these transport processes for mono-, di- and tricarboxylates and adenine nucleotides (61, 62). Although such transport systems have not been directly shown in T. pyriformis, there are indications that they are present. Recent work by Erecinska et al. (63) showed that a near equilibrium exists between the transfer of reducing equivalents from intramitochondrial NAD/NADH

to the phosphorylation of ADP to ATP in T. pyriformis, yeast, isolated liver cells and cultured kidney cells. This equilibrium occurs in T. pyriformis despite an unusual mitochondrial electron transport chain (64, 65) and suggests a specific translocation of adenine nucleotides, as has been demonstrated in animal mitochondria to maintain this constant $[ATP]/([ADP][P_i])$ ratio. ADP in the cytoplasm is transported into the mitochondrial matrix with orthophosphate (P_i) while ATP exits. This ATP-ADP translocase accounts in part for the constant tenfold higher $[ATP]/([ADP][P_i])$ ratio in the cytoplasm of animals. In mammalian systems this homeostatic regulation confirms the notion that changes in the mitochondrial ATP/ADP ratio are not a major regulatory factor simply because changes in this ratio are small (66).

Yet there is no doubt that adenine nucleotides have a dramatic effect upon the T. pyriformis NAD-Icdh, as well as its mammalian counterpart. The fact that ATP is not inhibitory to this enzyme's activity in T. pyriformis, but actually stimulates NAD-Icdh activity to a rate above that determined in the absence of any adenine nucleotide points out a divergence from the mammalian enzyme (24, 58). Activation by AMP has also been noted. The physiological significance of this activation of NAD-Icdh by adenine nucleotides other than ADP is unclear. It may simply represent nonspecific interactions, as appears to be the case with relatively high NAD concentrations acting as sub-

strate for the NADP-Icdh in this organism.

The precise role of ADP activation is itself unclear, since its levels are presumably always high in the mitochondrion, except under strictly anaerobic conditions. Studies with isolated heart mitochondria (67) and a soluble fraction from liver mitochondria (68) have indicated that the regulation of flux through NAD-Icdh by the ATP/ADP ratio is quantitatively much less than by the NAD/NADH ratio. Very recently Machado and Satrustegul (22) showed a large variation in the T. pyriformis NAD/NADH ratio that was dependent upon levels of oxygenation. Using the same experimental conditions, Raugi et al. (69) showed there was no variation in ATP, ADP or AMP levels. Paradoxically, cells adapted to lowered oxygen concentrations (during growth) increased the rate of oxidation through the TCA cycle, and these cells subjected to low oxygen during growth developed an improved capacity to utilize oxygen that persisted for over an hour after the cells were returned to a more oxygenated condition (69).

In any event, the high NADH levels that appear in cells subjected to hypoxia (not anaerobiosis) should inhibit isocitrate oxidation through NAD-Icdh. In the presence of ADP, however, I have shown that this NADH inhibition is not total as would be the case if ADP were not present (See Tables 9 and 13). Thus, the ADP activation of NAD-Icdh may be related to maintaining a mitochondrial ability to oxidize isocitrate rather than to actually augmenting this activity.

I should also mention that, despite the fact I have used the results of Machado and Satrustegul (22), I must disagree with many of their conclusions. Their entire work was founded on the assumption that there is no NAD-Icdh in T. pyriformis (22, 45), and that control of isocitrate metabolism (and gluconeogenesis from fats) rests in NADP-Icdh. Since this chapter refutes their notion that NAD-Icdh is absent in this organism, all other metabolic interpretations asserted should be reviewed. Much of their discussion centered around the NADPH/NADP ratio, although their results showed that NADH/NAD ratios were more affected by levels of oxygenation than the NADPH/NADP ratios. They felt that the NADH/NAD ratio had no regulatory significance. Yet a prerequisite to reversing glycolysis toward glucose production at the level of glyceraldehyde-3-phosphate dehydrogenase is a high NADH/NAD ratio in the cytosol.

The possibility that inhibition of isocitrate oxidation within the mitochondrion occurs during conditions favorable for the inducement of gluconeogenesis from fats (hypoxia) seems remote if both the TCA cycle and respiration are occurring afterward at normal rates. My own data showed that NAD-Icdh had the potential to continue to function under low oxygenation-high NADH conditions (See Table 14). However, Raugi et al. (69) and Stein and Blum (70) have shown that cells grown under hypoxic conditions develop the ability to use

oxygen more efficiently, with the Krebs cycle and respiration continuing at rates comparable to cells grown under higher oxygen tensions. Thus, it does not appear possible, except under strictly anaerobic conditions, that inhibition of NAD-Icdh controls the flux of isocitrate out of the mitochondrion as I had suggested in chapter 1. However, this does not preclude a normal flux of isocitrate out of the mitochondrion. Also, citrate exit from the mitochondria could constitute a net isocitrate flux out, because about 50% of the T. pyriformis aconitase is cytosolic (15, 71). Once the isocitrate (or citrate) leaves the mitochondria, its oxidation by NADP-Icdh could be prevented by high NADPH/NADP ratios in the cytosol, thus permitting isocitrate lyase to use the available isocitrate. Whether or not the NADPH/NADP ratio(1.7-Machado and Satrustegul) is sufficient to inhibit NADP-Icdh enough for isocitrate lyase to compete successfully with it for isocitrate cannot be stated with certainty. However, using approximately the same ratio of NADPH/NADP as Machado and Satrustegul found (1.5) I retained as much as 60% of the NADP-Icdh activity (See Tables 9 and 13). Thus, it seems that the NADP-Icdh is still functioning well enough to compete favorably with isocitrate lyase for isocitrate.

Alternatively, as presented in chapter 1, the source of isocitrate for the glyoxylate cycle may not be the mitochondrion at all. Since the isocitrate concentration in whole cells that are actively

synthesizing glucose is only 5 micromolar (23)-far too low a concentration for isocitrate lyase to function (71, 72)-there must be either a transport system involved in accumulating isocitrate or a synthesis of isocitrate near the site of the glyoxylate bypass reactions. Accumulating isocitrate would still require inhibition of the NADP-Icdh in both the cytosol and peroxisome. Instead, the high NADH/NAD or NADPH/NADP ratios that accompany conditions favorable for gluconeogenesis could fuel the reverse reaction of NADP-Icdh. As shown in chapter 1, the reductive carboxylation of α-ketoglutarate by NADP-Icdh was found to work with either NADH or NADPH (See Table 7). Also, CO_2 fixation into isocitrate is consistent with the available tracer data (8, 73). Van Niel et al. (73) found that CO_2 was fixed in the carboxyl groups of succinate. This is where it should be if α-ketoglutarate reacted with CO_2 and NAD(P)H to form isocitrate and this isocitrate then was cleaved to form succinate and glyoxylate by isocitrate lyase. Hogg (8) showed that 1-[^{14}C]-acetate incorporation into glycogen was exclusively into the third and fourth carbons of glucose. This is precisely where it should be located if the CO_2 generated from the labeled 1-carbon of acetate (labeled CO_2 or succinate must be generated from this 1-carbon position, if this acetate eventually condenses with oxaloacetate or glyoxylate) was fixed into α-ketoglutarate to form isocitrate. Isocitrate in turn would go through an aldo-like intercon-

version to labeled succinate and unlabeled glyoxylate by isocitrate lyase. If the carboxyl-labeled succinate then goes to glucose, only the third and fourth carbons should be labeled. An alternate explanation of this labeling pattern has the CO_2 fixation occurring on phosphoenolpyruvate, with equilibration of ;the carboxyls on oxaloacetate (74) with succinate via Krebs cycle reactions, and a subsequent return to phosphoenolpyruvate. However, such a path would be energetically wasteful.

Since the definitive work of Muller et al. (15) it has been assumed that gluconeogenesis through the glyoxylate cycle occurred at the expense of the tricarboxylic acid cycle (TCA) in T. pyriformis (8). The basis of this assertion stems from the fact that both the TCA cycle and gluconeogenesis require common intermediates and enzymes that are found in the mitochondrion. Yet Raugi et al. and Blum and Stein (69, 70) have shown that the TCA cycle is functioning as well or better while gluconeogenesis through the glyoxylate cycle is occurring. Thus, the possibility of a gluconeogenic pathway that is independent of the mitochondrion and/or the TCA cycle should be considered. The next chapter deals specifically with new evidence for this concept.

CHAPTER 3

SUBCELLULAR CHANGES AND THEIR RELATIONSHIP TO GLUCONEOGENESIS

INTRODUCTION

Two interrelated perspectives have dominated the study of intermediary metabolism for over 40 years: 1. the identification of intermediary compounds from substrates and 2. the discovery and characterization of those enzymes involved in the production and consumption of those intermediates. Over the last ten to fifteen years further clarification of the regulation of eucaryotic metabolism has focused on enzyme mechanisms, intracellular compartmentation of enzymes, determinations of the intracellular flux of intermediates from multi-enzyme pathways (or cycles) within each compartment and the various transport systems necessarily involved in linking overall cellular metabolism with that in each compartment. Types or kinds of compartments (organelles) have been further classified by their enzymic composition and by their appearance under the electron microscope. The combined facts that most or all of the protein components of these organelles are synthesized outside of them and that there is a uniformity of sequestration of these organelle-characterizing proteins into distinct particles have led to the rapidly growing study of organelle biogenesis. Although each organelle can be represented as a separate entity within eucaryotic cells, it is clear that each is simply part of a complex subcellular organization that is coordinated and controlled by

the needs of the whole cell. Removal and isolation of any particular part of the whole cell must be viewed with the understanding that its function has been disrupted.

In Tetrahymena pyriformis, the ability to synthesize glycogen from fats requires the integration of enzymes found in at least three subcellular compartments (mitochondrion, peroxisome and cytosol). The intracellular organization for such a pathway has been hypothesized to be exceedingly complex (8). Chapters 1 and 2 have, in fact, been attempts at explaining the possible role(s) that isocitrate metabolism plays in glycogen synthesis. Due to the parochial nature of singling out an enzyme activity and relating it to a complex metabolic pathway the conclusions of this work are tentative at best. I have, more recently, turned my attention to a phenomenon of intracellular structural change that may be involved in glyconeogenesis.

My interest in such phenomenon began with certain anomalous results obtained in development of the subcellular fractionation procedure described in chapter 2. Fractionation experiments of homogenates from log phase cells of T. pyriformis showed that enzyme markers for lysosomes, peroxisomes and mitochondria separate from each other by centrifugation through a discontinuous sucrose density gradient (Figure 7). Homogenates from stationary phase cells showed a very similar density gradient separation for

mitochondrial and peroxisomal enzymes. However, a large proportion of mitochondrial and peroxisomal enzymes, as well as almost all of the lysosomal marker were found together at a lower sucrose density (Figure 8). Instead of this phenomenon being an artifact of the separation procedure, electron micrographs have provided evidence for significant structural alterations within the cell that may be responsible for this accumulation of enzymes known to originate from different organelles. Inducing the stationary phase of growth in cells taken from log phase cultures by decreasing the oxygen tension generated a somewhat intermediate state with respect to both the marker enzyme distribution in the sucrose gradient and the structural alterations visualized by electron micrographs. I propose that this supramolecular regrouping of enzymes and subcellular structure has functional significance in facilitating the synthesis of glycogen from fats in T. pyriformis.

MATERIALS AND METHODS

Growth and harvesting of cells have been described in chapter 1.

Activation of gluconeogenesis in log phase cells. To induce log phase cells to develop the capability of synthesizing glycogen from fats, cell suspensions were resuspended in 100 ml of dilute Ringer phosphate buffer (17) such that all suspensions had a final concentration of 4% (v/v) as determined by centrifugal packing in a Constable protein tube. These cell suspensions were then placed in a 125 ml Erlenmeyer flask for 4 hours. The resultant decrease in oxygen tension that occurs in such "deep" cultures (14, 69, 70) has also been shown to rapidly terminate cell division (14, 70).

Subcellular fractionation and cell disruption. The methods used for these procedures have been described in chapter 2. In one set of experiments the density of the upper part of the gradient was altered to decrease the density of fraction 8. The gradient was prepared as before except that 2 ml of 0.25M D-mannitol was added on top of the 40% (w/w) sucrose. After 4-5 hours there was considerable mixing between the top layer of sucrose and the mannitol layer, thus reducing the density of the eventual fraction 8. Only 4 ml of freshly prepared homogenate was then layered on top of this gradient. All other procedures remained the same as before.

Enzyme assays, protein and glycogen determination. Succinate dehydrogenase was assayed according to the method described in Muller et al. (15); fumarase (51); citrate and malate synthase (75); isocitrate lyase (50); fatty acyl-CoA oxidase(76); catalase (49); malate dehydrogenase (77); acid phosphatase (53); aspartate-α-ketoglutarate transaminase (78); glutamate dehydrogenase (52); glucose 6-phosphate isomerase (79) and fatty acyl-CoA dehydrogenase (19). NAD- and NADP-Icdh were assayed by methods described here previously. Lactate oxidase was assayed in the manner of the fatty acyl-CoA oxidase, except that L-lactate at 30mM replaced butyryl-CoA. β-oxidation with butyryl- CoA and lauryl-CoA was measured according to the spectrophotometric method of Cooper and Beevers (18). All assays were performed on a Gilford 240 or 2400 recording spectrophotometer at 30°C. All enzymes were assayed in the presence of 0.067%(v/v) Triton X-100, except isocitrate lyase, malate synthase and citrate synthase.

The methods used for extracting and isolating protein were described in chapter 1. Glycogen was isolated from fresh cells, particles or supernatants by suspension in 1 N cold perchloric acid (1:1) to a final concentration of 0.5 N and sonicating with a Branson Sonifier Cell Disruptor (model W140D) for 30 seconds at setting 5. The ice-cold sonicate was centrifuged for 10 minutes at 1000 x g in an International centrifuge and the pellet (lipids, nucleic acids and

protein) was washed twice more with 0.5 N perchloric acid. All supernatants were combined, mixed vigorously with 1.2 volumes of absolute ethanol and allowed to stand at 0-5°C overnight. The glycogen precipitate was pelleted at 1000 x g for ten minutes in an International centrifuge and washed two times with absolute ethanol before the glycogen was redissolved in 0.05 N NaOH. For radiotracer experiments, 0.05-0.10 ml of this glycogen solution was added directly to 5ml of scintillation cocktail (80) and counted. Total glycogen was analyzed by the anthrone method, using glucose as a standard(81).

ELECTRON MICROSCOPY

Cell preparations. Suspensions of cell cultures were fixed for electron microscopy by adding an equal volume of 6% (v/v) glutaraldehyde prepared in 0.1M Sorensen's phosphate buffer (pH 7.2) at 25°C. Hence, the final fixative was 3% glutaraldehyde in 0.05M phosphate buffer. After 10 minutes at 25°C, the cell suspension was chilled to 5°C and fixed for an additional 50 minutes. Fixed cells were collected by gentle centrifugation (200 x g for 5 minutes) in an International centrifuge. The supernatant was removed and the pellet of cells was resuspended in a drop of 0.8% Ionagar that was cooled to 38°C before addition. The pellet was dispersed in the agar by flicking the tip of the centrifuge tube vigorously and immediately after addition of the agar drop. The agar

suspension was solidified by chilling in an ice bath and the resulting block was floated up in the centrifuge tube by adding chilled Sorenson's phosphate buffer. The agar block was cut into cubes approximately $1mm^3$ in volume, washed in cold buffer for 5 minutes and post-fixed for 2 hours at 5°C in 2% (w/v) osmium tetroxide prepared in 0.05M Sorenson's phosphate buffer (pH 7.2). The fixed cells, enclosed in the agar cubes, were washed in deionized water, dehydrated in a graded acetone series and embedded in LX112 epoxy resin (Ladd Research Industries, Burlington, Vt.).

Cell fraction preparations. Cell fraction suspensions were fixed for 1 hour at 5°C by adding an equal volume of glutaraldehyde fixative as prepared for whole cells. An aliquot of the suspension (0.1-0.3 ml) was collected on a 13mm diameter Millipore filter with 0.22 micrometer pore size (Millipore Corporation, Bedford, Mass.) under gentle nitrogen pressure (82). The thin layer of cell fraction was protected by covering it with an opposing layer of fixed red blood cells previously collected on a 0.45 micrometer pore size Millipore filter. The "sandwiched" preparation was gently secured in a screw clamp, washed in 0.05M phosphate buffer (pH 7.2) at 5°C and post-fixed for 2 hours in 2% osmium tetroxide (5°C) prepared as for whole cells. The fixed preparation was washed in deionized water and dehydrated in a graded ethanol series. The dehydrated wafer was released from

the clamp and deposited in 100% acetone in a sealed container. After 12 hours, the Millipore filters had dissolved releasing the thin disc containing the fraction which was further dehydrated in three changes of 100% acetone and embedded in a flat mold using LX 112 epoxy resin.

Section preparations. Ultrathin sections (silver-gray to silver-gold) were obtained using a diamond knife, mounted in a Porter-Blum MT-2 ultramicrotome, collected on uncoated copper grids, and stained using Reynolds' lead citrate (82) and/or uranyl acetate solution prepared in a 10% (v/v) ethanol/water solution. Sections were observed with a Philips EM 200 electron microscope operated at 60 kV.

RESULTS

Three types of particles, marked by enzymes specific to each show different and characteristic patterns of distribution within the sucrose density gradient (see Figures 7 and 8). When log phase cells are used, fractions of peak enzyme activity for each organelle marker are separated by at least one fraction (see Figure 7). Fraction 3 represents peroxisomes, fraction 5 represents mitochondria and fraction 7 represents lysosomes. NADP-linked isocitrate dehydrogenase has been found in the peroxisome, mitochondrion and cytosol of Tetrahymena pyriformis (15). The equilibrium densities reported for these organelles by de Duve's laboratory (15)— peroxisome-1.235; mitochondria-1.214; and lysosomes-1.182— fall within the range of these discontinuous-gradient fractions by appropriate enzyme markers.

Fraction	Density Range (mg/ml)
1	1.297-1.295
2	1.295-1.234
3	1.234-1.225
4	1.225-1.215
5	1.215-1.206
6	1.206-1.197
7	1.197-1.180
8	1.180-1.165
9	0.25M mannitol

When stationary phase cells are used the same peaks for mitochondrial and peroxisomal markers are found as in log phase, but all of these enzyme markers exhibit peaks in fraction 8. Lysosomes are found almost exclusively in fraction 8 (Figure 8g). There is a substantial redistribution of protein into fraction 8 when cells go from

log to stationary phase of growth (Figures 7h and 8h). Pyruvate kinase, previously associated with the cytosol of T. pyriformis (84) is found partly associated with the peroxisomes and fraction 8 from stationary phase cells(see Figures 15 and 16). This indicates that cytosolic uptake by peroxisomes and the particles of fraction 8 is partially responsible for the substantial protein redistribution.

This phenomenon of enzymes and total homogenate protein peaking at a lower density fraction when the cells are in the non-dividing state does not represent solubilization. An increase of soluble enzymes would be reflected by an increase in activity in fraction 9. With the exception of pyruvate kinase and NADP-Icdh, no enzyme studied here was found in any significant amount in fraction 9. Furthermore, many of the enzymes found in fraction 8 displayed latency(data not shown). Also, when the gradient is slightly alterred to decrease the density in fraction 8 (see Materials and Methods) the enzyme peaks found in fraction 8 shifted together into fraction 7(see Table 15).

Figures 17 and 18 show that this fraction 8 phenomenon is dependent on the culture age. Both fumarase-Figure 17 (mitochondrion) and catalase-Figure 18 (peroxisome) were selected here as the more critical markers since neither enzyme has ever been shown to be membrane-bound. Thus, their respective shifts of pattern could not be considered to be an artifact of membrane fragmentation resulting from the homogenization procedure.

FIGURE 15. Distribution of pyruvate kinase specific activities in the fractions from the sucrose density gradient in stationary phase cells (6 days). All activities are in terms of micromoles of pyruvate/minute/mg of protein.

FIGURE 15

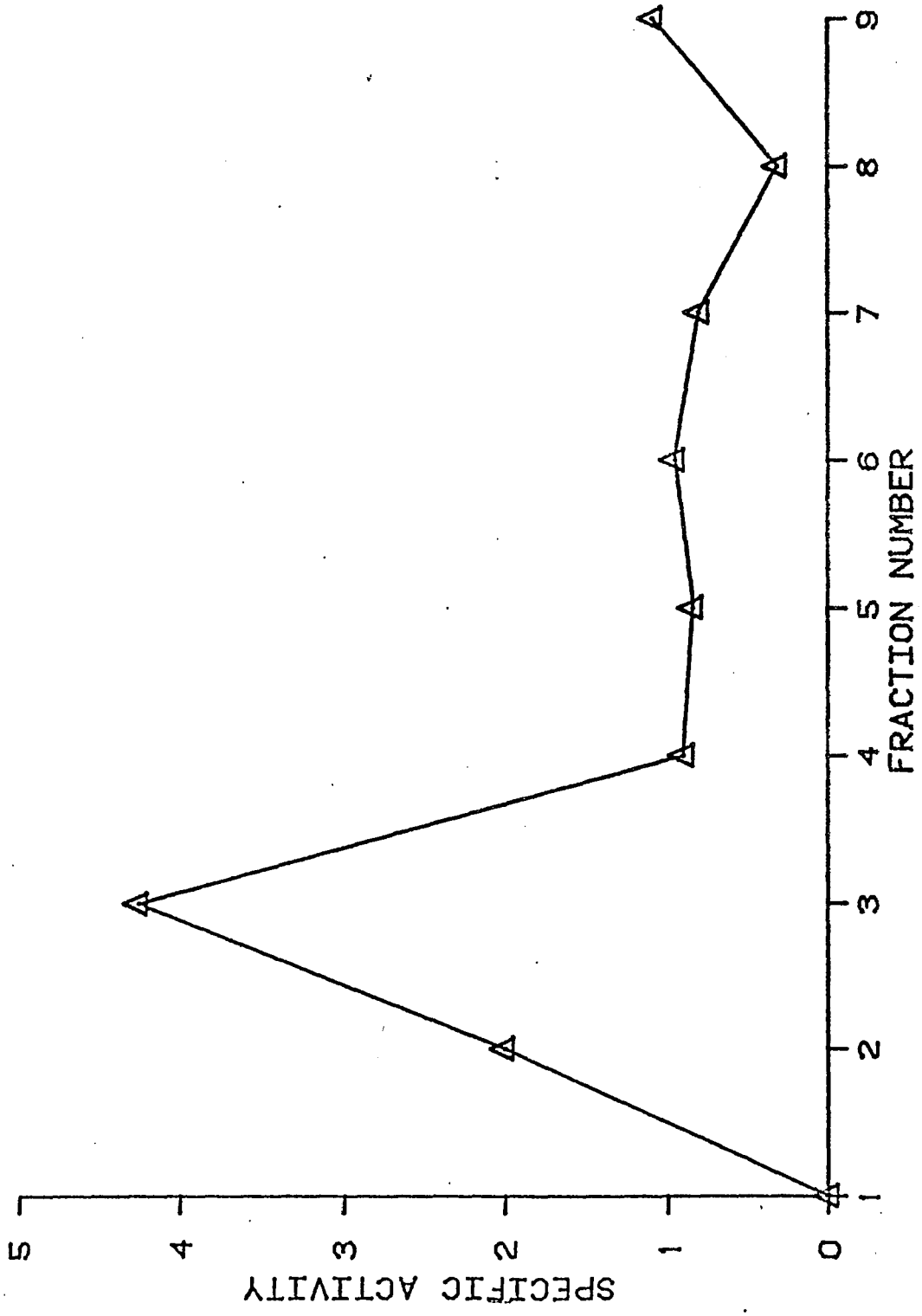

FIGURE 16. Distribution of pyruvate kinase in the sucrose density gradient using stationary phase cells (6 days).

FIGURE 16

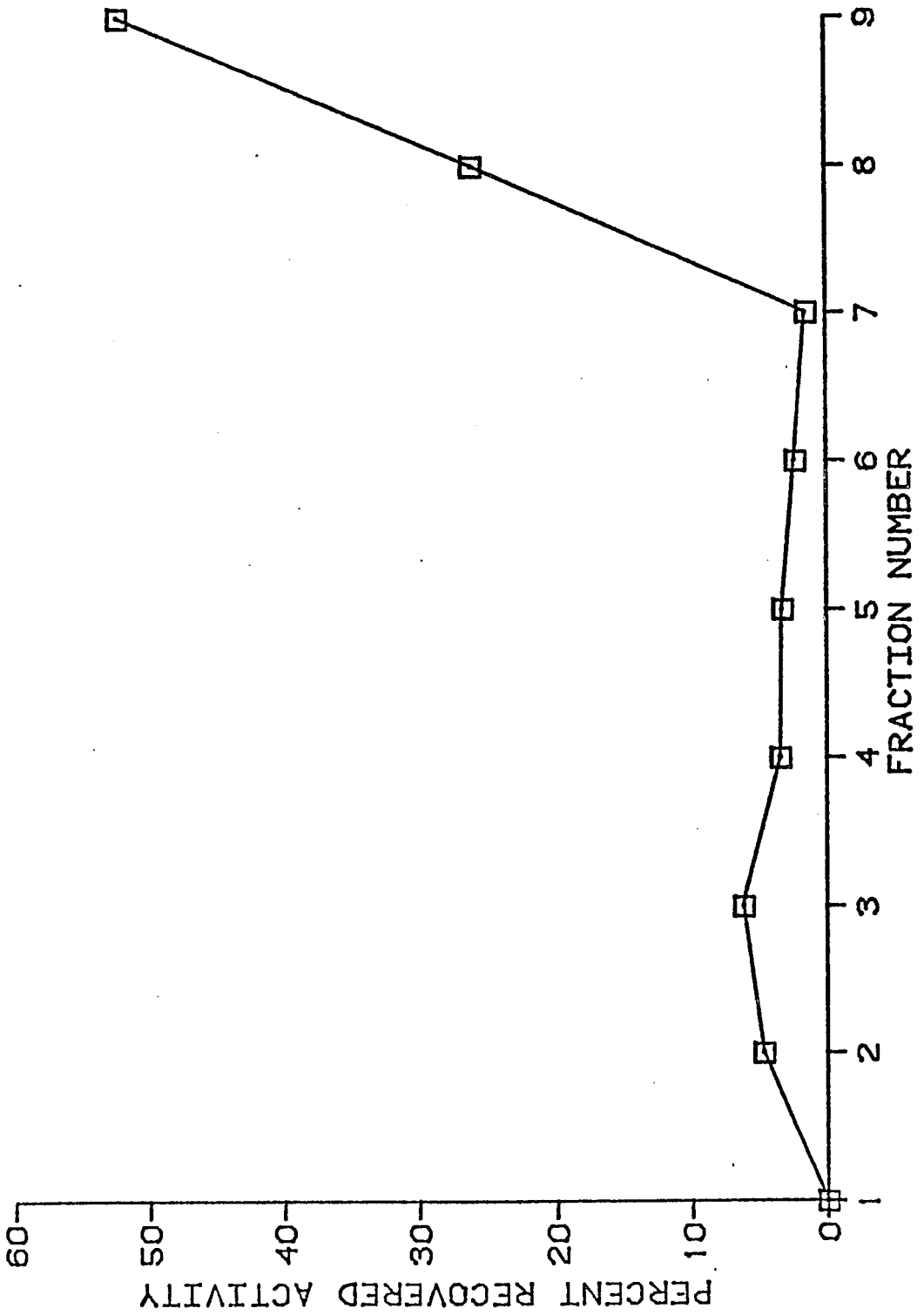
PERCENT RECOVERED ACTIVITY
0
10
20
30
40
50
60
1
2
3
4
5
6
7
8
9
FRACTION NUMBER

TABLE 15. Effects of altered gradient on the accumulation of protein and enzymes at a low sucrose density in stationary phase cells. Sucrose gradient was altered to decrease the density interface at fraction 8 (See Materials and Methods of this chapter). All values are in percent recovered activity from the gradient.

Enzyme	Control Gradient		Altered Gradient	
	Fraction 7	Fraction 8	Fraction 7	Fraction8
succinate dehydrogenase	2.7%	39.2%	37.6%	8.1%
fumarase	8.9%	35.2%	36.5%	7.3%
catalase	6.8%	40.2%	44.8%	6.4%
protein	1.3%	57.9%	38.7%	20.6%

FIGURE 17. Distribution of fumarase in the sucrose density gradient at various ages of culture. (◇)-37 hours; (△)-48 hours; (⬡)-96 hours; (□)-139 hours

FIGURE 17

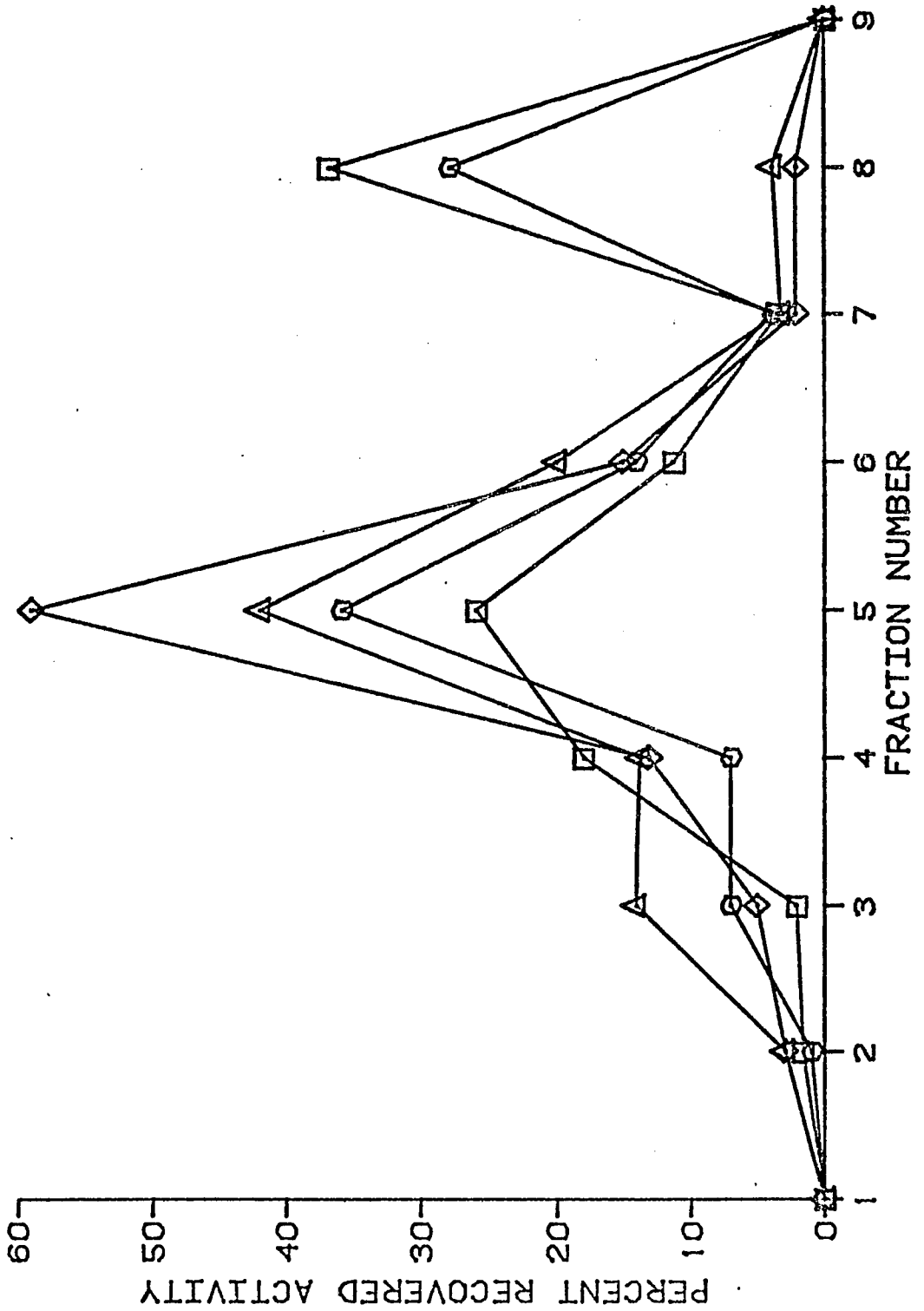
PERCENT RECOVERED ACTIVITY
0
10
20
30
40
50
60
1
2
3
4
5
6
7
8
9
FRACTION NUMBER

FIGURE 18. Distribution of catalase in the sucrose density gradient at various ages of culture. (◇)-43 hours; (△)-96 hours; (□)-116 hours; (⬡)-168 hours

FIGURE 18

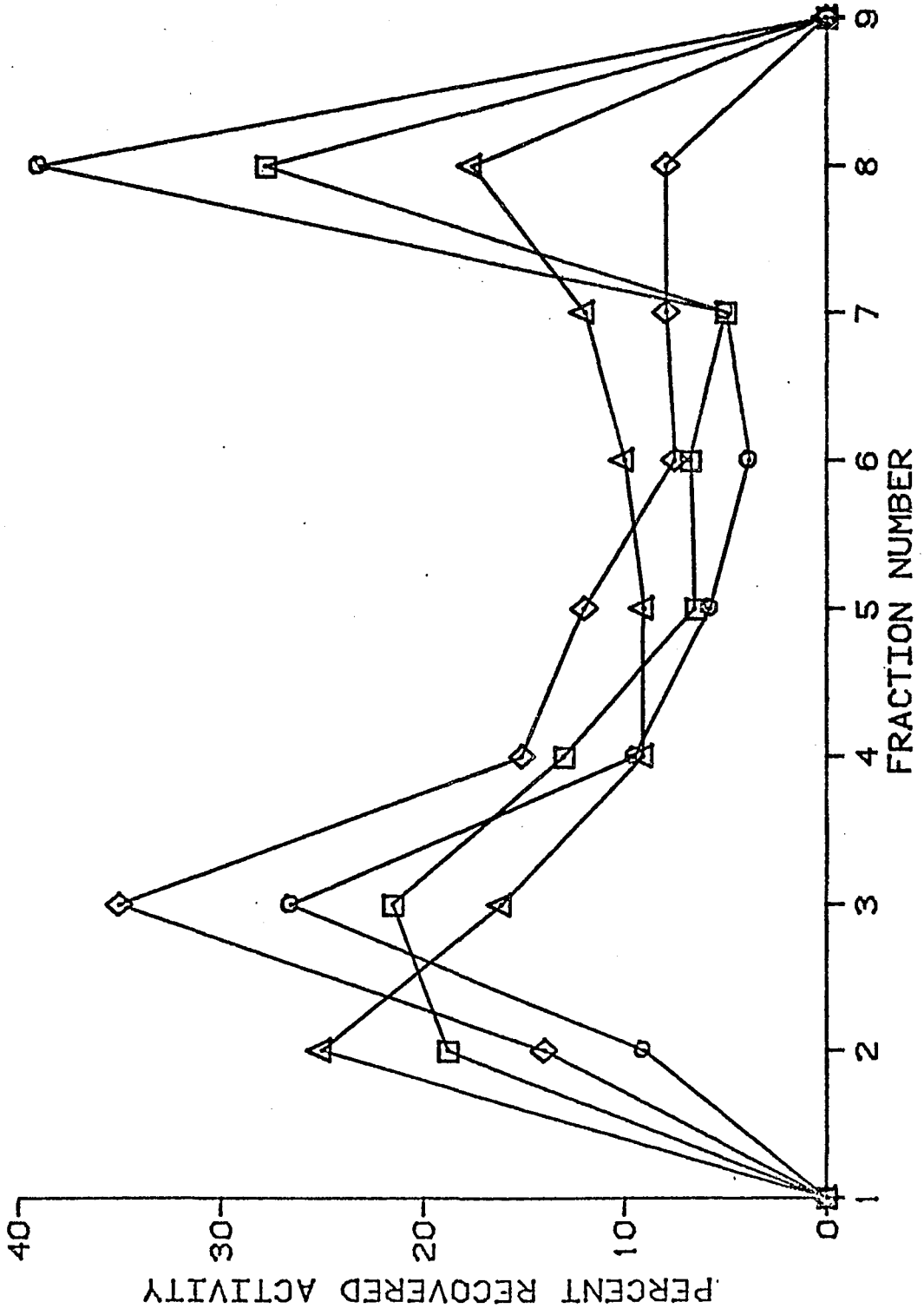
PERCENT RECOVERED ACTIVITY
0
10
20
30
40
1
2
3
4
5
6
7
8
9
FRACTION NUMBER

Enzyme distribution patterns in a sucrose density gradient were also examined for log phase cells that had been subjected to four hours of reduced oxygen tension (See Materials and Methods). Distribution of marker enzymes from these cells showed a pattern intermediate between those for log phase and stationary phase cells (See Figure 19). The peroxisomal marker, catalase, was found largely in fractions 3 and 8. The mitochondrial markers, fumarase and glutamate dehydrogenase, peaked in fractions 3 and 5. Lysosomes (acid phosphatase) were found to peak in fractions 3 and 8.

A wider survey of enzymes in stationary phase cells that have well-known subcellular localization showed that the accumulation of enzymes in fraction 8 does not occur for all mitochondrial and peroxisomal enzymes (See Table 16). [In order to avoid an unduly large number of figures, I have listed the type of distribution pattern found for each of the enzymes in this table, in accord with the patterns illustrated in Figures 7 and 8.] Specifically, citrate synthase, fatty acyl-CoA dehydrogenase, NAD-Icdh and lactate oxidase either could not be found in fraction 8 or exhibited only a neglibible fraction of their total activity in this fraction. In comparison, all other enzymes studied, with the exception of pyruvate kinase (See Figure 16), a cytosolic and glycolytic enzyme, showed substantial accumulation in fraction 8.

FIGURE 19. Enzyme and protein distribution in a sucrose density gradient for log phase cells (37 hours) after 4 hours of hypoxia. (a) glutamate dehydrogenase-102% recovered, (b) fumarase-89% recovered, (c) catalase-95% recovered, (d) acid phosphatase-92% recovered and (e) protein-97% recovered.

FIGURE 19

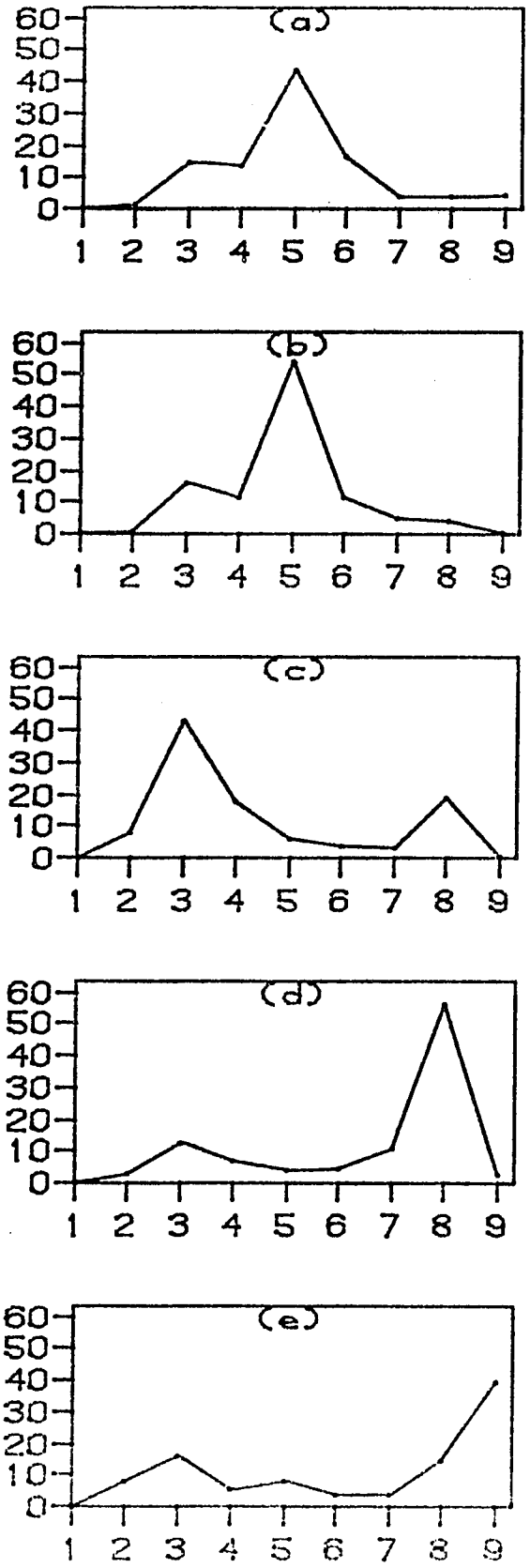

TABLE 16. Percent of total recovered activity of enzymes found in fractions 8 and 9 of stationary phase cells.

Enzyme	Distribution Pattern	Fraction 8	Fraction9
isocitrate lyase	peroxisome(P)	24.2%	0%
malate synthase	P	27.5%	3.9%
catalase	P	29.2%	1.9%
fatty acyl-CoA oxidase	P	30.7%	0%
NADP-Icdh	P-M-soluble	34.5%	35.7%
succinate dehydrogenase	Mitochon. (M)	29.1%	0%
malate dehydrogenase	M	30.0%	0.8%
glutamate dehydrogenase	M	29.4%	2.8%
fumarase	M	26.8%	0%
fatty acyl-CoA dehydrogenase	M	1.4%	3.1%
citrate synthase	M	0.4%	6.4%
asp.-α-ketoglut. transaminase	P-M	21.3%	0.3%
NAD-Icdh	M	1.6%	2.5%
lactate oxidase	P	0%	1.8%
acid phosphatase	lysosome(L)	67.6%	4.6%
glucose 6-phosphate isomerase	L	73.1%	1.7%
B-oxidation with butyryl CoA	-	100%	0%
B-oxidation with lauryl CoA	-	0%	0%
pyruvate kinase	soluble	27%	58%

Figure 20 provides the distribution patterns in the sucrose density gradient of glucose-6-phosphate isomerase from log phase, log phase after 4 hours of hypoxia and stationary phase cells. The patterns of the stationary phase and hypoxically induced non-dividing cells show an accumulation in fraction 8, with a small peak also occurring in fraction 3. All patterns observed for this enzyme most closely follow the acid phosphatase marker in their distribution. Surprisingly no significant amount of this glycolytic enzyme is found in the soluble fraction (number 9), where other studies have shown the glycolytic enzymes to be localized (85, 86). In these other studies a different strain of T. pyriformis (HSM) was used. Perhaps more important however, is the difference in the method used for cell disruption. The filtration method used here yielded quantitative recoveries ($100 \pm 10\%$) for all enzymes studied. More importantly the organelles do not appear to be disrupted, as indicated by the complete sedimentation of enzymes known to be particulate, and the pronounced latency displayed by them (15, 87). The other method of disruption specifies 100 up and down strokes of a Potter homogenizer to disrupt the cells (85, 86, 88). This procedure does not produce quantitative recoveries, nor does it seem to maintain the integrity of subcellular organelles, as witnessed by a 28% solubilization of glutamate dehydrogenase and 56% solubilization of isocitrate lyase (88). There is no indication on how well lysosomal integrity

FIGURE 20. Distribution of glucose-6-phosphate isomerase in a sucrose density gradient. (□)-45 hours; (○)-45 hours + 4 hours of hypoxia; (△)-138 hours

FIGURE 20

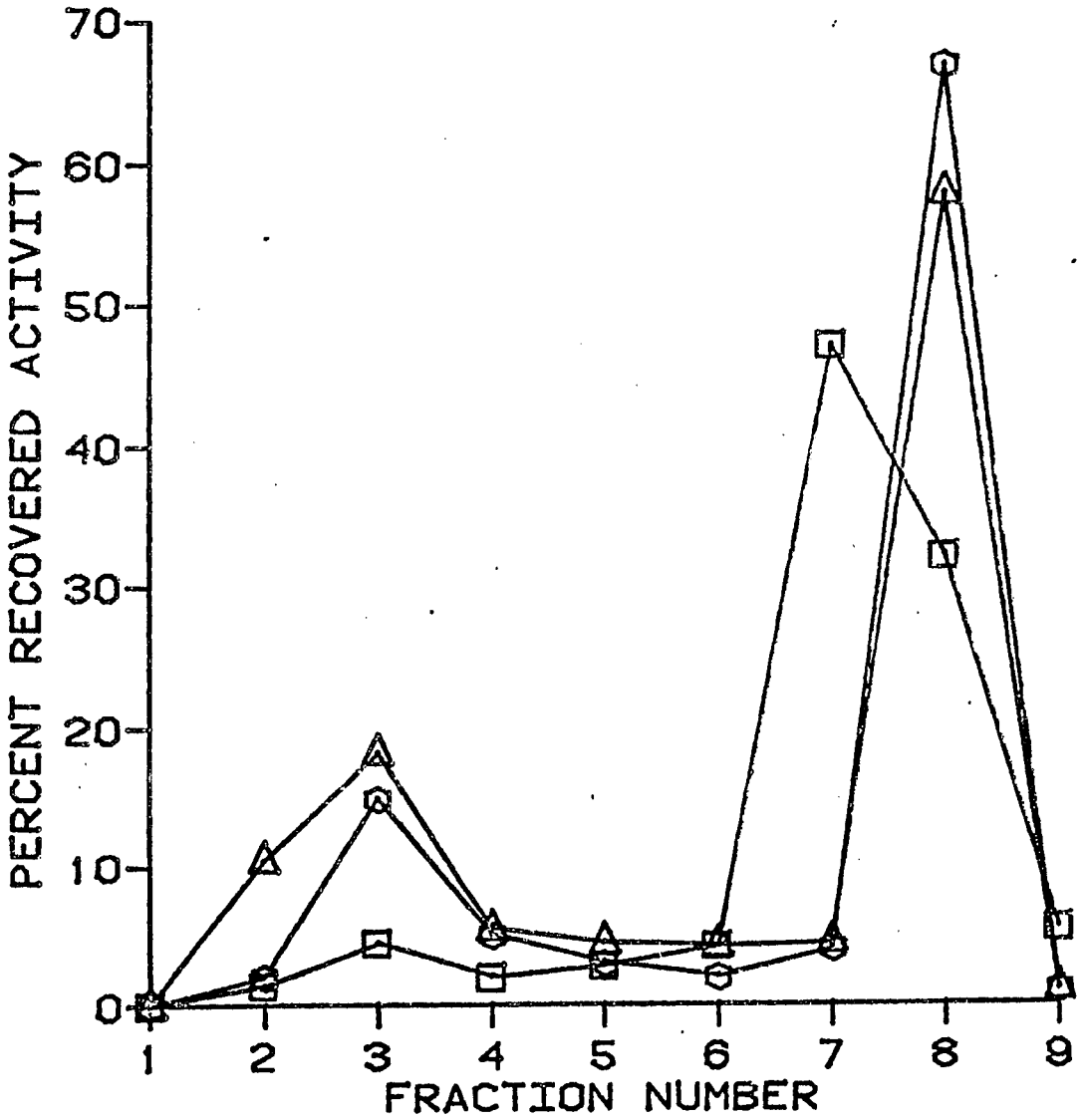
70
60
50
40
30
20
10
0
PERCENT RECOVERED ACTIVITY
1
2
3
4
5
6
7
8
9
FRACTION NUMBER

is preserved in these studies. In view of lysosomal fragility (89) and of my observation that glucose-6-phosphate isomerase occurs in lysosomal fraction(s) it may be important to restudy the subcellular location of all glycolytic enzymes of Tetrahymena. The recent finding that fructose-1,6-diphosphatase is activated by lysosomal cathepsins in rat liver (90) also suggests that this mammalian enzyme may function within lysosomes (or another organelle containing lysosomal enzymes).

Electron micrographs were prepared by O. Roger Anderson for log phase cells, log phase cells subjected to hypoxic conditions for 4 hours (See Materials and Methods) and stationary phase cells. Figure 21 shows the general structural features of cells in the log phase of growth. Large vacuoles, approximately 5-6 um in diameter (V, Figure 21) contain small amounts of a dispersed material that may be membranous debris or other cytoplasmic matter suggestive of limited autophagic activity. Numerous small granular deposits, densely-stained by lead show the vast stores of glycogen in the cytoplasm. The general cytoplasmic organization in log phase cells subjected to 4 hours of hypoxia is shown in Figure 22. The most prominent feature is the abundant autophagic vacuoles which contain mitochondria (Figure 24) and peroxisomes (Figures 25 and 26). A unique feature of these hypoxic log phase cells is the engulfment of glycogen granules by peroxisomes illustrated in

FIGURE 21.

Top. A section through the nuclear region of a log phase cell exhibits the macronucleus (N), large vacuoles (V), dense deposits of glycogen and mitochondria (M) at the periphery of the cell.

Bottom. Peroxisomes (P) and densely-stained vesicles that appear to be primary lysosomes (Ly) occur in the peripheral cytoplasm near the large vacuoles (V) of a log phase cell.

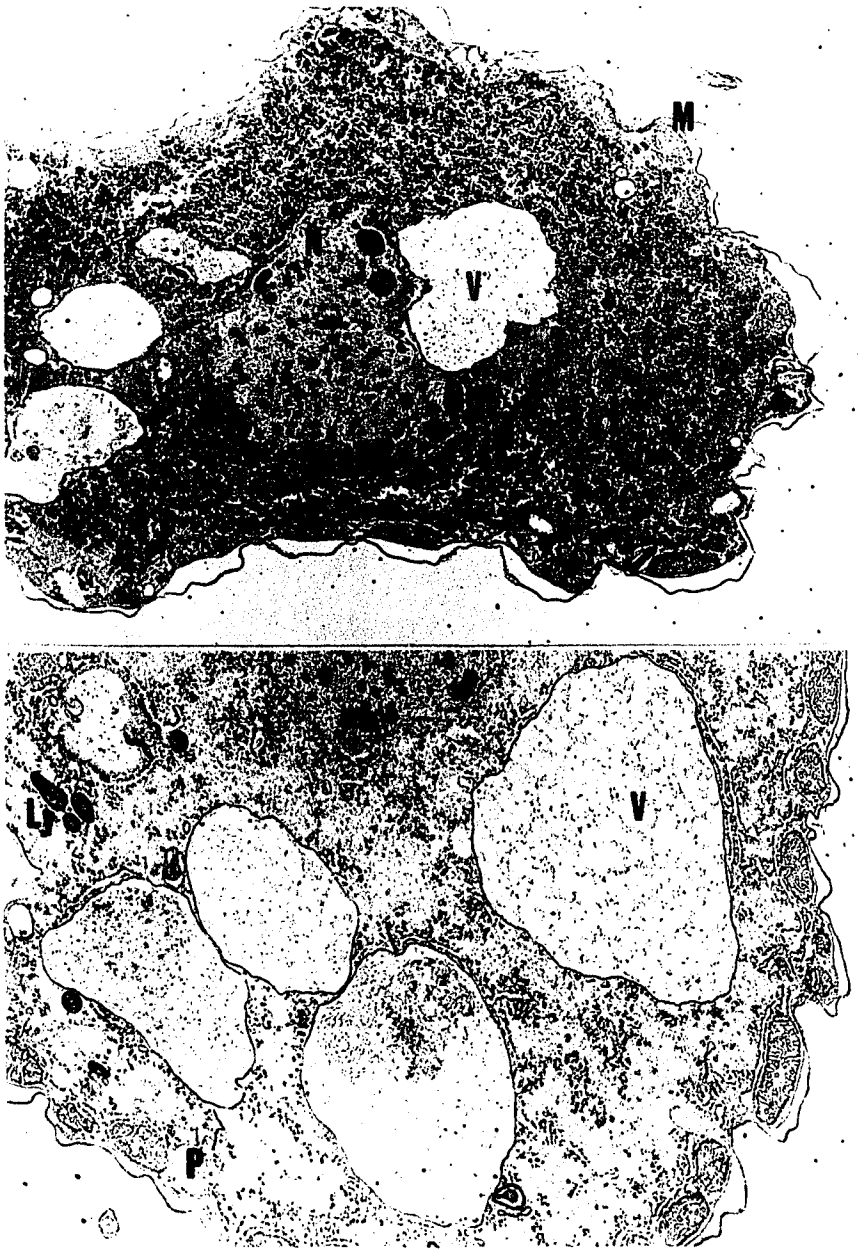

Figure 21

FIGURE 22. A section through the nuclear region of a log phase cell after 4 hours of hypoxia exhibits autophagic vacuoles containing densely-stained residual matter. Peroxisomes (P) occur in the vicinity of the nucleus and scattered throughout the cytoplasm which contains dense deposits of glycogen. Mitochondria appear largely at the periphery of the cell.

Inset: Autophagic vacuole contains a mitochondrion and some glycogen granules (arrow).

Figure 22

FIGURE 23. A stationary phase cell contains vacuoles filled with residual matter including membranes, lipid droplets and large masses of glycogen (arrow).

FIGURE 24. Log phase cell + 4 hours of hypoxia. A nearly intact mitochondrion is surrounded by membranes (arrow) of a presumptive autophagic vacuole while a nearby vacuole contains inclusions and a partially disrupted mitochondrion.

FIGURE 25. (middle-bottom) Log phase cell + 4 hours of hypoxia. Peroxisomes are surrounded by concentric layers of endoplasmic reticulum (arrow).

FIGURE 26. (bottom-right) Log phase cell + 4 hours of hypoxia. An intact peroxisome (P) with granular matrix and occasional tubule like membranous inclusions lies next to a vacuole containing degraded granular matter (asterisk) resembling a peroxisome.

Figure 23

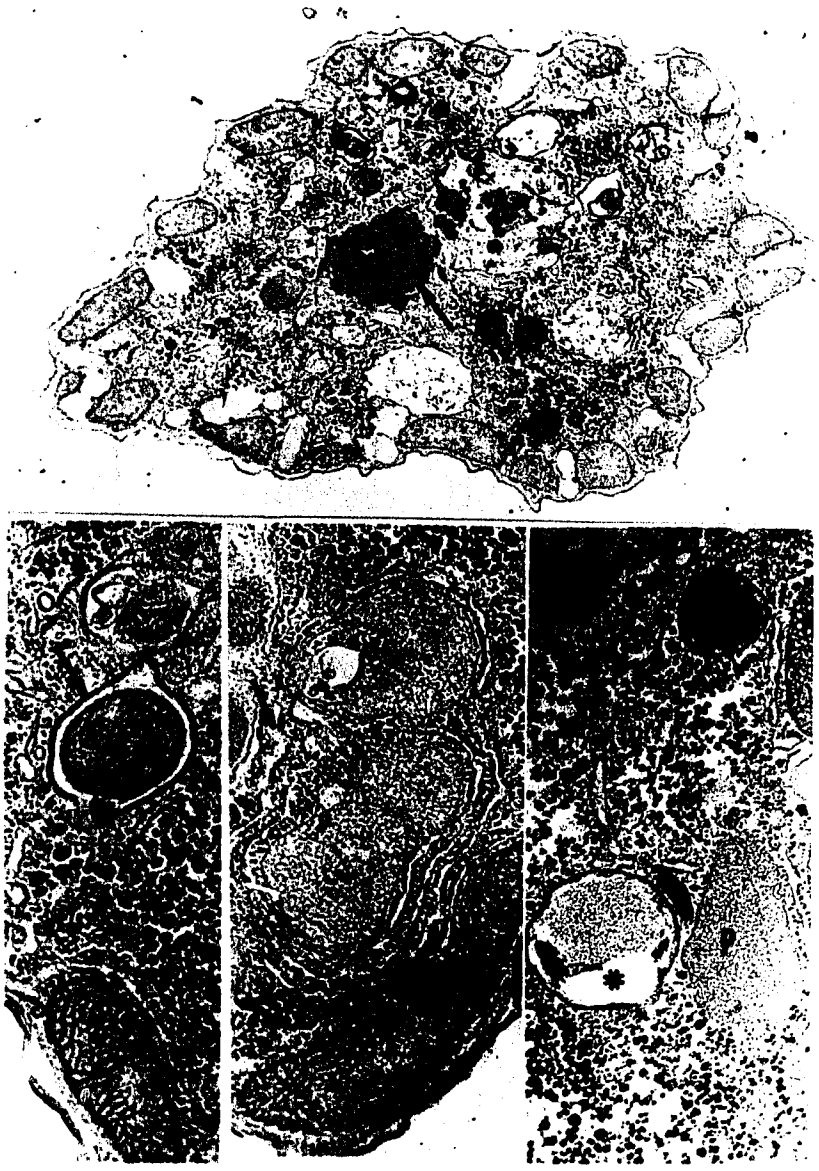

Figure 24 Figure 25 Figure 26

Figures 27, 28, 29 and 30. The engulfed glycogen is surrounded by a membrane which appears eventually to undergo degradation (Figure 30). Glycogen analyses confirm that limited glycogenolysis is occurring while these cells are subjected to a decreased oxygen tension (See Table 17). Upon returning these cells to a more oxygenated state, glycogen begins to increase, thus confirming the observations of Stein and Blum (70) on hypoxic cells.

Stationary phase cells exhibit varying stages of advanced vacuolar sequestration of cytoplasmic components (Figures 23 and 31). Some of the larger vacuoles contain residual membranous whorls and lipid droplets as are often observed in the late stages of digestive vacuoles (91). Other vacuoles contain abundant deposits of osmiophilic substances and large compact masses of glycogen (arrow, Figure 23). Table 18 compares low speed (20,000 g-min) sedimentable glycogen in both log and stationary phase cells. In confirmation of the electron micrographs (Figure 23) much of the glycogen in the stationary phase cells (55%) is found to sediment at low speeds, while less than 10% of the glycogen in log phase cells sedimented. Furthermore, of the radioactive acetate (2-^{14}C) incorporated into glycogen by stationary phase cells(42%), greater than 70% is found in the particulate glycogen (i.e. sedimentable at low speeds).

Fraction 8 from the sucrose density gradient was examined for both log and stationary phase cells. Fraction 8 from log phase

TABLE 17. Changes in glycogen content in log phase cells after exposure to extreme hypoxic conditions and subsequent aeration. All values are for 1ml of cell suspension, originating from the same suspension, but differing in treatment. Each value is based on six trials.

	glycogen in terms of glucose
log phase cells	2.75 ± 0.10 mg/ml
log phase cells + 4 hours hypoxia	2.00 ± 0.11 mg/ml
log phase cells + 4 hours hypoxia + only 30 minutes aeration	2.43 ± 0.08 mg/ml

FIGURE 27. (top-left) Log phase cell + 4 hours of hypoxia. A peroxisome engulfs a cytoplasmic mass containing glycogen.

FIGURES 28 (top right) and 29 (middle-left) Log phase cell + 4 hours of hypoxia. Peroxisomes containing glycogen within a membrane-bound compartment.

FIGURE 30. (middle-right) Log phase cell + 4 hours of hypoxia. The thin inner membrane surrounding glycogen in a peroxisome has been partially dissipated and the glycogen appears less dense than in peroxisomes with an intact boundary membrane.

FIGURE 31. (bottom) Stationary phase cell. Vacuoles containing thin, partially degraded deposits of lipid and lipid droplets are observed.

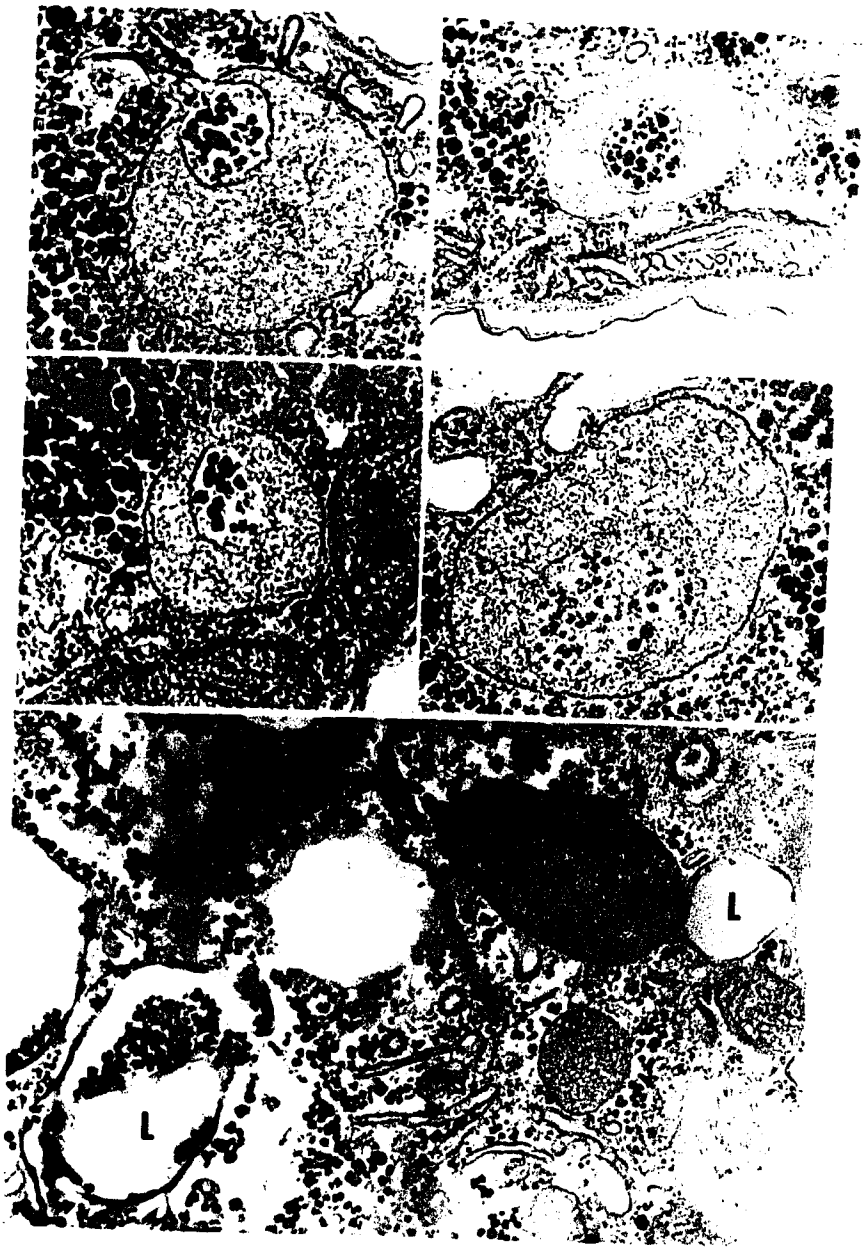

Figures 27-31

TABLE 18. Glycogen distribution between pellet and supernatant fractions in log and stationary phase cells, and the distribution of [2-^{14}C]-acetate incorporated into pelleted and soluble glycogen in stationary phase cells(42% of ^{14}C was found in total glycogen).

	Supernatant	Pellet
Log phase cells	93%	7%
Stationary phase cells	45.5%	54.5%
^{14}C-glycogen in stationary phase cells	29%	71%

cells (Figure 32) contained small vesicles and membrane fragments. The membranes however are thickened (160-210 Å thickness) and densely osmiophilic, thus resembling the membranes surrounding autophagic vacuoles. It may also be important to recall that there is no significant build-up of mitochondrial or peroxisomal enzymes in fraction 8 at this stage of cellular growth. Thus, the membranes in Figure 32 may be precursors to autophagic vacuolar membranes. Fraction 8 from stationary phase cells (Figures 33, 34, 35 and 36) contained large vacuoles filled with glycogen, autophagic vacuoles in various stages of digestive activity, membrane-enclosed lipid droplets and occasional ciliary fragments. The vacuolar membranes are thickened and osmiophilic, as was also observed in the smaller membrane fragments of fraction 8 from log phase cells; this may indicate they are rich in lipid, thus in part accounting for their low density. There is a clear resemblence between the vacuolar bodies found in fraction 8 from stationary phase cells, and the stages of autophagic vacuoles observed in hypoxia induced and later stages of stationary phase development. Thus, it appears that fraction 8 from stationary phase cells contains glycogen-enriched autophagic vacuoles enclosing the remains of engulfed mitochondria, peroxisomes and masses of cytoplasm. The presence of significant amounts of peroxisomal and mitochondrial enzymes in this fraction coupled with the electron micrographs showing no obvious peroxisomes and only mitochondria

in the later stages of degradation indicates these enzymes may now be enclosed together within a common vacuolar compartment. This may be similar to the P_1 fraction that Hogg and Kornberg (7) isolated from stationary phase cells.

FIGURE 32. (top) Fraction 8 of log phase cells showing thickened membranes with little or no glycogen or internal structure observable.

FIGURE 33. (middle) An electron micrograph of a section from fraction 8 obtained fromstationary phase cells contains membrane-enclosed glycogen.

FIGURES 34-36. (bottom) A section from fraction 8 obtained from stationary phase cells exhibiting varying stages of organelle degradation in autophagic vacuoles.

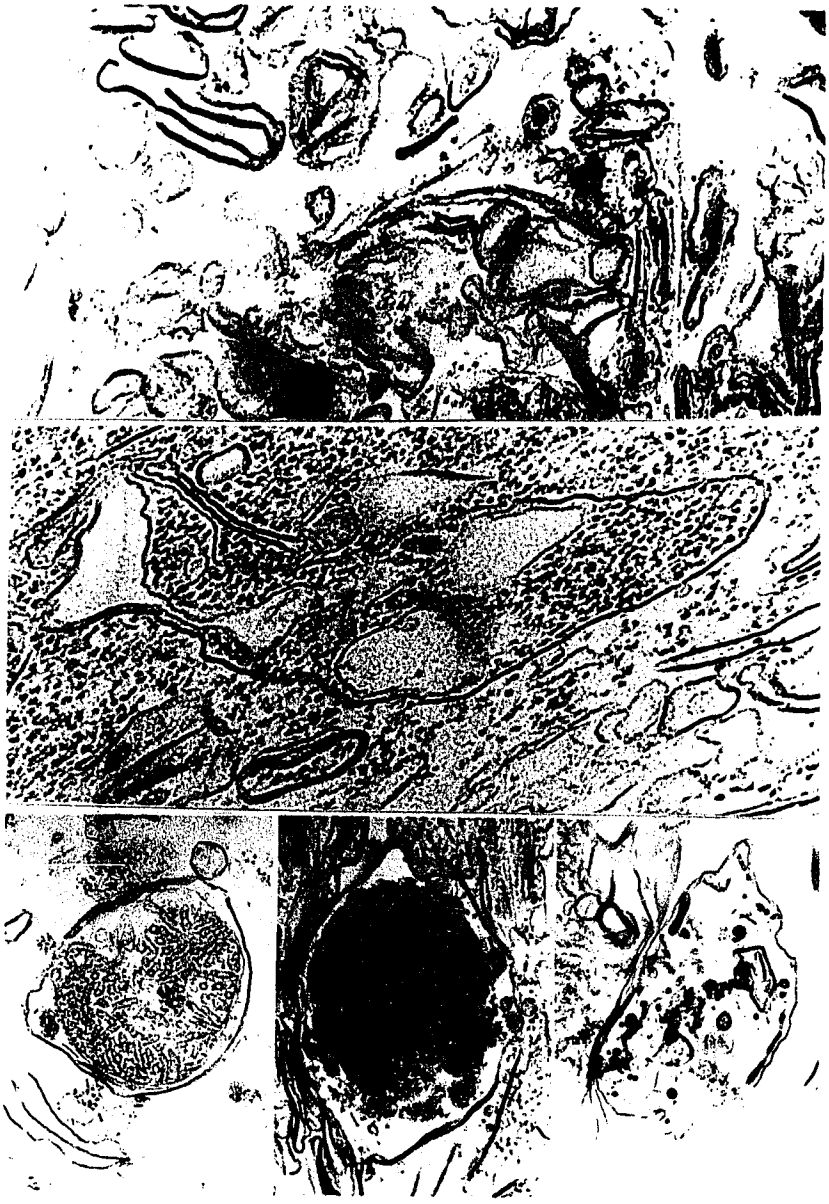

Figures 32-36

DISCUSSION

The electron microscopic evidence shows substantial reorganization of the cytoplasm during the transitions from log phase growth to an hypoxia induced stationary phase or stationary phase growth. Equilibrium density patterns of subcellular particles as marked by enzymic distribution likewise show distinctive changes in going from log to stationary phase growth. While the characteristic enzyme activity peaks for mitochondria and peroxisomes persist at or about the same equilibrium densities as in log phase cells, a low density particulate accumulation of enzymes from several organelles appears as the cells enter the stationary phase. Concurrent with the redistribution of a large portion of particulate enzymes to a lower equilibrium density is a dramatic increase in autophagic vacuole formation. Elliot and Bak (92) had associated this increase in autophagic events with the normal process of "ageing". Levy and Elliot (93) also noted that by inducing stationary phase growth by transfer to a non-nutrient medium, a large increase in autophagy of organelles and cytoplasm occurred, and acid phosphatase was localized in or on these autophagic vacuoles. In stationary or hypoxically induced non-dividing cells I find acid phosphatase to be situated almost entirely in a particulate fraction of low density (fraction 8). Furthermore, there is a clear resemblance

in the electron micrographs between the vacuolar bodies found in fraction 8 (Figures 33-36) from homogenate of stationary phase cells and the autophagic vacuoles observed in whole stationary phase cells or hypoxic log phase cells (Figures 23, 24, 25, 26 and 31). The seemingly aberrant peak of glutamate dehydrogenase at a peroxisomal density (fraction 3-1.235 grams/ml) in log phase cells subjected to 4 hours of hypoxia (Figure 19) is accompanied by acid phosphatase activity and thus may represent incipient autophagic activity (I have also shown in Figure 19 that fumarase follows a pattern identical to that of glutamate dehydrogenase).

Concomitant with the increase of autophagy there is an increased capacity to synthesize glycogen by T. pyriformis. Log phase cells are able to convert exogenous glucose very rapidly to glycogen (2, 94), but lack the ability to convert exogenous acetate or endogenous lipids into glycogen. Log phase cells can develop this ability when subjected to hypoxic conditions (8, 14, 69, 70), a procedure that also causes the rapid cessation of cell division. However, net glyconeogenesis in T. pyriformis absolutely requires the presence of oxygen (8, 17). Although the system involved in glycogen synthesis can be induced under extremely low oxygen conditions, the organism continues to use up its glycogen reserves (17, 70) until oxygen is present (8, 70). My data are in complete agreement with these previous studies. Table 17 shows

a decrease in total glycogen after 4 hours of hypoxia. When these same cells were vigorously aerated for 30 minutes (by shaking after providing for a large increase in the surface area available to absorb oxygen) there was a net increase (+22%) in the total glycogen content of these cells. Although no exogenous nutrients were added, endogenous sources, most notably phospholipids can account for this glycogen increase (2, 5, 95).

The engulfment of glycogen into peroxisomes and what appears to be an intraorganellar dispersal of this glycogen within the matrix of the peroxisome (Figures 27, 28, 29 and 30) could provide the site for glycogenolysis that was noted in log phase cells subjected to 4 hours of hypoxia (Table 17). From these hypoxic cells glucose-6-phosphate isomerase shows an equilibrium density pattern with two peaks (Figure 20). It has a high density peak that overlaps the peroxisomal fraction (fraction 3) and a lower density peak found in fraction 8. Thus, this enzyme, which is necessary for glycogenolysis, has a subcellular distribution that is in accordance with the proposal that glycogenolysis may take place in the peroxisome. (It had been previously postulated that a portion of glycolysis in T. pyriformis takes place within the mitochondria (96).) In these hypoxic cells, small amounts of glycogen have been found to be entrapped, along with mitochondria in an autophagic vacuole (Figure 22). However, at no stage of growth that was studied did I find

glucose-6-phosphate isomerase accumulating at the equilibrium density (1.21-1.22 grams/ml or fraction 5 in the gradient) accepted for T. pyriformis mitochondria (15). Thus, it does not seem possible that glycogenolysis can take place in mitochondria.

While glycolysis is occurring during periods of extreme oxygen deprivation in log phase cells, in contrast the capability to synthesize glycogen from exogenous acetate or endogenous lipids is concomitantly developing. But the fulfillment of this capability requires the presence of oxygen (8, 70). Induction of the key enzymes involved in glyconeogenesis from fats does not adequately explain this development, since both malate synthase and isocitrate lyase (the glyoxylate bypass enzymes) are present in log phase cells at levels that can exceed the rates required for glycogen synthesis in stationary phase cells (8). Furthermore, activation of glyconeogenesis by 3 hours of hypoxia resulted in a 14-fold increase in glyconeogenic capacity, but less than a 2-fold increase in isocitrate lyase activity (8). Moreover, the rise in isocitrate lyase, as well as malate synthase, can be prevented by addition of chloramphenicol or actinomycin D and hypoxia still activates glyconeogenesis (97). In spite of their apparent enzymatic competence to perform glyconeogenesis, log phase cells are not capable of gluconeogenesis from fats (2, 8, 14). Since the enzymatic capability for glyconeogenesis is present in both log and stationary phase cells, the poss-

ibility that control lies at the level of activating or inhibitory regulators of key enzyme(s) in the pathway cannot be excluded. However, the period of induction (3 hours) that fully activates glyconeogenesis in log phase cells (8) seems too long for such a mechanism. The data presented here suggest another and very different mechanism for this activation of glyconeogenesis.

The engulfment of mitochondria, peroxisomes and masses of glycogen-rich cytoplasm into autophagic vacuoles may provide a mechanism whereby mitochondrial and peroxisomal enzymes are brought together in a common membrane-bound compartment that will facilitate efficient glyconeogenesis. The essential enzymes for lipid gluconeogenesis-mitochondrial, peroxisomal and cytosolic-are therefore combined into a common vacuolar space with fatty acids from the breakdown of membrane lipids and glycogen acceptor molecules. Table 16 provides a partial list of the enzymes that accumulate and remain active in the putative synthetic autophagic vacuole (fraction 8 from the sucrose density gradient fractionation of stationary phase cells). The bulk of the acid phosphatase is found there also, thus suggesting that much of the lysosomal proteases are also present. Furthermore, there is evidence of digestive activity within the vacuoles that contain the engulfed cytoplasmic organelles. If the gluconeogenic enzymes released from the mitochondria and peroxisomes are to remain active, there must be either limited

proteolysis or these enzymes must exhibit unusual resistance to proteolysis. Table 16 provides circumstantial evidence for this point. Those enzymes absolutely required for lipid gluconeogenesis are spared, while those that might be deleterious to or unnecessary for glycogen synthesis are absent or present in very low amounts. At the present time there is very little known about the biochemical pathways leading to intracellular degradation of proteins. Very recently Levine et al. (98) have shown that a covalent modification is involved in inactivating glutamine synthetase of bacteria and thereby labelling it for digestion. Catalase blocks this modification step essential for intracellular proteolysis. In the proposed glycogen synthesis vacuole, catalase is found in abundance. Going further, the results of Pontremoli et al. (99) for mammalian liver indicate that lysosomal proteases are involved in activating fructose-1,6-diphosphatase, rather than in degrading this enzyme (100). Thus, the lysosome appears to achieve more than the mere destruction of biopolymers.

NAD-linked isocitrate dehydrogenase is a notable absentee from fraction 8, which contains many other mitochondrial enzymes. Its absence from the proposed gluconeogenic vacuole is vital since it has never been shown to be reversible and therefore it would compete strongly for isocitrate with isocitrate lyase. The fact that NADP-linked isocitrate dehydrogenase is present in large amounts in

fraction 8 from the sucrose density gradient of stationary phase cells could represent a significant obstacle for gluconeogenesis by competing for the isocitrate required for isocitrate lyase to act in the glyoxylate cycle. Alternatively, as explained in chapters 1 and 2, this enzy me may act as a source of isocitrate and thus eliminate any need for citrate synthase as the primary source of isocitrate. A potential source of NADH, as well as acetyl-CoA has been confirmed with the finding that uncoupled (a peroxisomal type of) β-oxidation takes place in the putative glycogen synthetic vacuole (see Table 16). The first enzyme of this novel β-oxidation system is the fatty acyl-CoA oxidase (19). Its requirement for oxygen as a substrate may account for the need for oxygen in gluconeogenesis from fats. It may be important that the β-oxidation found here was neither peroxisomal nor mitochondrial. Virtually all of the activity was found in fraction 8 of the sucrose density gradient, and butyryl-CoA but not lauryl-CoA had activity. This short chain length specificity has been associated with peroxisomal β-oxidation of T. pyriformis (19, 76). This association of uncoupled, short chain length β-oxidation with peroxisomes was based on relatively simple differential centrifugation method (7) which has only 3 fractions (P_n, P_1, S), and cannot distinguish between peroxisomes and the lower density accumulation of peroxisomal and other particulate enzymes. In fact Hogg and Kornberg (7) had proposed the P_1 fraction was a "glyoxylate cycle granule" whose accumulation of

mitochondrial enzymes (succinate dehydrogenase, malate dehydrogenase and citrate synthase) along with other key enzymes of the glyoxylate cycle (isocitrate lyase and malate synthase) gave it gluconeogenic potential. Expanding on this concept, by using a different subcellular fractionation method I have separated peroxisomes (fraction 3) from fraction 8 particles which have been postulated to be involved in glyconeogenesis. The finding that uncoupled β-oxidation takes place only in this fraction and that its products-acetyl-CoA and NADH-could fuel gluconeogenesis supports and extends the old concept of a "glyoxylate cycle granule!"

In stationary phase cells, many of the large, late-stage autophagic vacuoles contain copious amounts of glycogen which may be products of lipid glyconeogenesis. The occurrence of large autophagic vacuoles containing masses of glycogen (found both in fraction 8 and in whole stationary phase cells) in conjunction with the biochemical evidence of enriched peroxisomal and mitochondrial enzyme activity in fraction 8 lends support to the concept of compartmentalization of gluconeogenesis and/or glyconeogenesis through autophagic vacuolarization. These findings suggest a much more diversified role for autophagic vacuoles in cellular metabolism.

There is now evidence that autophagic events also may govern gluconeogenesis from amino acids in liver (101). However, there has not been any evaluation of the constituent enzymes of these

autophagic vacuoles with respect to gluconeogenesis. A further complication is the mechanical and osmotic fragility of the liver vacuoles (89), as indicated by the nonlatent activity of acid hydrolases in liver homogenates. Thus, any study of a postulated glycogen-synthesizing vacuoles in liver necessarily will require very mild cell disruption methods as a precondition to success.

REFERENCES

1. Manners, D.J. and Ryley, J.F. (1952) Biochem. J. 52, 480-482.

2. Wagner, C. (1956) Ph. D. Thesis, University of Michigan, Ann Arbor, Michigan.

3. Manners, D.J. and Ryley, J.F. (1963) J. Protozool. 10, 28.

4. Barber, A.A., Harris, W.W. and Padilla, G.M. (1965) J. Cell Biol. 27, 281-292.

5. Warnock, L.G. and Van Eys, J. (1962) J. Cell. Comp. Physiol. 60, 53-59.

6. Barnekow, A. (1978) Biochem. Soc. Trans. 6, 184-187.

7. Hogg, J.F. and Kornberg, H.L. (1963) Biochem. J. 86, 462-468.

8. Hogg, J.F. (1969) Ann. N.Y. Acad. Sci., 168, 281-291.

9. Goodman, D.B.P., Davis, W.L. and Jones, R.G. (1980) Proc. Natl. Acad. Sci. U.S.A., 77, 1521-1525.

10. Jones, C.T. (1980) Biochem. Biophys. Res. Commun., 95, 849-856.

11. Jones, R.G., Davis, W.L. and Goodman, D.B.P. (1981) J. Histochem. Cytochem. In press.

12. Kornberg, H.L. and Krebs, H.A. (1957) Nature, 179, 988-991.

13. Campbell, J.J.R., Smith, R.A., and Eagles, B.A. (1953) Biochim. Biophys. Acta 11, 594-597.

14. Levy, M.R. and Scherbaum, O.H. (1965) J. Gen. Microbiol.

38, 221-230.

15. Muller, M., Hogg, J.F. and deDuve, C. (1968) J. Biol. Chem. 243, 5385-5395.

16. Eldan, M. and Blum, J.J. (1975) J. Protozool. 22(1), 145-149.

17. Ryley, J.F. (1952) Biochem. J. 52, 483-492.

18. Cooper, T.C. and Beevers, H. (1969) J. Biol. Chem. 244, 3514-3520.

19. Hryb, D.J. (1980) Ph. D. Thesis, City University of N.Y., N.Y., N.Y.

20. Levy, M.R. (1972) Arch. Biochem. Biophys. 152, 463-471.

21. Lord, J.M., Mcfadden, B.A. and Kornberg, H.L. (1974) Proc. R. Soc. Lond. B. 185, 19-31.

22. Machado, A. and Satrustegul, J. (1981) Biochimie 63, 247-249.

23. Dorsey, T. (1975) Ph. D. Thesis. City University of N.Y., N.Y., N.Y.

24. Plaut, G.W.E. (1970) Curr. Top. Cell. Regul. 2, 1-27.

25. Chen, R.F. and Plaut, G.W.E. (1963) Biochem. 2, 1023-1032.

26. Smith, C.M. and Plaut, G.W.E. (1979) Eur. J. Biochem. 97, 283-295.

27. Kornberg, A. and Pricer, W.E. Jr. (1951) J. Biol. Chem. 189, 123-136.

28. Kobiyashi, S. (1965) J. Biochem. 58, 444-457.

29. Kornberg, A. (1955) M. in Enzym. 1, 705-707.

30. Andrews, P. (1965) Biochem. J. 96, 595-606.

31. Gabriel, O. (1971) M. in Enzym. 22, 565-578.

32. Dietz, A. and Lubrano, T. (1967) Anal. Biochem. 20, 246-257.

33. Weichselbaum, T.E. (1946) Am. J. Clin. Path. Suppl. 10, 40-49.

34. Cook, R.A. and Sanwal, B.D. (1969) M. in Enzym. 13, 42-47.

35. Cox, G.F. and Davies, D.D. (1969) Biochem. J. 113, 813-821.

36. Carlier, M.-F. and Pantaloni (1973) Eur. J. Biochem. 37, 341-354.

37. Dalziel, K. (1980) FEBS letters 117(suppl.), K45-K55.

38. Colman, R.F. (1976) Adv. in Enzy. Regul. 13, 413-433.

39. Atkinson, D.E., Hathaway, J.A. and Smith, E.C. (1965) J. Biol. Chem. 240, 2682-2690.

40. Nishi, A. and Scherbaum, O.H. (1962) Biochim. Biophys. Acta 65, 411-418.

41. Macfarlane, N., Matthews, B. and Dalziel, K. (1977) Eur. J. Biochem. 74, 533-559.

42. Illingworth, J.A. and Tipton, K.F. (1970) Biochem. J. 118, 253-258.

43. Vidal, P. and Machado, A. (1978) Molec. and Cell. Biochem. 17, 151-156.

44. Nanney, D.L., Cooper, L.E., Simon, E.M. and Whitt, G.S. (1980) J. Protozool. 27(4), 451-459.

45. Bautista, J., Satrustegul, J. and Machado, A. (1979) FEBS Letters 105, 333-336.

46. Ragland, T.E., Kawasaki, T. and Lowenstein, J.M. (1966) J. Bacteriol. 91, 236-244.

47. Hampton, M.L. and Hanson, T.S. (1969) Bacteriol. Proc. 118-122.

48. Rahat, M., Judd, J. and Van Eys, J. (1964) J. Biol. Chem. 239, 3537-3545.

49. Luck, H. (1963) In: Methods of Enzymatic Analysis, edited by H.U. Bergmeyer. New York: Academic Press, Inc., p885.

50. Dixon, G.H. and Kornberg, H.L. (1959) Biochem. J. 72, 3P.

51. Bergmeyer, H.U., Gawehn, K. and Grassl, M. (1974) In: Methods of Enzymatic Analysis, edited by H. U. Bergmeyer. New York and London: Academic Press Inc. Vol. 1, pp452-453.

52. Hooper, A.B., Terry, K.R. and Kemp, K.D. (1974) Biochim. Biophys. Acta 358, 14-20.

53. Torriani, A. (1960) Biochim. Biophys. Acta 38, 460-469.

54. Stadtman, E.R. (1957) M. of Enzym. 3, 931-934.

55. Denton, R.M., Richards, D.A. and Chin, J.G. (1978) Biochem. J. 176, 899-906.

56. Goebell, H. and Klingenberg, M. (1964) Biochem. Z. 340, 441-447.

57. Klingenberg, M., Goebell, H. and Wenske, G. (1965) Biochem.

Z. 341, 199-208.

58. Plaut, G.W.E. and Aogaichi, T. (1968) J. Biol. Chem. 243, 5572-5583.

59. Scherbaum, O.H., Chou, S.-C., Seraydarian, K.H. and Byfield, J.E. (1962) Can. J. Microbiol. 8, 753-760.

60. Warnock, L.G. (1962) Diss. Abstr. 23, 3623.

61. Klingenberg, M. (1976) In: "The Enzymes of Biological Transport" (A. Martinose editor) Vol. 3, pp383-438, Plenum Press, N.Y.

62. Williamson, J.R. (1976) In: "Mitochondria: Bioenergetics, Biogenesis and Membrane Structure" (L. Packer editor) pp79-107, Academic Press, N.Y.

63. Erecinska, M., Wilson, D.F. and Nishiki, K. (1978) Am. J. Physiol. 3, C82-C89.

64. Shug, A.L., Ferguson, S. and Shrago, E. (1968) Biochem. Biophys. Res. Commun. 32, 81-85.

65. Kilpatrick, L. and Erecinska, M. (1977) Biochim. Biophs. Acta 462, 515-530.

66. Williamson, J.R. and Cooper, R.H. (1980) FEBS Letters 117(suppl.), K73-K83.

67. Hansford, R.G. and Johnson, R.N. (1975) J. Biol. Chem. 250, 8361-8375.

68. Smith, C.M., Bryla, J. and Williamson, J.R. (1974) J. Biol. Chem. 249, 1497-1505.

69. Raugi, G.J., Lliang, T. and Blum, J.J. (1975) J. Biol. Chem. 250, 445-460.

70. Stein, R.B. and Blum, J.J. (1981) J. Biol. Chem. 256, 2752-2760.

71. Eichel, H.J. (1961) J. Protozool. 8(suppl.), 16.

72. Levy, M.R. (1970) Biochim. Biophys. Acta 201, 205-214.

73. van Niel, C.B., Thomas, J.O., Rubens, T.S. and Kamen, M.D. (1942) Proc. Natl. Acad. Sci., U.S.A. 28, 157-161.

74. Diestershaft, M.D., Hsieh, H.-C., Elson, C., Sallach, H.J. and Shrago, E. (1972) J. Biol. Chem. 247, 2755-2762.

75. Durchschlag, H., Biederman, G. and Eggerer, H. (1981) Eur. J. Biochem. 114, 255-262.

76. Hryb, D.J. and Hogg, J.F. (1976) Fed. Proc. FASEB 35, 1501.

77. Ochoa, S. (1955) M. of Enzym. 1, 735.

78. Muller, M. (1969) Ann. N.Y. Acad. Sci. 168, 292-302.

79. Slein, M.W. (1955) M. of Enzym. 1, 304-306.

80. Patterson, M.S. and Greene, R.C. (1965) Anal. Chem. 37, 854-860.

81. Morris, D.L. (1948) Science 107, 254-257.

82. Baudhuin, P., Evrard, P. and Berthet, J. (1967) J. Cell Biol. 32, 181-195.

83. Baudhuin, P., Muller, M., Poole, B. and deDuve, C. (1965) Biochem. Biophys. Res. Commun. 20, 53-57.

84. Levy, M.R. and Wasmuth, J.J. (1970) Biochim. Biophys. Acta 201, 205-214.

85. Eldan, M. and Blum, J.J. (1973) J. Biol. Chem. 248, 7445-7448.

86. Risse, H.J. and Blum, J.J. (1972) Arch. Biochem. Biophys. 149, 329-335.

87. Muller, M., Baudhuin, P. and deDuve, C. (1966) J. Cell Physiol. 68, 165-175.

88. Porter, P., Blum, J.J. and Elrod, H. (1972) J. Protozool. 19, 375-378.

89. Deter, R.L. and deDuve, C. (1967) J. Cell Biol. 33, 437-449.

90. Pontremoli, S., Melloni, E. and Horecker, B.L. (1981) Biochem. Soc. Trans. 9(2), 258P.

91. Novikoff, P.M. and Novikoff, A.B. (1972) J. Cell Biol. 53, 532-560.

92. Elliot, A.M. and Bak, I.J. (1964) J. Cell Biol. 20, 113-129.

93. Levy, M.R. and Elliot, A.M. (1968) J. Protozool. 15, 208-222.

94. Borowitz, M.J., Stein, R.B. and Blum, J.J. (1977) J. Biol. Chem. 252, 1589-1605.

95. Hogg, J.F. and Wagner, C. (1957) Fed. Proc. 15, 275.

96. Shrago, E. and Elson, C. (1980) In: "Biochemistry and Physiology of Protozoa" Vol. 3, pp287-312. Academic Press, N.Y.

97. Levy, M.R. (1967) J. Cell. Physiol. 69, 247-252.

98. Levine, R.L., Oliver, C.N., Fulks, R.M. and Stadtman, E.R.

(1981) Proc. Natl. Acad. Sci., U.S.A. 78, 2120-2124.

99. Pontremoli, S., De Flora, A., Salamino, F., Melloni, E. and Horecker, B.L. (1975) Proc. Natl. Acad. Sci., U.S.A. 72, 2969-2973.

100. Melloni, E., Pontremoli, S., Salamino, F., Sparatore, B., Michetti, M. and Horecker, B.L. (1981) Arch. Biochem. Biophys. 208, 175-183.

101. Aronson, N.N., Jr. (1980) Life Sciences 27, 95-104.

102. Conner, R.L., Cline, S.G., Koroly, M.J. and Hamilton, B. (1966) J. Protozool. 13, 377-379.